ROBUST OPTIMIZATION APPLIED TO A HYDROTHERMAL UNIT COMMITMENT PROBLEM WITH DISPATCHABLE WIND POWER

Cindy Carolina Viviescas Latorre

Tese de Doutorado apresentada ao Programa de Pós-graduação em Planejamento Energético, COPPE, da Universidade Federal do Rio de Janeiro, como parte dos requisitos necessários à obtenção do título de Doutor em Planejamento Energético.

Orientadores: Roberto Schaeffer

André Luiz Diniz Souto Lima

Rio de Janeiro

Dezembro de 2019

ROBUST OPTIMIZATION APPLIED TO A HYDROTHERMAL UNIT COMMITMENT PROBLEM WITH DISPATCHABLE WIND POWER

Cindy Carolina Viviescas Latorre

TESE SUBMETIDA AO CORPO DOCENTE DO INSTITUTO ALBERTO LUIZ COIMBRA DE PÓS-GRADUAÇÃO E PESQUISA DE ENGENHARIA (COPPE) DA UNIVERSIDADE FEDERAL DO RIO DE JANEIRO COMO PARTE DOS REQUISITOS NECESSÁRIOS PARA A OBTENÇÃO DO GRAU DE DOUTOR EM CIÊNCIAS EM PLANEJAMENTO ENERGÉTICO.

Examinada por:

_____

Prof. Roberto Schaeffer, Ph.D.

_____

Dr. André Luiz Diniz Souto Lima, D.Sc.

_____

Prof. Alexandre Salem Szklo, D.Sc.

_____

Prof. André Frossard Pereira de Lucena, D.Sc.

_____

Dr. Arild Helseth, PhD.

_____

Prof. Bruno Fânzeres, dos Santos, D.Sc.

RIO DE JANEIRO, RJ - BRASIL

DEZEMBRO DE 2019

Latorre, Cindy Carolina Viviescas

Robust optimization applied to a hydrothermal unit commitment problem with dispatchable wind power/ Cindy Carolina Viviescas Latorre – Rio de Janeiro: UFRJ/COPPE, 2019.

XIX, 135 p.: il.; 29,7 cm.

Orientadores: Roberto Schaeffer

André Luiz Diniz Souto Lima

Tese (doutorado) – UFRJ/ COPPE/ Programa de Planejamento Energético, 2019.

Referências Bibliográficas: p. 100- 113.

1. Robust Optimization. 2. Unit commitment. 3. Hydropower modeling. 4. Wind power uncertainty. I. Schaeffer, Roberto *et al*. II. Universidade Federal do Rio de Janeiro, COPPE, Programa de Planejamento Energético. III. Título.

"*Si no hay viento, rema*"

Provérbio Latino

Agradecimentos

Son tantos *Gracias, Obrigados,* y *Thank you* a todas las personas que me ayudaron a llegar a mi meta, que decidí escribir mis agradecimientos en el idioma que mejor lo sé hacer.

Agradezco a mi familia, especialmente a mi madre, Luz Imelda, que siempre ha sido la roca en la que he basado la construcción de mi vida.

Agradezco a mi esposo, Oscar, que en los momentos felices, estresantes o tristes siempre ha estado a mi lado sosteniendo mi mano, y en algunos momentos mi cordura.

A mi orientador, Roberto Schaeffer que me dio la bienvenida al PPE. Gracias por haberme dado el privilegio de aprender y trabajar con Ud., por siempre tener una palabra gentil hacia mí y por permitirme ser parte de la familia CENERGIA, este tal vez sea el mejor regalo que Brasil me dio.

A mi orientador, André Diniz, de quien tanto aprendí. Gracias por todas las conversaciones y discusiones técnicas que me condujeron durante el desarrollo de esta tese, un agradecimiento especial por permitirme ser parte de la familia Cepel.

A los colegas y amigos del PPE, quienes, cada uno a su manera, fueron haciendo el camino más fácil y agradable, especialmente a Susi, Esperanza, Murilo, Gabi, Eve, Rafael Morais, Bruno, Rafael G, Fernanda, Camila O, Fabio T, Fran, Leticia, Camila L, Lucas, Otto, Mauro, Gerd, Rebeca, Talita. Un agradecimiento especial a Fabio D alias Fabito, por ser un excelente compañero de pesquisa, pero sobre todo por la amistad.

A Paula, Isabela y Mari por siempre escuchar mis neurosis, por ser mis confidentes, por ser mi familia brasilera.

A los profesores del PPE que se dedicaron no solo a transmitir su conocimiento sino también a generar un espacio de pensamiento crítico y a ser una mano de ayuda en momentos de incertidumbre, en especial Pedro Rochedo, Joana Portugal, Alexandre Szklo y André Lucena.

A la profesora Paula Ferreira de la Uminho que me introdujo a los modelos de despacho y a la herramienta de optimización GAMS.

A los colegas y amigos de PIK, em especial a Falko Ueckerdt y Gunnar Luderer que me permitieron mejorar mi modelo usando las herramientas computacionales de su centro de investigación.

A mis amigos Colombianos y algunos que adoptamos como colombianos por las tantas comidas y charlas que nos hacían recodar la “tierrita”: Marcela, Diego, Lizeth, Diogo, Judy, Jeniffer M, Vivian, Joanna, Jorge, Mabel, Santi, Chepe, Kathe, Gustavo, David, Jeniffer y un especial agradecimiento a Rafael Soria que fue el “culpable” de que encontrara en mi carrera aquello que me apasiona.

A mis compañeros de sala D26 por hacer mis días en Cepel más divertidos.

A los miembros de la banca por haber aceptado participar y prestigiar este trabajo. Su revisión crítica será fundamental para mejorar la calidad de este documento.

A los funcionarios do Programa de Planejamento Energético – PPE/COPPE, especialmente a Paulo por la ayuda para navegar a través de los requisitos burocráticos.

Y finalmente agradezco el apoyo financiero de Capes y Cepel que hicieron todo esto posible.

¡Gracias!

Resumo da Tese apresentada à COPPE/UFRJ como parte dos requisitos necessários para a obtenção do grau de Doutor em Ciências (D.Sc.)

OTIMIZAÇÃO ROBUSTA APLICADA AO DESPACHO HIDROTÉRMICO CONSIDERANDO GERAÇÃO EÓLICA

Cindy Carolina Viviescas Latorre

Dezembro /2019

Orientadores: Roberto Schaeffer
André Luiz Diniz Souto Lima
Programa: Planejamento Energético

A variabilidade e a incerteza inerentes da energia eólica exigem que os operadores do sistema elétrico refinem suas políticas de *Unit Commitment* (UC) e despacho econômico. A implementação de metodologias eficazes que produzam decisões de UC resistentes a variações repentinas na geração eólica é fundamental para garantir uma operação confiável. Esta tese propõe aplicar uma abordagem de otimização robusta a um modelo hidrotérmico de UC que considera a energia eólica como uma fonte incerta de geração de energia. O modelo, que é formulado como um problema de UC de dois estágios, tem como objetivo minimizar o custo operacional no pior cenário de energia eólica dentro do conjunto de incerteza definido. A metodologia de solução é baseada no algoritmo de decomposição de Benders. Uma abordagem de amostragem de Monte Carlo é usada para avaliar o desempenho da solução determinada por este modelo. Os resultados apresentados mostram que o modelo robusto ofereceu uma solução econômica para todos os níveis considerados de incerteza. Além disso, foi formulado um modelo de despacho hidrotérmico (considerando a função detalhada de produção hidrelétrica, bem como o efeito cascata) para o sistema elétrico brasileiro, denominado STORM. Os resultados mostraram que o modelo STORM representa as principais características do sistema elétrico brasileiro, e pode ser usado como ferramenta para analisar as interações de mercado, os custos de eletricidade e os possíveis impactos das políticas / iniciativas regulatórias nacionais.

Abstract of Thesis presented to COPPE/UFRJ as a partial fulfillment of the requirements for the degree of Doctor of Science (D.Sc.)

ROBUST OPTIMIZATION APPLIED TO A HYDROTHERMAL UNIT COMMITMENT PROBLEM WITH DISPATCHABLE WIND POWER

Cindy Carolina Viviescas Latorre

Dezembro/2019

Advisors: Roberto Schaeffer

André Luiz Diniz Souto Lima.

Department: Energy Planning

The inherent variability and uncertainty of wind power require that system operators refine their Unit Commitment (UC) and economic dispatch policies. Implementing effective methodologies that produce UC decisions strong enough to deal with wind power variations is critical to ensure a reliable operation. This thesis proposes to apply a Robust Optimization approach to a hydrothermal UC model that considers wind energy as an uncertain source of power generation. The model is formulated as a two-stage UC problem with the objective of minimizing the total operational cost under worst wind power output scenario. The methodology solution is based on the Benders' decomposition algorithm. A Monte Carlo sampling approach is used to evaluate the Robust UC solution. Results show that the robust optimization model delivered a cost-efficient solution for all considered levels of uncertainty. Additionally, a deterministic optimization model for the Brazilian hydrothermal UC problem, called STORM, was formulated. This model considers technical restrictions of thermal and hydro power plants (including detailed hydro production function and cascade effect), as well as transmission capacity limitations between major electricity markets. Results show that STORM model can represent the main characteristics of the Brazilian power system, in such a way that it can be used as a tool to analyze and better understand market interactions, electricity costs and possible impacts of national energy policy/regulatory initiatives.

Index

Index of Figures

Index of Tables

List of Abbreviations and Acronyms

Table I-1. Sets Definition.

Symbol	Description
bus	Set of power grid buses
$busWind \subseteq bus$	Subset of bus with wind generation
$cutset \subseteq iter$	Subset of Iterations that generated an optimality cut
$GB(bus, x)$	Bi-dimensional set linking generation unit x with bus *bus*, and $x = \{hT, j, ncl, pen\}$
$hd \subseteq hT$	Set of hydropower plants with reservoir
$hr \subseteq hT$	Set of run-of-river (ROR) hydropower plants
hT	Set of hydropower plants
$iter$	Set of iterations in benders' decomposition method
j	Set of thermal power plants
MCs	Set of Monte Carlo Sampling scenarios
$lim \pm$	Set of power flow directions (positive or negative)
ncl	Set of nuclear power plants
pen	Set of penalty power plants
pln	Set of planes that describe the hydropower production function (HPF)
$plnR$	Set of planes that describe the ROR- HPF
t	Set of time periods (h)s
$TblCasc(hT, hx)$	Set of hydropower units (hx) upstream of unit hT
$line$	Set of transmission lines
$utt \subseteq t$	Subset of set t for min UP/down time
$week$	Set of operative weeks
w_n	Set of wind hotspots
sr	Set of solar hotspots
su	Set of small generation units
$\Lambda_{wn-busWind}$	Bi-dimensional set linking wind hotspot w_n with bus *busWind*
Λ_{sr-bus}	Bi-dimensional set linking solar hotspot s_r with bus *bus*
Λ_{su-bus}	Bi-dimensional set linking small generation unit su with bus *bus*

Table I-2. Parameters Definition.

Symbol	Description
$Bgt_{busWind}$	Uncertainty budget for wind power generation at *busWind*
$CapTx_{line,limx}$	Transmission line capacity of $line$ for the $limx$ power flow direction (MW)
$ColdS_j$	Startup cost of thermal power unit *j* ($)
$COVF$	Fuel and O&M cost of nuclear power plants ($/MWh)
$CPen$	Operation cost for penalty units ($/MWh)
$CVOMdEq$	Variable O&M cost of RES hydropower plants ($/MWh)
$CVOMt_J$	Variable O&M cost of thermal power unit j ($/MWh)
CSd_j	Shutdown cost of thermal power unit j ($)
$CWater_{hd,week}$	Water value for RES hydropower plants per *week* ($\$/hm^3$)
$Demand_{bus,t}$	Demand by *bus* at time *t* (MWh)
DT_j	Minimum down time of thermal power unit *j* (h)
$IndA_j$	Slope of the fuel cost curve of *j* power unit ($/MWh)
$IndB_j$	Constant coefficient of the Fuel cost curve of *j* power unit ($)
$InflowhT_{hT,t}$	Incremental Inflow of *hT* hydropower unit at time *t* (m^3/s)
$InitVal_{hd}$	Initial Reservoir Level of *hd* unit (hm^3)
$MaxLevel_{hd}$	Maximum reservoir level of *hd* unit (hm^3)
$MaxNcl_{ncl}$	Nominal capacity of nuclear thermal power unit *ncl* (MW)
$MinLevel_{hd}$	Minimum reservoir level of *hd* unit (hm^3)
$MinNcl_{ncl}$	Minimal power generation of unit *ncl* (MW)
$Pcap_j$	Nominal capacity of thermal power unit *j* (MW)
$PhdMax_{hd}$	Nominal capacity of *hd* hydropower plant (MW)
$PmaxROR_{hr}$	Nominal capacity of *hr* hydropower plant (MW)
PLD_{hd}	Electricity price in spot markets ($MWh/\$$)
$Pmin_{hd}$	Minimal power generation of *hd* hydropower plant (MW)
$Pmin_j$	Minimal power generation of thermal power unit *j* (MW)
$Ppch_{bus,t}$	Small hydro power generation by *bus* and time *t* (MWh)
$Produt_{hT}$	Hydropower plant productivity of *hT* unit ($MW/(m^3/s)$)
$PsmPU_{sm,t}$	Seasonal "capacity factor" for small power unit *sm* at time *t*
$PsolarPU_{sr,t}$	Hourly capacity factor for sr solar hotspot at time *t*
$Psolar_{bus,t}$	Solar PV power generation by bus and time (MWh)

$Pstm_{bus,t}$	Small units thermal power generation by bus and time (MWh)
$PTDF_{line,bus}$	Distribution factor for DC power flow of *line* connected to *bus*
$PVCap_{sr}$	Nominal capacity of sr solar hotspot (MW)
$PwindCap_{busWind}$	Maximum wind power generation capability link to *busWind*
$PwindFcast_{busWind,t}$	Forecast wind power generation link to *busWind* and time *t* (MWh)
$PwindUP_{busWind,t}$	Upper bound of wind power generation at *busWind* and *t*
$PwindDW_{busWind,t}$	Lower bound of wind power generation at *busWind* and *t*
$PwindPU_{wn,t}$	Hourly capacity factor for wm wind hotspot
$Qmax_{hd}$	Maximum water discharge of hd power unit (m^3/s)
$QmaxROR_{hr}$	Maximum water discharge of *hr* power unit (m^3/s)
$Qmin_{hd}$	Minimum water discharge of the *hd* power unit (m^3/s)
$Ramp_j$	Online ramp rate of thermal power unit *j*
Rmp_{ncl}	Online ramp rate of nuclear thermal power unit *ncl*
$RoRCost_{hr}$	Variable O&M cost of ROR hydropower plants ($\$/m^3$)
$SmUnCap_{sm}$	Nominal capacity of small power units (MW)
$SpilMax_{hd}$	Maximum spillage of the hd hydropower plant (m^3/s)
$Spin$	Spin reserve requirement
$SRamp_j$	Start ramp of thermal power unit j (MW)
$tviag_{hT}$	water transport delay for each *hT* unit in cascaded (h)
T	Total analysis period
UT_j	Minimum up time of thermal power unit j (h)
$WindCao_{wn}$	Nominal capacity of wn wind hotspot (MW)
$\gamma_o^{hT,pln}$	Constant term of the HPF for power unit *hT* and plane *pln* (MW)
$\gamma_V^{hT,pln}$	Volume coefficient of the HPF for power unit *hT* and plane *pln* (MW/hm³)
$\gamma_Q^{hT,pln}$	Water discharge coefficient of the HPF for power unit *hT* and plane *pln* (MW·s/m³)
$\gamma_S^{hT,pln}$	Spillage coefficient of the HPF for power unit *hT* and plane *pln* (MW·s/m³)

Table I-3. Variables Definition.

Symbol	Description
$cutcost_{iter}$	Constant coefficient of Benders algorithm for the *iter*th loop cycle
$cutcoeffU_{iter,j,t}$	Proportional coefficient of Benders algorithm for the binary variable of *j* thermal unit at time *t* and *iter*th loop cycle
$cutcoeffVh_{iter,hd,t}$	Proportional coefficient of Benders algorithm for the binary variable of *hd* hydro unit at time *t* and *iter*th loop cycle
$DeltaVol_{hd}$	Reservoir level variation over the simulation time frame.
$HydroCost_{hd,t}$	Total hydropower generation cost of hd unit at time t ($)
$HRORCost_{hr,t}$	Total hydropower generation cost of hr unit at time t ($)
LB	Lower bound of Benders solution algorithm
$PenCost_{pen,t}$	Total deficit cost at time t ($)
$GenPen_{pen,t}$	Power generation of penalty power unit *pen* at time t (MWh)
$NCLCost_{ncl,t}$	Total nuclear power generation cost of ncl at time *t*– ($)
$Ph_{hd,t} \parallel HPF_{hd}^{t}$	Power generation of RES hydropower unit *hd* at time t (MWh)
$Pncl_{ncl,t}$	Power generation of nuclear thermal power unit *ncl* at time t (MWh)
$Pror_{hr,t} \parallel HPF_{hr}^{t}$	Power generation of ROR hydropower unit *hr* at time t (MWh)
$Pt_{j,t}$	Power generation of thermal power unit j at time t (MWh)
$PwindEq_{busWind,t}$	Power generation of wind farms at bus *busWind* and time *t* (MWh)
$PwindTemp_{busWind,t}$	Available wind generation power at bus *busWind* and time *t* (MWh)
$rm_{busWind,t,MCs}$	Random variable, per *busWind*, time *t*, and scenario *MCs* used for Monte Carlo sampling analysis
$Rsrv_{hd,t} \parallel V_{hd}^{t}$	Reservoir level of hydropower unit hd at time $t(hm^3)$
$ThermCost_{j,t}$	Total thermal generation cost of j unit at time t($)
$Spil_{hd,t} \parallel S_{hd}^{t}$	Spillage in *hd* unit at time t (m^3/s)
$SpilROR_{hr,t} \parallel S_{hr}^{t}$	Spillage in *hr* unit at time t (m^3/s)
$TurbROR_{hr,t} \parallel Q_{hr}^{t}$	Turbinated outflow in *hr* unit at time t (m^3/s)
$TurbWat_{hd,t} \parallel Q_{hd}^{t}$	Turbinated outflow of hd hydropower unit at time t (m^3/s)
UB	Upper bound of Benders solution algorithm
$U_{j,t}$	Binary variable - Indicates if thermal unit *j* is online at time t
$Uoff_{j,t}$	Binary variable - Indicates if thermal unit j switches off at time t
$Uon_{j,t}$	Binary variable - Indicates if thermal unit j switches on at time t
$VazaoInEq_{hT,t}$	Inflow of hydropower units (considering cascade) at time t (m^3/s)
$Vh_{hd,t}$	Binary variable - Indicates if hydropower unit *hd* is online at time t

$Zneg_{busWind,t}$	Binary variable - indicates if wind power output at bus $busWind$ reaches the lower bound at time t
$Zpos_{busWind,t}$	Binary variable - indicates if wind power output at bus $busWind$ reaches the upper bound at time t
$\vartheta_{j,t}$	Fuel cost function of j thermal unit at time t (\$)
Θ	Auxiliary variable for solution of Master problem (Benders algorithm)
$x.l$	Nomenclature that refers to the actual level of a variable x
π_1 to π_{29}	Dual variables of the slave problem, defined in Section 4.1.2
$\Phi()$	Cumulative standard normal distribution function

Chapter 1

Introduction and Thesis Overview

The power sector is leading an ongoing energy transition driven by the growing need for energy sources with net-zero direct greenhouse (GHG) gas emissions and the rapid decline on renewable electricity costs, particularly for wind and solar generation [1]. Due to the inherent characteristic of renewable energy, increasing levels of uncertainty and variability are being introduced into power systems, calling for more flexible systems. Flexibility in power systems can be defined as "the ability of a power system to cope with variability and uncertainty in both generation and demand, while maintaining a satisfactory level of reliability at a reasonable cost, over different time horizons" [2]. Besides system flexibility, enhanced transmission system capacity, geographical dispersion and complementarity between energy sources are pointed out as key components to ensure the reliability of power systems with high levels of renewable energy [3] [4].

The impacts of intermittent and renewable energy generation differ based on the time frame. Long-term impacts (1 year – 5 years) can be seen in energy models solutions that, without considering renewable energy variability, could lead to unfit investment portfolios that create generation and load mismatches, especially at peak load and/or high energy variability moments [5]. Short-term impacts (1 day - 1 week) can be seen in unit commitment (UC) models and real time operation as higher operating costs and/or load sheading due to required efforts to maintain the stability and reliability of power systems e.g. stricter ramping requirements and higher management of the reserves [6], [7]. The unit commitment problem is defined by [2] as "the determination of generating units to be committed during each interval of a short-term scheduling period (hours, a day or a week)" (p.1). The UC models are employed to ensure that sufficient resources are available for hours or days ahead to meet system demand and reserve requirements in an optimal and cost-efficient manner through the expected range of system operation conditions [2].

Unit Commitment models are often used as a tool to better understand system flexibility [8]–[11]. However, determinist UC models generally require the use of operational reserve levels to increase system flexibility and handle uncertainty [12]. In this case, system operators make sure that there is enough power reserve to maintain system balance according to local reliability standards. Yet, these standards have been affected by the level of intermittent energy generation. In [13] was reported that an addition of 1500 MW (10% of peak demand) of wind energy into New York's power system increased the regulation[1] requirements by 8 MW, and an addition of 3300 MW (20% of peak demand) caused an increment of 36 MW [7]. In the Ontario case study [14] the impacts of wind penetration through different penetration scenarios (4%, 17%, 20%, 27% and 33%) and regulation requirements were analyzed. According to the study, even with high levels of wind energy penetration the 1-min regulation[2] requirements were not highly impacted due to aggregation and spatial distribution effect. However, for levels of penetration above 17% (5 GW) the 5-min load following requirement may exceed the capability of existing generators, and from scenarios beyond 20% (6 GW wind capacity) the 10-min operating reserve requirement should be increased in order to accommodate extreme drops of wind generation. Additionally, high renewable energy penetration levels could result in transmission congestions and therefore higher transmission capacity requirements [15].

The day-ahead UC scheduling in purely thermal systems aims to minimize the operating cost through the reduction of fuel consumption subject mainly to system power balance constraints and generation power limits [16]. The day-ahead hydrothermal UC problem, on the other hand, is more challenging since the availability of water resources for electrical generation at each stage of the operation-planning horizon depends on the previous and future planned use of water, which establishes a dynamic and inter-temporal relationship among the operational decisions made along the whole horizon [17] [18]. Even more, in hydrothermal power systems is essential to a soft/hard link between the UC problem and the long-term operation planning problem, usually formulated as a multistage stochastic problem, in order to correctly define the value of water. Additionally, several technical constraints such as the hydropower

[1] "Regulation is the balancing of fast second-to-second and minute-to-minute random variations in load or generation" [158].

production function, water balance constraints and reservoir storage limits increase the problem complexity [19], [20], [21], making the hydrothermal UC problem one of the most challenging optimization problems in the economic operation of power systems [12].

In general terms, the UC problem is a large-scale mixed integer nonlinear constrained optimization problem [22] that determines an hourly or sub-hourly generation dispatch for each committed unit without violating operational constraints taking into account water values and/or daily generation/discharge targets that, in the case of hydrothermal power systems, are calculated in the mid-term level scheduling problem (seasonal level) [18]. The UC model nonlinearities stem from the inclusion of quadratic curves for fuel and emissions costs [23], non-linear transmission constraints [2] and from the modeling of the hydro plant's production curve, which is a nonlinear and non-concave function [24]. Additionally, even though linear programming models have been successfully used for solving UC problems, mixed integer programming models must be used when binary variables are associated with non-convexities, such as minimum run levels and minimum up and downtimes of thermal power plants [25]. The combinatorial characteristic of the problem formulation and the need of binary and non-linear variables have encouraged researchers to focus on the development of efficient, optimal or near-optimal UC algorithms for large-scale power systems (as described on the review of [2]).

Renewable energy (such as wind or solar power) increases the complexity of hydrothermal UC problems, mainly because of their unpredictability and variability. This renewable energy's characteristics challenge power grid operation as affect conventional generation plants, which must follow the resultant power variations. Therefore, a higher share of renewable energy tends to induce an increase in the frequency of startups and ramping operation and periods of operation at low load levels. In other words, it can lead to a most costly and less reliable system operation [26]. Even though good forecasting and prediction tools can contribute to better deal with this scenario, the intermittent characteristic of renewable sources can still lead to curtailment and suboptimal operation of conventional power plants due to complexities in balancing

[2] Power sources online, on automatic generation control, that can respond rapidly to system-operator requests for up and down movements; used to track the minute-to-minute fluctuations in system load [159].

load with generation while obeying system constraints in a minimization cost problem [2] [27].

The cost of the reduced system efficiency depends on the unit commitment of conventional plants, renewable energy uncertainties, and system flexibility [12]. As mentioned, during conventional real-time operation, system operator dispatches the committed generation resources to satisfy the actual demand and reliability requirements. However, if the actual system condition deviates significantly from the expected one, system operators take corrective actions to maintain system stability, such as committing expensive fast-start generators or, in emergency cases, load shedding [28].

With intermittent renewable energy playing an increasing role in the electrical power sector, short-term models or UC models must have enough robustness to determine unit commitment decisions that guarantee a stable and reliable system operation, even with high levels of uncertainty [29]. UC models that consider the economic and technical aspects of intermittent and renewable energy integration can be useful to: i) assess the extra costs on hydrothermal power operation, ii) check the technical feasibility of the solutions of power system planning models, iii) guarantee a reliable energy supply, iv) help the integration of non-conventional sources in a more robust and controllable way, v) reduce the possibility of technical infeasibilities and/or contingencies in real-time operation and vi) analyze the adverse impacts of renewable power integration, such as the increment of cyclic operations, thermal stress, EFOR (Equivalent Forced Outage Rate) levels of thermal power plants, among others. [30]. In this context, it becomes important for system operators to have an effective methodology that produces robust unit commitment decisions considering the stochasticity of renewable energy generation and ensures system reliability in the presence of increasing real-time uncertainty [28].

1.1. Objectives

The first objective of this thesis is to develop and validate a robust hydrothermal unit commitment model that considers wind energy as an uncertain source of power generation. The model is named R-STORM. In order to test the robust model's ability to hedge against wind power uncertainty, the performance of R-STORM was compared against its equivalent deterministic model, using a Monte Carlo sampling method. The comparisons were made considering two fictional case studies (system A and system

B). The main difference between these systems is the greatest complexity of system B, which allows to test the robust approach in large scale systems and analyze computational performance characteristics of R-STORM.

The second objective of this thesis is to validate the capability of the deterministic UC Model (STORM) to represent the Brazilian power system main characteristics. This validation was performed through numerical comparisons between the STORM dispatch and the power system dispatch made by the Brazilian power system operator (ONS), for four representative days. Therefore, the following specific objectives are considered:

- To formulate and validate a deterministic optimization model for the hydrothermal unit commitment (UC) problem as a large-scale mixed-integer linear problem, based on previous formulations presented in the literature [23], [31] [32], [33]. Technical restrictions of thermal and hydro power plants (including detailed hydro production function and cascade effect), as well as transmission capacity limitations between major electricity markets, are considered. The model formulation is implemented in GAMS[3].
- To employ the Robust Optimization framework[4] to hedge the system from wind energy uncertainty. This problem is formulated as a two-stage UC problem with the objective of minimizing the total operational cost under worst wind power output scenarios. The uncertainty set of this model is defined as a polyhedral set [34], [35],[36].
- To apply the dual-based formulation and Benders' decomposition algorithm[5] as an heuristic solution methodology [37]. The problem formulation and solution algorithm are implemented in GAMS.
- To employ a Monte Carlo sampling approach to evaluate the Robust UC solution.

[3] GAMS is a software system that combines the language of mathematical algebra with traditional programming concepts in order to efficiently describe and solve optimization problems [160].
[4] Methodology aimed at dealing with uncertain optimization problems where constraints must remain feasible for all *reasonable* realizations.
[5] The Benders decomposition implemented approach is a partitioning procedure for solving mixed-variables programming problems.

1.2. Contribution

The main contribution of this thesis is the development of two open-source models for the solution of the UC problems of large-scale hydrothermal power systems. The developed models can be especially useful to model power systems with high share of hydropower generation due to its highly sophisticated representation of hydropower reservoirs. These models (STORM and R-STORM) can be applied to other power systems beyond the case studies analyzed in this thesis, and therefore, they are an excellent starting point for many future analyses. STORM can be used, for example, to analyze the technical viability of scenarios related to energy policies and/or energy transactions. R-STORM, on the other hand, can be used in power systems with high penetration of non-dispatchable power generation, as an economically option to deal with uncertainty. Furthermore, different approaches to define the uncertainty set can be explored in order to better represent wind uncertainty in robust UC optimization.

The methodological and practical contribution of this thesis is the development of an approach for implementing a Robust Optimization Unit Commitment problem in a large-scale hydrothermal context, considering a detailed hydro production function and the cascade effect in the water balance of hydropower plants. Hydropower modelling tend to be overlooked in UC formulations that deal with wind power uncertainty. However, for power systems that presents high levels of hydropower, such as the Brazilian one, appropriate reservoir modelling is crucial to reach accurate results. The robust optimization approach is an extension of a previous work [35] to hydrothermal systems with wind energy uncertainty. Nonetheless, R-STORM introduces the use of a piece-wise linear production function for hydroelectrical power plants that takes into account the water head as a function of the forebay and tailrace levels and considers spillage effects, proposed in [24].

1.3. Thesis synopsis

The remainder of this thesis is structured as follows: Chapter 2 provides a literature review on Unit Commitment (UC) models with special focus on Robust Unit commitment approaches. The advantages and disadvantages of Robust UC models, related to deterministic UC models with spinning reserve and stochastic UC models, for power systems with high levels of uncertainty, is presented.

Chapter 3 presents the problem formulation for a deterministic hydrothermal unit commitment model considering wind power. This model takes into account individual unit constraints and system-wide constraints. Additionally, the operation of hydropower plants is modeled through its production function, individual technical restrictions and water balance, considering the cascade effect.

Chapter 4 presents the formulation and the solution methodology for the Robust hydrothermal UC problem. The constraints considered in the formulation of this model are the ones presented in Chapter 3. However, in this analysis wind energy is a decision variable and it is optimized within an uncertainty set. Benders' decomposition method is used as a solution framework.

Chapter 5 is divided in two main sections. The first one validates the Brazilian deterministic UC model and the second one presents the Robust UC solutions for a reduced power system using different uncertainty budgets. A comparison is made between Robust UC Solutions and deterministic UC solutions with spinning reserve requirement; also called reserve adjustment method. A Monte Carlo sampling is employed to evaluate Robust UC solutions. Finally, an analysis of the scalability of the proposed model for higher dimensional uncertainty is presented. Chapter 6 provides the final remarks, the study limitations and future work suggestions.

Chapter 2

Literature review

2.1. Short-Term Operation Planning: The Unit Commitment Problem

Traditionally, the unit commitment (UC) problem is a cost minimization problem that seeks for optimal unit commitment decisions and generation level (economic dispatch) decisions of power plants to meet the forecasted system load, while satisfying individual unit constraints, inter-temporal constraints of generating sources and system-wide constraints such us reliability requirements and transmission constraints [28], [38]. The UC problem is generally formulated as a large-scale mixed-integer nonlinear and non-convex combinatorial problem, which can be modeled with binary variables to represent on/off status of the generation units and continuous variables to represent the amounts of energy to be generated by the committed units [2], which makes it a complex mathematical problem [16],[39].

Several efficient methods capable of finding optimal or near–optimal UC solutions, in reasonable computational times, have been studied in the past decades (as described on the review of [2]). Commonly adopted methods to solve deterministic UC problems are Lagrangian relaxation-based methods [40] and Mixed Integer Programming-based methods (MIP)[41] [42]. The Lagrangian relaxation method is one of the most realistic and efficient method for large-scale systems. However, its disadvantage of inherent sub-optimality means that its convergence to a feasible solution after a limited number of iterations is not guaranteed. Mixed Integer Linear Programming-based method (MILP) has become more popular since more efficient general-purpose MILP solvers, like CPLEX and GUROBI, have become available. Branch-and-Bound [16] is often used by commercial solvers to solve MIP problems because it guarantees global optimality. Nonetheless, it is important to highlight that its good performance for solving large-scale systems requires large memory and high computational cost.

Traditionally, given that global UC optimal solutions can be challenging to find, uncertainty from sources like customer load, renewable generation, and unit availability have been often neglected or managed with reserve requirements [43]. However, higher penetration levels of variable generation resources (such as wind power, solar power, and distributed generators) and more price-responsive demand participation have posed new challenges to the UC problem. In the case of wind power, the inherent variability and uncertainty of the resource requires that both utility companies and system operators refine their unit commitment and economic dispatch policies. It has become increasingly important to have an effective methodology that produces robust UC decisions and ensures system reliability for electric power grids that everyday are more volatile due to increasingly real-time uncertainty [28].

In traditional approaches, uncertainty management is handled by imposing conservative reserve requirements to maintain the power grid reliability [34]. This approach is usually called “reserve adjustment method” and it is widely used in today’s power industry [28]. Much of the research related to this area, including [44]–[47], has focused on analyzing the levels of reserve requirements needed to implement preventive or corrective actions in order to handle outages. This kind of approach is usually based on deterministic criteria, such as loss of the largest generator or a number of system components [48]–[51]. Even though this approach is easy to implement, in the case of wind power uncertainty, for example, it can lead to an economically inefficient or even infeasible way to handle uncertainty, because the UC decision only considers the expected operating condition. Then, even with enough reserve available, the power system may still suffer capacity inadequacy when the real-time condition deviates significantly from the expected value. This is specially the case when the reserve requirement is determined by some *a priori* system-wide rules, rather than by a systematic analysis [36].

To tackle this situation, two alternative methods for uncertainty management have been proposed in the literature: the Stochastic programming based method [52]–[54] and the Robust optimization based method [29], [30], [55], [56]. Stochastic optimization methods for UC problems represent the uncertainty by using a set of scenarios based on a chosen Probability Distribution Function (PDF) with the objective of minimizing the total expected cost [57]–[59]. However, this approach has some practical limitations. For once, this approach is effective when the PDF is available, which is not a realistic

assumption since in most cases the detailed probability information is hard to obtain and, in the case of wind power, for example, the wind distribution is difficult to be defined day-ahead, especially when there is a lack of accurate large amounts of data [29]. Additionally, stochastic methods are computationally intensive since the problem size increases dramatically due to the large number of samples needed to generate the scenarios. To reduce this restriction, scenario reduction methods can be adopted [52], [60], [61]. Nonetheless, this approach does not guarantee the feasibility for all the uncertainties, as only limited sample points are considered [38]. Even more, due to the objective of minimizing the total expected cost, in order to achieve the optimal objective value, a significant portion of wind energy may be curtailed due to operative restrictions such us minimum on/off time of slow and cheap thermal power plants. This means a waste of available resources and does not allow to use renewable energy as much as possible [62] [30].

The Robust Optimization (RO) approach has gained substantial popularity as a modeling framework led by Ben-Tal and Nemirovski [63]–[65], El Ghaoui et al.[66], [67] and Bertsimas and Sim [68], [69]. The main idea of RO based methods for Unit Commitment problems is to find a UC solution which is feasible for all possible realizations so that the total operating cost under the worst case scenario is minimized [34]. The appealing of RO stems from the fact that it only requires moderate information about the underlying uncertainty, such as the mean and the range of the uncertain data [28]. This makes the RO approach an appropriate framework to model optimization problems where the optimal solution must remain feasible for the parameter variations in a given user-defined set, called “uncertainty set” [70]. This concept is consistent with the risk-averse fashion in which power systems are operated. The developments performed in this thesis are focused on the RO approach. Nonetheless, it is important to mention that since the robust commitment decisions must be feasible for any realization within the uncertainty set, and neglects any underlying probabilistic information, over-conservative or too expensive schedules regarding stochastic optimization solutions can be produced.

2.2. Robust Unit Commitment Optimization

The decision environment in real world optimization problems is large scale and tends to be characterized by uncertain or inexact data, which can make the optimal

solution difficult to implement and in some cases infeasible in face of changes on the nominal data [71]. Ben-Tal and Nemirovski [71] showed that, from the practical point of view, nominal solutions can be meaningless since its optimality is damaged by small implementation errors. In order to "immunize" the system against implementation errors, one can use the Robust Counterpart methodology [72].

Robust optimization for linear programming problems was first introduced in the early 1970s by Soyster [73]. In the late 1990s and early 2000s, robust optimization was further developed by Ben-Tal and Nemirovski's works [64] [71], El Ghaoui et al.[66], [67] and Bertsimas and Sim [68], [69]. In the Robust Optimization methodology, one associates an uncertain problem with its robust counterpart, which is a usually a semi-infinite optimization program [64]. Robust optimization (RO) became an attractive framework for decision makers to tackle real problems with parameter ambiguity and stochastic uncertainty, when it is challenging to construct a stochastic model to capture randomness and the system reliability is a critical concern e.g. the operational problems in power industry [28], [29], [74]–[77]. Different from classical stochastic programming models, an RO formulation does not suffer from the curse of dimensionality (regarding the number of scenarios), does not assume any probabilistic information on random factors (it assumes "uncertainty sets", described in Section 2.2.2, to capture randomness) and instead of seeking for solutions with the optimal expected value, it derives a best performance solution with respect to the worst cases in the uncertainty set [78]. Consequently, a RO model is less demanding on data to capture randomness and its solution is more reliable towards uncertainty.

Nonetheless, decision makers generally have different attitudes with respect to infeasibility and sub-optimality. Therefore, what does it mean for the decision-maker a robust solution? Robust Optimization concept relies on finding a solution whose feasibility is guaranteed for any realization of the uncertain parameters using the worst-case analysis. In other words, a solution is obtained through the use of the uncertain value that would create "the most damage" to the system [64] [71]. However, how should the worst-case analysis be defined? Should it use a finite number of scenarios, such as historical data, or continuous convex uncertainty sets? As presented by Gabrel et al. [79], RO solutions tends to be overly conservative and may not be cost-effective since it must hedge against any possible realization. The correct definition of uncertainty sets can be seen as a trade-off between system performance and protection

against uncertainty [77]. The major challenges associated with the RO methodology are: i) how to specify reasonable uncertainty sets in specific application [71], ii) how can we reformulate the problem as a "computationally tractable" optimization problem, or at least approximate it by a tractable problem.

In RO complete protection from adverse realizations often comes at the expense of severe deterioration in the objective value [28]. Therefore, to make the robust methodology more appealing, robust optimization focuses on obtaining a feasible solution for any realization of the unknown coefficients within a ''realistic'' set, called the **uncertainty set**, described in Section 2.2.2. In this context, RO seeks for the optimal objective value, over a set of solutions that are feasible for all coefficient realizations within the uncertainty set. As mentioned before, the specific choice of the uncertainty set should be carefully analyzed since it will be crucial for ensuring computational tractability and limiting the over-conservatives' solutions [79].

Multistage RO Unit Commitment problems [80], [81], guarantee both the robustness and non-anticipativity[6] of both UC and economic dispatch (ED) decisions [82]. However, multistage RO in its most general form [83] is currently computationally intractable. Some approaches such as affine policies[7] have been studied as an effective approximation [80], [81], reducing the computational burden. Nonetheless, the affine policies are only an approximation to the full adaptive policies and can reduce the feasible region of the UC problem. In other words, the price of the convexification is that it shrinks the feasible set due to the strong assumptions and sacrifices the optimality of the solution [38] [84].

Because of the difficulty in incorporating multiple stages in RO, many works have focused on two-stages RO approaches to solve practical system design and operation problems [28], [34], [62], [85]–[87]. Two-stage RO was introduced to support decision making where decisions are partitioned into two stages; i.e., before and after uncertainty is disclosed. In this approach, the first stage decisions still need to be made with respect to any realization in the uncertainty set while the second stage decisions can be made after the first stage decisions are determined and the uncertainty is revealed, which essentially enables the decision maker a recourse opportunity [71], [72], [77]. This

[6] Non - anticipative constraints are related with the fact that the uncertainty is unfolded sequentially over time, and the dispatch decisions are made accordingly [82].

decision-making structure matches the day-ahead UC problem [84]. The uncertainty set and the consideration of the worst case performance with recourse opportunities provide a very flexible mechanism that can be used to satisfy more complicated modeling needs [77]. Under this direction, this thesis will discourse with more detail on two-stage robust UC models in Section 2.2.1.

2.2.1. Two stage adaptive robust unit commitment

Robust optimization claims "*All decision variables represent **here and now** decisions: they should get specific numerical values as a result of solving the problem before the actual data "reveals itself"* " [78] (p.2). Adaptive robust optimization , on the other hand, relaxes this paradigm and considers that "*some decision variables can be adjusted at a later moment in time according to a decision rule, which is a function of the uncertain data*" [78] (p.6). In other words, in the adaptative robust optimization the unit commitment decision variables are the first-stage "here and now" decisions made before the uncertainty is revealed and the second-stage "wait and see" decision are the dispatch decision (amounts of generated energy) that can be adjusted according to the actual data of uncertain variables.

Various adaptive two-stages robust UC models dealing with nodal injection uncertainty associated with both supply (e.g., wind power) and demand (e.g., demand forecast errors and price elasticity) have been studied. A robust formulation for the contingency constrained UC problem is proposed in Street et al. [36], [88]. Moreira et al. [89] proposed a contingency-constrained model for the co-optimization of energy and spinning reserves under both demand uncertainty and a deterministic security criterion, considering the correlation effect between nodal demands. Naversen et al. [90] present a two-stage model for scheduling power and procuring symmetric spinning reserves in a hydropower system with uncertain net load. Bertsimas et al. [28] present a security constrained robust UC formulation with system reserve requirements under nodal net injection uncertainty. Zhao and Zeng [29] present a robust UC formulation with demand response under wind uncertainty. Jiang et al. [91] used a two-dimensional uncertainty set to describe the uncertain problem parameters allowing uncertainty correlations among different grid nodes and among different time periods. Liu and

[7] Affine policies replace the unit dispatch decision variables with affine functions of the uncertain power injections.

Tomsovic [92] present a robust UC model to minimize the generalized social cost taking into account uncertainty of demand price elasticity. Duan et al. [93] propose a data-driven affinely adjustable distributionally RO for UC considering uncertain load and renewable generation forecasting errors. Wei et al. [94] propose a two-stage distributionally RO model for the joint energy and reserve dispatch of bulk power systems with renewable energy penetration. Morales-España et al. [95] demonstrate that, by considering dispatchable wind energy and a box uncertainty set for wind availability, an adaptive two-stage robust UC formulation can be translated into an equivalent single-level MIP. Apostolopoulou et al. [96] proposed an optimal dispatch scheme for a cascade hydroelectric power system that maximizes the head levels of each dam taking into account uncertainty in the net load variation. Lee et al. [87] propose a column-generation method for a two-stage robust UC problem considering transmission line constraints using the cutting-plane algorithm for the master problem, which dynamically includes critical transmission line constraints.

The UC problem with uncertain node injections is usually formulated as a two-stage problem with a tri-level structure, or as two-stage problem with a two-level structure by dualizing the inner level of the slave problem [87], [35]. Due to the multi-level structure, the Benders' Decomposition duality-based approach [28], [35] and the Column and Constraints Generation method (C&CG) [87] [29], [55], [96] are often applied. These optimization methods iteratively add vertex scenarios, found in the second-stage or slave problem, into the first-stage problem. In other words, if the first-stage UC decisions cannot immunize against some specific vertex scenarios, the "worst" realizations of the uncertain parameter are obtained by solving the second-stage problem and then adding them as constraints (or cuts) into the first-stage problem.

Nonetheless, solving a two-stage Robust UC is a hard task since the problem formulation is usually a bi-level problem where the outer level is a mixed-integer linear program (MIP), and the inner level is a bilinear program, which is non-deterministic polynomial-time hard (NP-hard) problem [28]. Solving bilinear problems typically requires sub-optimal heuristic methods [28], [91] or computationally expensive exact methods [55] [97]. Furthermore, due to the iteratively nature of the methodology solution algorithm (usually Benders decomposition or C&CG method), the bilinear problem is solved multiple times; which also requires solving a difficult master MIP

problem repeatedly [35] [55]. This computational difficulty highlights the challenges of creating efficient methods to find effective robust UC solutions.

As mentioned, the presence of bilinear and non-convex terms makes it difficult to get the exact two-stage Robust UC optimal solution in acceptable time [87]. Bertsimas et al. [28] find the local optimal solution of the sub-problem (second stage) using an iterative heuristic through an outer-approximation algorithm with general polyhedral uncertainty sets. The authors in [29], [34], [35], [98] transform the separable bilinear sub-problem into an equivalent mixed-integer linear program (MILP) using the big-M method in which they represent the extreme points of the uncertainty set using a set of binary variables. In such cases the presence of bilinear and non-convex terms prevents the Benders decomposition from guaranteeing the attainment of global optimality. Thus, such approaches rely on Monte Carlo sampling [35] in order to assess the quality of the achieved solutions. It is also possible to solve approximately the bilinear version of the sub-problem through the mountain climbing procedure of Konno [99]. This approach provides a lower bound for the master problem. Statistical upper bounds for the master problem are obtained using a Monte Carlo simulation. Other studies like [95] [36] [100] proposed acceleration techniques by recast the min-max-min problem as a single-level MIP problem under assumptions such as defining the uncertainty set as a box set or in the case of [100] by eliminating active flow constraints and decomposing time-coupled uncertainty budget constraints.

As presented in this section, several two-stages Robust UC studies have been proposed in the literature. However, these studies have been focused mainly on thermal power systems; only a few of them have considered hydropower generation as a relevant element in the UC problem formulation. Among the ones that consider hydropower generation there is Jiang et al. [35], which presented a robust UC formulation including pumped-storage hydropower plants under wind uncertainty. Peng et al. [101] propose a RO model for a hybrid wind/photovoltaic/hydro/thermal power system ensuring robustness in the presence of uncertainties caused by renewable energy; This UC problem takes into account a run-of-river hydropower plan and its production function considers a constant height and a max/min flow restriction. Chen et al [20] also propose a two-stage robust wind-hydrothermal UC model, in which wind generation is assumed to be able to vary in a pre-defined uncertainty set. Their formulation considers run-of-river hydropower plants with a production capability curve

linearized by using binary variables separation and the piecewise linear (PWL) function. Soroudi [102] uses a RO model for optimal self-scheduling of a hydrothermal generating company considering electricity prices uncertainties. This proposed model is suitable for price takers Gencos (generation companies) which seek the optimal schedule of their thermal and hydro generating plants for a given operating horizon. Chen et al. [103] present a distributionally robust hydrothermal-wind economic dispatch where wind power uncertainty is described through an ambiguous PDF set and the hydro energy is modeled with the net head and the total water usage fixed.

Yet, it was identified that there is still a gap in the literature related to Robust Optimization problems applied to large scale hydrothermal UC problems considering the operation of large water reservoirs for hydropower generation in detail. That is taking into account characteristics as water balance with the cascaded effect and a production function that considers variable net head and spillage effects. Unlike thermal power energy resources, hydropower generation depends on a variety of factors and is simultaneously coupled both in time and space [20]. Due to its high flexibility and low operation cost, a method for optimizing the hydrothermal UC problem (HTUC) with wind power penetration is desired, especially in power systems that are mainly hydro like the Brazilian power system with increasing wind energy participation. According to [104], for 2027 it is expected a installed capacity of 27GW of wind power in Brazil, which would represent 12.7% of the total installed capacity.

2.2.2. Uncertainty set

The RO methodology, first presented by Soyster [73], caused concern due to issues of over- conservatism for considering the uncertain parameter as the “worst one” since it is highly unlikely that stochastic perturbations, in coefficients of an uncertain linear inequality, will simultaneously take the “most dangerous” values. One way to tackle this issue is by making the uncertainty set smaller and therefore less conservative, through the use of ellipsoidal [43] or polyhedral sets [28], [91], uncertainty budgets [70], and/or combing stochastic and robust approaches [105]. Different from probabilistic scenarios, the uncertainty set modeling method captures the randomness nature without any explicit description of the distribution function [34]. This makes the uncertainty set a key component of any robust optimization model [79]. The trade-off

between the probability of constraint violation and the effect to the objective function of the nominal problem, is what [68] calls *the price of robustness*.

Robust optimization UC focuses on worst-case optimization where the worst case of the constraints is computed over a convex uncertainty set of the parameters, which bounds the maximum allowable deviation of the parameters from their nominal values [106]. Among the types of uncertainty sets, box sets are simple, easy to derive and promise to protect against uncertainties to a high degree [70]. For instance, when considering the uncertain parameter $d_{bus,t}$ for power system bus *bus* at time *t*, with its point estimator $\overline{d_{bus,t}}$ and its sample deviation $\widehat{d_{bus,t}}$; it is possible to use a box (D) for $d_{bus,t}$ with a confidence interval (C_x) [70]; as follow: .

$$D\colon \max\left\{0, \overline{d_{bus,t}} - C_x\,\widehat{d_{bus,t}}\right\} \le d_{bus,t} \le \overline{d_{bus,t}} + C_x\,\widehat{d_{bus,t}} \quad \forall t, \forall bus \tag{2.1}$$

However, this kind of set does not consider correlations between adjacent buses or consecutive time periods and, thus, tends to be very conservative in general. Its conservatism can be reduced by imposing budget constraints. This gives the frequently used ellipsoidal and polyhedral uncertainty sets [107]. Ben-Tal and Nemirovski [64] proposed the use of an ellipsoidal uncertainty set that allowed the user to define a much more accurate description of the uncertainty factors while maintaining the robustness. However, this approach leads to conic quadratic problems which, although convex, are more demanding computationally than the earlier linear models of Soyster [73]. Advances by Bertsimas and Sim [68] allow an easy control of the degree of conservatism with polyhedral uncertainty sets and a user-defined parameter, usually called uncertainty budget, that controls the number of uncertainty coefficients that can deviate from their nominal value. The main advantage of this technique is that the robust model does not increase in complexity compared to its original formulation presented by Soyster [73] [36]. An illustrative example of an ellipsoidal and polyhedral uncertainty set is presented in Figure 2.1. The figure shows the aggregation effect of wind power measurement prediction error.

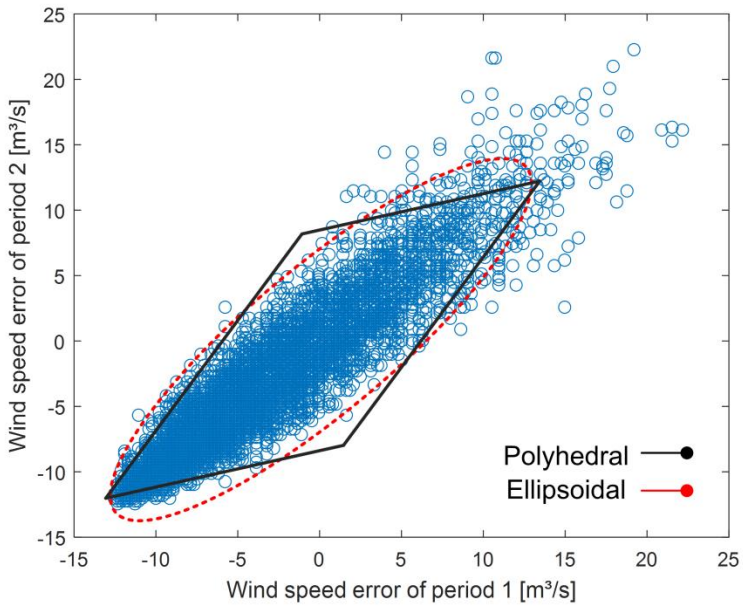

Figure 2.1 Ellipsoidal and Polyhedral uncertainty set models for dispatch periods 1 and 2 of a wind farm.

For instance, in the case of demand uncertainty and polyhedral uncertainty sets, budget constraints can be added in the form of the summation of the weighted demands at all grid buses [34], as depicted by (2.2).

$$\sum_{bus} \pi_{bus,t} \cdot d_{bus,t} \leq \pi_t \ \forall t \tag{2.2}$$

Where π_t is the given upper bound for time period *t* and $\pi_{bus,t}$ is the weight of the demand at bus *bus* at time *t*. The above approach can be extended to multidimensional cases to make the uncertainty set even smaller [70]. We can consider a two-dimensional case and add one more budget constraint such us the summation of the weighted demands within the planning horizon (eq. (2.3)).

$$\sum_{bus,t} \pi_{bus,t} . d_{bus,t} \leq \pi_o \ \forall t \tag{2.3}$$

Where π_o is the given upper bound for the planning horizon [34].

Furthermore, Bertsimas and Sim proposed in [68] a simplified type of budget called the cardinality budget Bgt_{bus} which represents a polytope type uncertainty set. This approach restricts the number of time periods in which the uncertain parameter is deviated from its forecasted value at power system bus *bus* [108]. Considering, for instance, a UC problem in which the uncertainty variable is the wind power generation in bus *b*, the cardinality budget can be defined using eq. (2.4):

$$\sum_{t} z^{+}_{bus,t} + z^{-}_{bus,t} \leq Bgt_{bus} \ \forall t, \forall b, \qquad z_{bus,t} \in \{0,1\} \tag{2.4}$$

where $z^{+}_{bus,t} = 1$ and $z^{-}_{bus,t} = 1$ represent when wind power output reaches the upper and lower bound, respectively. Therefore, the cardinality budget (Bgt_{bus}) limits the total number of periods in which wind energy differs from its forecasted value, i.e., if $Bgt_{bus} = 0$ the wind energy fluctuation at bus b is assumed to be small and the power injection can be approximated by its forecasted value. If $Bgt_{bus} = 2$, for instance, significant fluctuations of wind power output are assumed to occur in no more than two-time intervals at bus *bus*. An illustrative example (considering only one bus) of the polytope uncertainty set with cardinality budget Bgt is presented in Figure 2.2. It presents the set of combinations a wind farm power output can deviates from its forecasted value considering the uncertainty budget presented in eq. (2.5).

$$z_t = |z^{+}_t| + |z^{-}_t| \leq Bgt \quad t \in \{1,2,3\}; \ z^{+}_t \in \{0,1\}; \ z^{-}_t \in \{-1,0\} \tag{2.5}$$

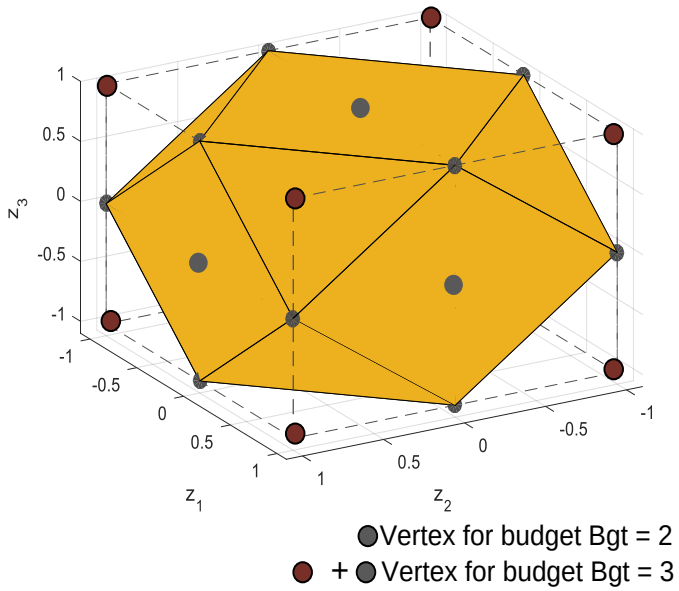

Figure 2.2 Set of worst-case scenarios for a wind farm with T=3.

According to the formulation and mathematical proofs presented by Bertsimas and Sim [68], the consideration of the extreme points of the uncertain parameter guarantee feasible and bounded solutions for all realization of $z_{bus,t}$ over $Bgt_{bus} \in [0, |T|]$. Additionally, the budget constraint defined by (2.4) can guarantee that the optimal solution is feasible with high probability, under any realization of the model of data uncertainty, as a function of the uncertainty budget Bgt_{bus}. Therefore, Bgt_{bus} is the

parameter that controls the trade-off between the probability of constraint violation and the effect of the Robust approach on the objective function of the nominal problem. In [68] it is show that for an uncertain parameter z_t having a discrete probability distribution: $\Pr(z_t = 1) = 1/2$ and $\Pr(z_t = -1) = 1/2\ \forall t$ the relation between Bgt_{bus} and the probability of feasible solution is given by:

$$Bgt_{bus} = \theta\sqrt{n}. \tag{2.6}$$

Where n represents the number of random variables and $\Phi(\theta)$ is the cumulative distribution function of a standard normal. For instance, the UC Robust optimal solution of a problem with 24 uncertain variables (n) is feasible with probability approximately greater than 95% if the cardinality uncertainty budget Bgt_{bus} exceeds the value of 8. An example of a possible worst-case scenario considering $Bgt_{bus} = 8$ for a wind farm in bus *bus* is presented in Figure 2.3. Alternative, the numerical value for the uncertainty budget parameter can also be defined by the central-limit theorem or Chebyshev inequality [109] [20].

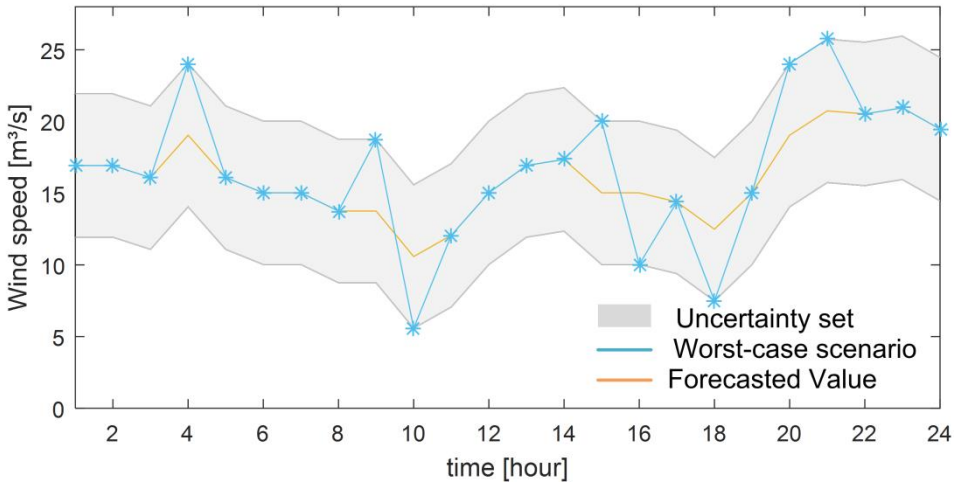

Figure 2.3 Example of a worst-case scenario for a wind farm.

It can be observed from Figure 2.2 and Figure 2.3 that the budget parameter (Bgt_{bus}) is used to adjust the conservatism of the system. Due to its simplicity and intuitiveness, this thesis uses a polyhedral uncertainty set based on a box set definition as presented in eq. (2.1) and an uncertainty budget based on eq. (2.4) (see Section 4.1.1).

Due to the challenge that is to capture the correlational structure of uncertain parameters, most of the existing literature considers static uncertainty sets where temporal and spatial correlations are not systematically represented [80], [110].

However, some important efforts have been undertaken to improve the uncertainty set definition. In [89], nonparametric correlations between nodal demands were accounted for. In [111], state-space representable uncertainty sets were considered. In [110], the idea of dynamic uncertainty sets is proposed to capture temporal and spatial correlations in wind speeds. In [112] is proposed a two-stage robust UC method that takes into account a polyhedral uncertain set that describe the spatiotemporal correlation of uncertainty prediction error. In [109] the temporal correlation of continuous uncertainties (wind power output and load) and discrete characteristics of the uncertain set N-k fault are also considered. In [80], it was developed a data-driven approach to construct dynamic uncertainty sets for capturing joint temporal and spatial correlations of multiple wind and solar farms, including a critical enhancement to reduce the dimensionality of these sets. In dynamic uncertainty sets the uncertainty budget can be related with the variable representing a random vector with uncorrelated components over time and space [80].

A more recent approach proposed to merge the ideas of Stochastic UC (SUC) with Robust UC (RUC), the resulting formulations are called Hybrid Unit Commitment (HUC) and aim at delivering low-cost solutions that can guarantee system reliability [107], [113]. In literature, the term HUC is ambiguous since various and essentially different hybrid formulations can be found. Zhao and Guan [105] present the so-called unified UC in which the expected operating costs from the SUC and the worst-case operating costs from the RUC are taken into consideration in the objective function by a user-defined weight factor. The main challenge resides in finding a proper weight term to balance the cost terms; the weight term should be determined heuristically in order to avoid sub-optimal results.

Distributionally robust UC formulations [84] have also been presented as a HUC. This approach can be divided into two broad subgroups: (i) robust optimization directly on the probability distributions [114] [94]: in which the probability distribution that models the uncertainties is chosen as a family of possible distributions, commonly referred to as ambiguity set, and in a second stage the expected cost under the worst-case distribution within the ambiguity set is minimized, and (ii) robust optimization using moment information [93] [115]: where the method is data-driven in the sense that no prior knowledge about the probability distribution of the uncertainties is needed and

the historical data is directly incorporated in the solution process. The more historical data is available, the less conservative the solution is.

Another option to reduce the over conservatism of RO is to, instead of using a single convex set for the uncertainty set, construct a group of smaller sets $D = D_1 \cup D_2 \cup D_3$ as described by [70]. This uncertainty set can be constructed based on the different possible scenarios and it could be much less conservative, while maintaining the same level of robustness. The so-called Robust Stochastic UC [116] [107] [117] approach, also presented as a HUC, relies on partitioning the uncertainty set into several subsets. By varying the number of partitions, the focus of this hybrid formulation can intuitively be shifted more towards reliability (Robust UC) or cost-efficiency (Stochastic UC), based upon preferences. However, practical applications with HUC approaches are restricted since they can be very complex and suffer from high computational costs.

Chapter 3

Deterministic Hydrothermal Unit Commitment Model

The UC problem is a short-term optimization model that seeks to translate the complexity associated with the dispatch of electrical power systems into computational language through inequalities that model operational restrictions. Due to the complexity and large-scale of national/regional power systems, the solution of this problem tends to be highly computational resource consuming. Pereira et al. [23] addresses the UC problem of an electricity system supported mainly by hydro, thermal and wind power plants as a binary mixed integer non-linear optimization model. In Pereira et al. [31] it is proposed a simplified approach for the thermal power units modelling, that uses quadratic penalty functions instead of on/off binary variables. Miranda et al, [19], [32], Oliveira et al. [118] and Soria et. Al [33] presented technical, social and environmental restrictions, for hydro and thermal power plants in Brazil, that should be considered when modeling Brazilian power system. These previous works inspired the formulation described in this chapter.

This Chapter describes the problem formulation of a deterministic Hydrothermal Unit Commitment (HTUC) model with renewable energy as a minimization cost problem. The proposed model is a mixed integer linear programming problem (MILP), programed in GAMS and solved with CPLEX, that aims to minimize the scheduling cost (i.e., costs for startup/shutdown) and the operating cost of both thermal and hydropower plants. This model is subjected to operational unit constraints and system-wide constraints. This model is named STORM (Short-Term power system OpeRation Model) in the following parts of this thesis. The definition of the sets, parameters and variables used in the developed formulation is listed from Table I-1 to Table I-3.

3.1. Objective function

The primary objective of STORM is to provide optimal utilization of the available resources in order to minimize the total operation cost over a scheduling period *T*, subject to hydro and thermal power constraints, as presented in eq.(3.1).

$$\text{Min} \sum_{t=1}^{T} \left(\sum_{j=1}^{J} ThermCost_{j,t} + \sum_{hd=1}^{Hd} HydroCost_{hd,t} + \sum_{hr=1}^{Hr} HRORCost_{hr,t} + \sum_{pen=1}^{Pen} PenCost_{pen,t} + \sum_{ncl=1}^{Ncl} NCLCost_{ncl,t} \right) \quad (3.1)$$

The variable $ThermCost_{j,t}$ encompasses the variable Operation and Maintenance (O&M) costs, fuel cost ($\vartheta_{j,t}$) and the costs for startup/shutdown for each thermal power plant as presented in. eq.(3.2).

$$ThermCost_{j,t} = CSd_j * UOff_{j,t} + ColdS_j * UOn_{j,t} + U_{j,t} * IndB_j + Pt_{j,t} * \left(IndA_j + CVOMt_j\right) \quad \forall t, \forall j \quad (3.2)$$

In practice, the fuel cost ($\vartheta_{j,t}$) is a quadratic function that variates with the operational load factor at a given time. However, to simplify the model, it was approximated as a linear curve presented in eq. (3.3) and it is already included in eq.(3.2).

$$\vartheta_{j,t} = U_{j,t} * IndB_j + Pt_{j,t} * IndA_j \quad \forall t, \forall j \quad (3.3)$$

The coefficient values of the fuel curve are shown in Appendix A; these coefficients are based on typical data of thermal power technologies. STORM considers five general thermal power technologies: i) Open cycle gas turbine; ii) Combined cycle gas turbine, iii) Coal/Biomass steam turbine, iv) Internal combustion generator and v) Nuclear power reactor. For the last one, this dispatch model does not consider the costs for startup/shutdown, under the premise that, due to the great inertia of this technology, it will take longer than a day to turn off/on. In other words, the nuclear power plants will be always online for the scheduling period (24 hours). The model also considers

"penalty" thermal generation plants to represent energy deficit and thus avoid infeasible cases; this generation plant is highly flexible and very expensive.

The operation cost of nuclear power plants ($NCLCost_{ncl,t}$) and penalty plants ($PenCost_{pen,t}$) is represented by an equivalent parameter for fuel and O&M costs as presented in eq. (3.4)- (3.5), respectively.

$$NCLCost_{ncl,t} = Pncl_{ncl,t} * COVF \quad \forall ncl, \forall t \tag{3.4}$$

$$PenCost_{pen,t} = GenPen_{pen,t} * CPen \quad \forall pen, \forall t \tag{3.5}$$

The hydropower operation cost (for units with reservoir, $HydroCost_{hd,t}$) is more complex to define. Hydrothermal power systems with significant hydropower generation units use long term operation models, such as Newave [119] to provide the operation planning of water resources that minimizes the total operation cost (future cost + immediate cost) over the simulated period. To achieve this objective, decisions about how much energy should be generated by hydroelectric and consequently by thermoelectric power plants in the long and medium term are made. In this context, the immediate cost refers to the decisions taken in the present (days or weeks) and the future cost for those to be adopted in the future (months or years). In predominantly hydroelectric systems, the immediate and future costs are time dependent; i.e. the future cost curve is a consequence of the decisions taken in the present. For example, an empty water reservoir (due to large amount of hydro energy generation) means that in the future it will be necessary to use significant thermal power energy to meet the demand and, therefore, the future cost will be high.

Consequently, HTUC problems tend to use a future cost curve to estimate a "cost" for the water stored in reservoirs. However, finding a future cost curve for a large hydrothermal power system with several water reservoirs can be challenging since it is usually described as a multi-dimensional curve [119]. Therefore, this thesis uses a simplified form to represent the water value for the HTUC model in which the parameter *Cwater* considers the productivity of each plant and electrical energy price, as shown in eq. (3.8). For the case study presented in Section 5.1, a sensibility analysis with different energy prices (PLD_{hd}) was made in order to better represent the value of water, considering Brazilian power dispatch characteristics. For hydropower plants in cascade, the accumulated productivity is considered. This gives higher water values for

the stored water in upstream reservoirs. The variable Operation and Management (O&M) cost for hydropower plants is also considered for both hydropower plants with reservoir (eq.(3.6)) and run-of-river power plants (eq. (3.7))

$$HydroCost_{hd,t} = -DeltaVol_{hd} * CWater_{hd} + Phd_{hd,t} * CVOMdEq \tag{3.6}$$

$$HRORCost_{hr,t} = TurbROR_{hr,t} * RoRCost_{hr} \tag{3.7}$$

$$CWater_{hd}\left[{}^{\$}/_{hm^3}\right] = \frac{1x10^6}{3600} * Produt_{hd}\left[\frac{MW}{m^3/s}\right] * PLD_{hd}\left[{}^{\$}/_{MWh}\right] \tag{3.8}$$

The final form of the objective function is presented in eq. (3.9).

$$\begin{aligned} \underset{\substack{U, Uon, Uoff, Pt,\\ TurbWat, TurbROR,\\ Pncl, GenPen}}{\text{Min}} \sum_{t=1}^{T}\Bigg(\sum_{j=1}^{J}\{&CSd_j * UOff_{j,t} + ColdS_j * UOn_{j,t} + U_{j,t} * IndB_j \\ &+ Pt_{j,t} * (IndA_j + CVOMt_j)\} \\ &+ \sum_{hd=1}^{Hd}\{-DeltaVol_{hd} * CWater_{hd} + Phd_{hd,t} * CVOMdEq\} \\ &+ \sum_{hr=1}^{Hr}\{TurbROR_{hr,t} * RoRCost_{hr}\} \\ &+ \sum_{pen=1}^{Pen} GenPen_{pen,t} * CPen + \sum_{ncl=1}^{Ncl} Pncl_{ncl,t} * COVF\Bigg) \end{aligned} \tag{3.9}$$

The variable $DeltaVol_{hd}$ used in eq (3.6), eq. (3.9) and defined in eq. (3.10) is the difference between the initial reservoir volume and the reservoir volume at the end of the simulation period. It can be understood as an approximate value of the turbined outflow.

$$DeltaVol_{hd} = Rsrv_{hd,T} - InitVal_{hd} \tag{3.10}$$

3.2. Hydrothermal UC problem constraints

The adopted set of constraints for the HTUC problem includes constraints derived from physical processes, demand requirements and capacity limitations. These constraints are inequalities that impose conditions to the model formulation.

For instance, thermal power plants at full power are able only to decrease power, as well as plants out of operation require a minimum time to reach the nominal power (operative ramp) and minimum time online once started up. On the other hand, the power plant technology and its operational costs need to be considered in UC problems, since it indicates in which power stage a specific power plant is more likely to be (based, mi-merit or peak). For hydropower plants, specific operational guidelines such as flood maintenance in rivers for environmental restrictions or for domestic use, reservoirs operational limits, outflow requirements for cascade operation and spillage effects are strict delimiters of their flexibility capacity. Renewable and variable energy may increase system operation costs since fluctuations in wind and sun energy-outputs need to be balanced by conventional power units, and in some cases energy curtailment is needed. Transmission systems capacity also imposes physical upper bounds in the system flexibility, therefore, power flows need to be calculated as accurate possible, to avoid over positive renewable energy integration scenarios.

3.2.1. Constraints for thermal power plants

The binary variables associated with the startup/shutdown status of the thermal power plants are defined in eq. (3.11) - (3.13). Equation (3.11) defines when the thermal power plant *j* is turn on, i.e. $UON_{j,t} = 1$ and eq. (3.12) when the power plant is turn off i.e. $UOff_{j,t} = 1$.

$$-U_{j,t-1} + U_{j,t} - UON_{j,t} \leq 0 \quad \forall t, \forall j \tag{3.11}$$

$$U_{j,t-1} - U_{j,t} - UOff_{j,t} \leq 0 \quad \forall t, \forall j \tag{3.12}$$

$$U_{j,t}\,, UOn_{j,t}\,, UOff_{j,t} \in \{0,1\} \text{ and } U_{j,-1} = 0 \quad \forall j \tag{3.13}$$

Minimum Up and Down time constraints enforce the system feasibility in terms of proper technical operation of units. Once a shutdown is verified, the thermal power plant (*j*) must remain off for a certain period (*DT*) (eq. (3.15)). The same logic applies if

a startup happens the power plant must remain online over a certain time (*UT*) (eq. (3.14)).

$$U_{j,t-1} - U_{j,t} + U_{j,t+utt} \leq 1 \; \forall t, \forall j; \;\; utt \in \{1, \dots, DT_j\} \tag{3.14}$$

$$-U_{j,t-1} + U_{j,t} - U_{j,t+utt} \leq 0 \;\; \forall t, \forall j; \;\; utt \in \{1, \dots, UT_j\} \tag{3.15}$$

Power capacity constraints ensure that power plants will not produce more than its install capacity ($Pcap_j$) for each hour of the scheduling period. In other words, the power output must be equal or less than its nominal value, eq. (3.16). A minimum generation value for a stable operation is imposed by eq. (3.17). This minimum value is defined according to the technical characteristics of each thermal power technology.

$$Pt_{j,t} \leq Pcap_j * U_{j,t} \; \forall t, \forall j \tag{3.16}$$

$$Pt_{j,t} \geq Pmin_j * U_{j,t} \;\; \forall t, \forall j \tag{3.17}$$

Start-up, shut-down and operation ramp constraints are also considered. The mathematical representation of the startup/operation ramp is presented in eq. (3.18) and the shutdown/ operation ramp constraint is shown in eq. (3.19).

Start up:

$$Pt_{j,t} - Pt_{j,t-1} \leq \left(2 - U_{j,t-1} - U_{j,t}\right) * SRamp_j + \left(1 + U_{j,t-1} - U_{j,t}\right) * Ramp_j \quad \forall j, \forall t \tag{3.18}$$

Shutdown:

$$Pt_{j,t-1} - Pt_{j,t} \leq \left(2 - U_{j,t-1} - U_{j,t}\right) * Pmin_j + \left(1 - U_{j,t-1} + U_{j,t}\right) * Ramp_j \quad \forall j, \forall t \tag{3.19}$$

For nuclear power plants, power capacity (eq.(3.20)), minimum generation value (eq. (3.21).) and up/down operation ramp (eq. (3.22) - (3.23)) constraints are considered.

$$Pncl_{ncl,t} \leq MaxNcl_{ncl} \quad \forall t, \forall ncl \tag{3.20}$$

$$Pncl_{ncl,t} \geq MinNcl_{ncl} \quad \forall t, \forall ncl \tag{3.21}$$

$$Pncl_{ncl,t} - Pncl_{ncl,t--1} \leq Rmp_{ncl} \quad \forall ncl, \forall t \tag{3.22}$$

$$Pncl_{ncl,t--1} - Pncl_{ncl,t} \leq Rmp_{ncl} \quad \forall ncl, \forall t \tag{3.23}$$

3.2.2. Hydro production function

The energy generated by a hydropower plant (hpg) depends on its turbinated outflow (q), its design characteristics (represented by both turbine (η_t) and generator (η_g) efficiency factors) and the net water head of its reservoir (h), as shown in eq. (3.24). The numerical factor $\zeta = 9.81x10^{-3}$ considers the gravity acceleration, water density and the unit conversion factor. The unit of hpg is MW.

$$hpg = \zeta \eta_t \eta_g q h \tag{3.24}$$

The reservoir net head is given by (3.25). The forebay level h_{up} depends on the reservoir volume (V_{hd}). The tailrace level h_{dw} is a function of the turbined outflow (Q_{hd}) of the whole hd plant and, depending on the geography and design of the hydropower plant, of the spillage (S_{hd}) as well. The term $h_{loss_{hd}}$ accounts for penstock head losses.

$$h_{hd} \ = h_{up}(V_{hd}) - h_{dw}(Q_{hd}, S_{hd}) - h_{loss_{hd}} \tag{3.25}$$

The expression in eq. (3.26) gives the power generation of a hydropower plant *hd* with xh units.

$$HPG_{hd} = \sum_{x=1}^{xh} hpg_x(q_x, V_{hd}, Q_{hd}, S_{hd}) \tag{3.26}$$

The daily variation of the forebay level has little effect on the energy production of hydropower plants with large dams. However, the tailrace level increases with the plant discharge; this causes a decrease in the net head and has a negative effect on the power plant generation. Consequently, the productivity of a hydropower plant MW/(m3/s)) decreases with the turbinated outflow, leading to a concave behavior. Even more, as presented by [24], there are complicating issues when modeling an equivalent production curve such as the forbidden zones [120], number of online units and the sequence in which the units are turned on/off. These difficulties can lead to a production

curve with non-convex regions and nonlinearities e.g. discontinuous derivatives at operational points where units are switched on.

In order to alleviate the computational burden, some studies have presented approximated models of hydro production functions for the dispatch problem. For instance, the nonlinearity is circumvented by assuming a constant net head resulting in a piecewise linear curve [121] or in a quadratic curve [40]. Nonetheless, this assumption is only adequate for hydropower plants in which their reservoir water levels vary across a narrow range. For head dependent reservoirs, the production curve can be approximate by a family of piecewise-linear [122], quadratic [123] or piecewise quadratic [124] functions. Binary variables are usually used to determine which linear or quadratic part is active. In [24] the production function is proposed as a four-dimensional piecewise linear model that considers head variation in a single multivariate linear function of turbinated outflow, storage, and spillage.

Other characteristics such as the turbine efficiency as a function of net head and turbinated outflow, the generator efficiency based on the generation output and the penstock head losses considering the turbinated outflow are also important in hydro UC problems [125] [126]. Yet, there are limitations for considering such restrictions in the unit commitment problem due to the computational burden involved with highly detailed hydropower modeling. Therefore, it becomes important to use a hydropower model that finds a balance between an accurate representation of water head variation and low computational times.

This thesis uses the 4-D piecewise linear model proposed by [24] for the hydro generation curve. This approach has the advantage of using a single function that considers the main elements that cause head variation in hydro plants: storage, turbinated outflow and spillage. The procedure first finds the hyperplanes that define the convex hull of the region below the Hydro Production Function (HPF) considering zero spillage, which lead to an initial 3-D piecewise linear approximation. Then the spillage effect is included using a secant approximation. For this approach the following assumptions were made:

- A constant turbine-generator efficiency
- Penstock losses are calculated as a percentage of the power output
- Forbidden zones are neglected

- The forebay level (h_{up}) is a fourth-degree polynomial function of the storage
- The tailrace level (h_{dw}) is a fourth-degree polynomial function of turbinated outflow and spillage.
- The productivity of each plant, defined as the water-power conversion rate per unit of head ((MW/(m^3/s))/m), is considered known.
- Storage, turbinated outflow, spillage and generation max/min limits are all known values.

The steps needed to reach the 4-D piecewise linear model for each hydro power generation plant include:

a) Definition of the Grid for the Approximation

To perform this first step a number of points, of the VxQ plane, are chosen. The size of the grid (number of points and their distribution) depends on the required precision for the model and the performance of the real plant production function. For each pair of points (V_{hd}, Q_{hd}), the power generation HPG_{hd} is calculated by the equation (3.27), considering $S = 0$. This provides a set of points $(\overline{V_{hd}}, \overline{Q_{hd}}, \overline{HPG_{hd}})$ in the 3-D space. The maximum turbinable outflow was defined as a curve dependent of the reservoir net head using the information provided by the software HydroExpert [127]. Figure 3.1 presents an example of the resulting grid for Boa Esperança hydropower plant using a 5x5 size grid.

$$\overline{HPG_{hd}} = product * \overline{Q_{hd}} * \overline{h_{hd}} \tag{3.27}$$

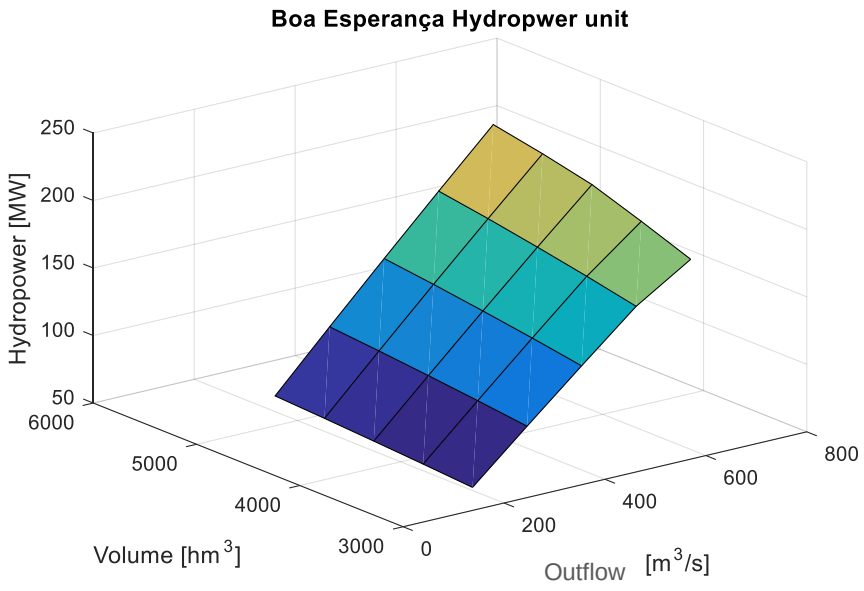

Figure 3.1 A 5x5 size grid of the $VxQxHPG$ plane.

b) Determination of the coefficients for the HPF model without considering spillage

Once the set of points $(\overline{V_{hd}}, \overline{Q_{hd}}, \overline{HPG_{hd}})$ is defined, the 3-D convex hull (convex envelope) of the grid can be calculated. To do this, this thesis used the MATLAB function *Convhull.* The outputs of this function are the vertices of the triangular planes that make up the convex hull. Next, it was established, for each plane $\tilde{P}$ with vertices (p_1, p_2, p_3), the equation that describes it, which has the form of $HG = \gamma_o + \gamma_Q Q + \gamma_V V$. The shape of the convexified region below Boa Esperança hydropower production function (HPF) curve is illustrated in Figure 3.2. The equations of the K_{hd} hyperplanes compose the initial approximated HPF model, given by eq. (3.28).

$$HPF_{hd}{}^{pln'}(V_{hd}, Q_{hd}) = \gamma_o^{hd,pln} + \gamma_V^{hd,pln} V_{hd} + \gamma_Q^{hd,pln} Q_{hd} \quad pln = 1, \dots, k \qquad (3.28)$$

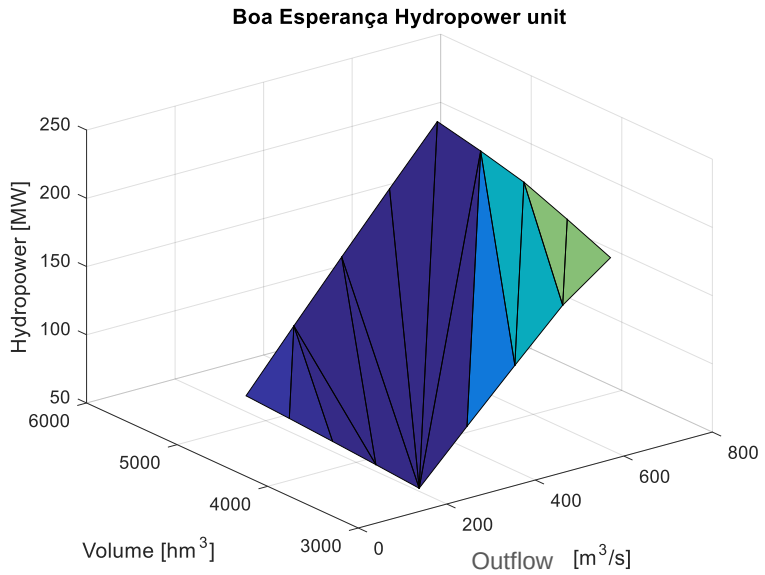

Figure 3.2 The convexified region below a hydropower production function curve.

c) Adding the spillage effect to the HPF

The shape of the production function for hydropower plants tends to be, for a fixed pair (V_{hd}, Q_{hd}), non-convex in the spillage dimension [24]. This behavior indicates that the piecewise linear approximation made in the volume and inflow dimensions would not be appropriate for the spillage dimension. Instead, a secant approximation is used to calculate the spillage coefficient. This secant approximation minimizes the average square error between the HPG (eq.(3.27)) and the HPF (eq. (3.28)) for M points between $(V_{hd}^{\dot{pln}}, Q_{hd}^{\dot{pln}}, 0)$ and $(V_{hd}^{\dot{pln}}, Q_{hd}^{\dot{pln}}, S_{ref})$; where $V_{hd}^{\dot{pln}}$, $Q_{hd}^{\dot{pln}}$ are the centroid's

coordinates of each plane (*pln*). The spillage coefficient $\gamma_S^{hd,pln}$ is calculated for each plane as shown by eq. (3.29). The value S_{ref}^{hd} is based on the plant spillage historical data, and it should not be too high, as more accurate representation is preferred for small values of spillage.

$$\gamma_S^{hd,pln} \in \arg\min_{\gamma} \left[M \sum_{m=1}^{M} \left(HPG_{hd}\left((\dot{V_{hd}}, \dot{Q_{hd}}, S_m\right) - \left(HPF_{hd}^{pln'}\left((\dot{V_{hd}}, \dot{Q_{hd}}\right) + \gamma S_m \right) \right)^2 \right] \tag{3.29}$$

with

$$S_m = \left(\frac{m}{M}\right) S_{ref}^{hd} \tag{3.30}$$

The final form of the approximated HPF is presented in eq. (3.31) and an example of evaluation of this 4-D piece-wise function over the volume and inflow axes, considering the case of the Boa Esperança power generation plant is illustrated in Figure 3.3.

$$HPF_{hd}^{pln}(V_{hd}, Q_{hd}, S_{hd}) = \gamma_o^{hd,pln} + \gamma_V^{hd,pln} V_{hd} + \gamma_Q^{hd,pln} Q_{hd} + \gamma_S^{hd,pln} S_{hd} \tag{3.31}$$

$$pln = 1, \dots, K_{hd}$$

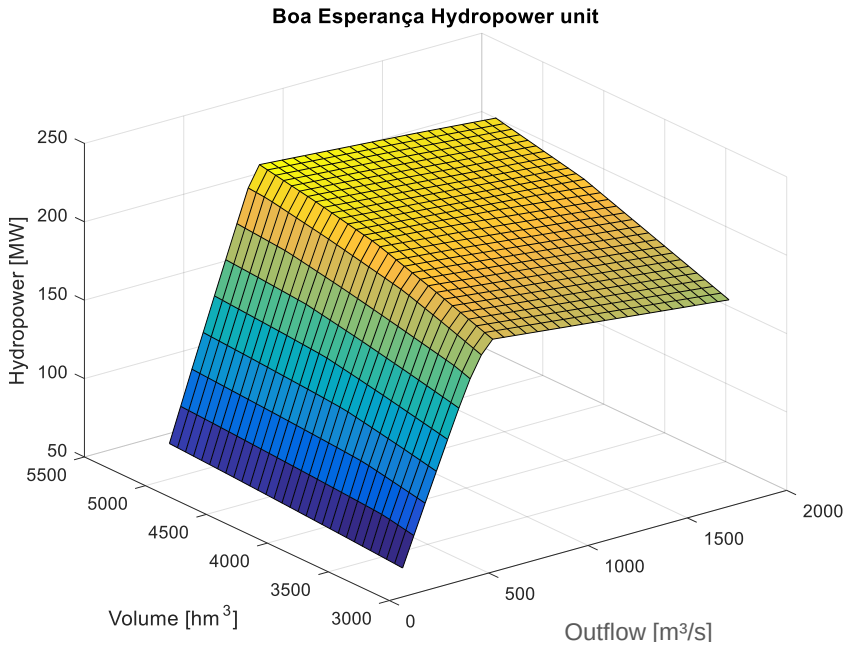

Figure 3.3 - HPF for a hydropower plant with reservoir.

All hydropower plants have a reservoir, even the ones called run-of-river plants have a small reservoir, and therefore this analysis was applied for all hydro power plants. However, since the reservoir volume does not impact significantly the production function of run-of-river plants, the representation of these plants can be simplified by establishing the volume as a fixed value. Therefore, for the HPF definition of run-of-river plants it was first considered that the reservoir volume could vary within [$MaxLevel_{hr}$(%), $Minlevel_{hr}$(%)] of the nominal value and once the coefficients of the HPF were defined using the methodology here described, a "cut" was made at $MB = (MaxLevel_{hr} + Minlevel_{hr})/2$ (%) of the nominal reservoir volume (V_{hr}^{nom}). The HPF for run-of-river plants is presented in eq. (3.32). It depends only of the turbinated outflow and, in some generation plants, according to the EPE register [128], of the spillage.

$$HPF_{hr}^{plnR}(Q_{hr}, S_{hr}) = \gamma_o^{hr,plnR} + MB * V_{hr}^{nom} * \gamma_V^{hr,plnR} + \gamma_Q^{hr,plnR} Q_{hr} + \gamma_S^{hr,plnR} S_{hr} \quad (3.32)$$

$$plnR = 1, \dots, K_{hr}$$

The mathematical formulation of the HPF model to be used in hydrothermal UC problem for reservoir and run-of-river plants is shown in eq.(3.33) and eq. (3.34), respectively. The coefficient values of the production function for each hydropower plant considered in the case studies of this thesis are shown in appendix D.

$$HPF_{hd}^{t}(V_{hd}, Q_{hd}, S_{hd}) \leq \gamma_o^{hd,pln} + \gamma_V^{hd,pln} * V_{hd}^{t-1} + \gamma_Q^{hd,pln} Q_{hd}^{t} + \gamma_S^{hd,pln} S_{hd}^{t} \quad \forall t, \forall hd, \forall pln \tag{3.33}$$

$$HPF_{hr}^{t}(Q_{hr}, S_{hr}) \leq \gamma_o^{hr,plnR} + \gamma_V^{hr,plnR} * MB * V_{hr}^{nom} + \gamma_Q^{hr,plnR} Q_{hr}^{t} + \gamma_S^{hr,plnR} S_{hr}^{t} \quad \forall t, \forall hr, \forall plnR \tag{3.34}$$

3.2.3. Constraints for hydroelectric power plants

Hydroelectric power plants are divided in two main categories. Hydro power plants with regularization capacity, here called as units with reservoir (Hydro-Res), and Hydro power plants without regularization capacity, here called as run-of-river units (Hydro – ROR). The hydropower production functions for Hydro-Res (*hd* plants) and for Hydro – ROR (*hr* plants) are considered and presented in equations (3.35) and (3.36), respectively. The methodology to define the production function coefficients is presented in Section 3.2.2

$$Phd_{hd,t} \leq \left[\gamma_o^{hd,pln} + TurbWat_{hd,t} * \gamma_{\mathrm{Q}}^{\mathrm{hd,pln}} + Rsrv_{hd,t-1} * \gamma_{\mathrm{V}}^{\mathrm{hd,pln}} + spil_{hd,t} * \gamma_S^{hd,pln}\right] \quad \forall t, \forall hd, \forall pln \tag{3.35}$$

$$Pror_{hr,t} \leq \gamma_o^{hr,plnR} + TurbROR_{hr,t} * \gamma_Q^{hr,pnlR} + SpilROR_{hr,t} * \gamma_S^{hr,pnlR} \quad \forall t, \forall hr, \forall plnR \tag{3.36}$$

Power capacity constraints were also considered for Hydro-Res (eq.(3.37)) and for Hydro-ROR (eq.(3.38)). Additionally, capacity constraints were also imposed to hydraulic turbines through eq. (3.41) - (3.40), which represent the maximum allowed turbinated outflow for *hd* and *hr* power plants, respectively.

$$Phd_{hd,t} \leq PhdMax_{hd} * Vh_{hd,t} \quad \forall t, \forall hd \tag{3.37}$$

$$Pror_{hr,t} \leq PmaxROR_{hr} \quad \forall t, \forall hr \tag{3.38}$$

$$TurbWat_{hd,t} \leq Qmax_{hd} \quad \forall t, \forall hd \tag{3.39}$$

$$TurbROR_{hr,t} \leq QmaxROR_{hr} \quad \forall t, \forall hr \tag{3.40}$$

Restrictions of minimum operational power level and minimum outflow (which is met by turbinated outflow or by spillage) are considered using eq. (3.41) and eq. (3.42). Minimum outflow restrictions are relevant to ensure navigability and water use in urban areas and agricultural projects, and in the case of generation in cascade mode it can play a central role in flow regulation of generation plants downstream [19].

$$Phd_{hd,t} \geq PhdMin_{hd} * Vh_{hd,t} \quad \forall t, \forall hd \tag{3.41}$$

$$TurbWat_{hd,t} + Spil_{hd,t} \geq Qmin_{hd} \quad \forall t, \forall hd \tag{3.42}$$

Upper bounds for spillage in hydro-Res (*hd*) plants are imposed as a security measure (eq. (3.43)).

$$Spil_{hd,t} \leq SpilMax_{hd} \quad \forall t, \forall hd \tag{3.43}$$

For hydro-ROR (*hr*) plants the spillage restriction is defined by eq. (3.44)

$$SpillROR_{hr,t} = VazaoInEq_{hr,t} - TurbROR_{hr,t} \quad \forall t, \forall hr \tag{3.44}$$

Upper and lower bounds for volume limits in water reservoir are also considered through eq. (3.45) - (3.46). The initial volume value of the reservoir is known data as indicated by eq. (3.47).

$$Rsrv_{hd,t} \leq MaxLevel_{hd} \quad \forall t, \forall hd \tag{3.45}$$

$$Rsrv_{hd,t} \geq MinLevel_{hd} \quad \forall t, \forall hd \tag{3.46}$$

$$Rsrv_{hd,-1} = InitVal_{hd} \tag{3.47}$$

The coming inflow for each hydropower plant (*hT* is the set that considers *hd* and *hr* plants) is calculated in eq (3.48). This formulation considers the cascade effect, i.e. the inflow of plant *hT* considers its incremental flow plus spillage and/or turbinated outflow from the upstream hydropower plants considering the travel time of each power plant.

$$\begin{aligned} VazaoInEq_{hT,t} &= InflowhT_{hT,t} \\ &+ \sum_{\forall hd \in TblCasc(hT,hd)} \left[TurbWat_{hd,t-tviag(hT)}\right. \\ &\left. + Spil_{hd,t-tviag(hT)}\right] \\ &+ \sum_{\forall hr \in TblCasc(hT,hr)} \left[TurbROR_{hr,t-tviag(hT)}\right. \\ &\left. + SpilROR_{hr,t-tviag(hT)}\right] \quad \forall t, \forall hT \end{aligned} \tag{3.48}$$

The reservoir water balance equation is presented in equation (3.49). Since the simulation period is a day and to simplify the model the water balance does not consider evaporation rate or inflow withdrawal due to other uses different from electricity generation, it considers the total coming inflow, calculated in eq (3.48). The scalar CF is a conversion factor from m^3/s to hm^3/h equal to 0.0036.

$$\begin{aligned} Rsrv_{hd,t} &= Rsrv_{hd,t-1} + CF \\ &* \left[VazaoInEq_{hd,t} - TurbWat_{hd,t} - Spil_{hd,t}\right] \quad \forall t, \forall hd \end{aligned} \tag{3.49}$$

3.2.4. Transmission system – DC power flow for UC problems

A power grid can be described by its incidence matrix $\bar{A}$ and its admittance matrix $\bar{Y}$**.** The incidence matrix is a *LinesxBuses* size matrix that describes the topology of the grid; i.e., which lines are connected to which buses; $a_{line,bus} = 1$ if line *line* starts at bus *bus*, $a_{line,bus} = -1$ if line *line* end at bus *bus* and $a_{line,bus} = 0$ if line *line* is not incident to bus *bus*. The incidence matrix relates the bus parameters (injected current I_{bus} and voltage V_{bus} at bus *bus*) with the line parameters (current I_{line} flowing through transmission line *line* and voltage drop V_{line} over transmission line *line).*

The admittance matrix $\bar{Y}$ is a *busxbus* size matrix, that relates the voltages V_{bus} with the injected nodal current I_{bus}. The admittance matrix is defined by eq. (3.50), where $\overline{Y}_d$ is the LxL-diagonal matrix with the line admittances on the diagonal (i.e. the primitive admittance matrix).

$$\bar{Y} = \overline{A^T} \cdot \overline{Y_d} \cdot \bar{A} \tag{3.50}$$

The most common calculation of static grid flows is the AC power flow. However, an AC power flow is computationally heavy within the scope of UC models. The DC power flow is a linearized version of the AC power flow with acceptable use of computational resources that can be used in UC models. The methodology used in this thesis to model the transmission system is based on [130],[131],[132].

DC power flow only considers active power flow, assumes perfect voltage support and reactive power management, and neglects transmission losses. In summary, the DC power flow is based on three assumptions:

1. Line resistances are negligible compared to line reactance ($R_{line} \ll X_{line}$). This assumption implies that grid losses are neglected, and line parameters are simplified.
2. The voltage amplitude is equal for all buses (in per unit values) $|V_{bus}| \approx 1\ p.u$
3. Voltage angle differences between neighboring buses are small. This assumption results in a linearization of the sine and cosine terms in the AC power flow equations.

The active power flow through a lossless transmission line and with the DC power flow assumptions is given by eq.(3.51). Where $\overline{B_d}$ is the matrix line suceptances ($\overline{Y}_d$ without any conductance term) and $\overline{\delta_{bus}}$ is the matrix voltage angle of bus *bus*.

$$\overline{P_L} = \overline{B_d} \cdot \bar{A} \cdot \overline{\delta_{bus}} \tag{3.51}$$

The nodal active power balance with the DC power flow equation is given by eq. (3.52):

$$\begin{aligned} P_{bus} &= \sum_{Q} B_{line}(\delta_{bus} - \delta_q) \\ \overline{P_{bus}} &= \overline{A^T} \cdot \overline{B_d} \cdot \bar{A} \cdot \overline{\delta_{bus}} \end{aligned} \tag{3.52}$$

The positive direction of the active power flow P_{line} is from node *bus* to node *q* and B_{line} refers to the susceptance of line *line* between bus *bus* and bus *q*. Substituting the nodal voltage angle δ_{bus} from (3.52) in (3.51) gives the DC power flow equations, showed by eq (3.53).

$$\overline{P_{line}} = \left((\overline{B_d} \cdot \bar{A}) \cdot \left(\overline{A^T} \cdot \overline{B_d} \cdot \bar{A} \right)^{-1} \right) \cdot \overline{P_{bus}} = PTDF^{LxN} * \overline{P_{bus}} \tag{3.53}$$

The Power Transfer Distribution Factor ($PTDF^{LxB}$) describes the linear relationship between the power injections in the grid (P_{bus}) and the active power flows through the transmission lines (P_{line}). An element of the $PTDF^{LxB}$ matrix gives the power flow through transmission line *line* caused by the injection of 1 unit of active power at node *bus* and withdrawal at node *q*.

3.2.5. Constraints for the transmission system

Based on eq. (3.53) the DC power flow and transmission capacity constraints are defined in eqs. (3.54) and (3.55). The sum of all nodal injection using the $PTDF^{LxB}$ factor guaranties that the power flow through line *l* will not be higher than its capacity, for both directions of the power flow, positive and negative.

$$\begin{aligned} \sum_{bus=1}^{B} PTDF_{line,bus} \Bigg\{ & \sum_{j \in \Lambda_{jb}} Pt_{j,t} + \sum_{ncl \in \Lambda_{ncl-b}} Pncl_{ncl,t} + PwindEq_{bus,t} \\ & + Psolar_{bus,t} + \sum_{pen \in \Lambda_{pen-b}} GenPen_{pen,t} \\ & + \sum_{hr \in \Lambda_{hr-b}} Pror_{hr,t} + \sum_{hd \in \Lambda_{hd-b}} Phd_{hd,t} + Ppch_{bus,t} \\ & + Pstm_{bus,t} - Demand_{bus,t} \Bigg\} \\ & \leq CapTx_{line,"lim+"} \quad \forall t, \forall line \end{aligned} \tag{3.54}$$

$$\sum_{bus=1}^{B} PTDF_{line,bus}\left\{\sum_{j\in\Lambda_{jb}} Pt_{j,t} + \sum_{ncl\in\Lambda_{ncl-b}} Pncl_{ncl,t} + PwindEq_{bus,t} + Psolar_{bus,t} + \sum_{pen\in\Lambda_{pen-b}} GenPen_{pen,t} + \sum_{hr\in\Lambda_{hr-b}} Pror_{hr,t} + \sum_{hd\in\Lambda_{hd-b}} Phd_{hd,t} + Ppch_{bus,t} + Pstm_{bus,t} - Demand_{bus,t}\right\} \geq -CapTx_{line,"lim-"} \quad \forall t, \forall line \tag{3.55}$$

To make sure that the DC power flow has one unique solution the sum of all nodal injections must be equal zero as presented in eq.(3.56), also known as the demand balance constraint.

$$\sum_{j=1}^{J} Pt_{j,t} + \sum_{ncl=1}^{Ncl} Pncl_{ncl,t} + \sum_{bus=1}^{B}\{PwindEq_{bus,t} + Psolar_{bus,t} + Ppch_{bus,t} + Pstm_{bus,t}\} + \sum_{pen=1}^{Pen} GenPen_{pen,t} + \sum_{hr=1}^{Hr} Pror_{hr,t} + \sum_{hd=1}^{Hd} Phd_{hd,t} \geq \sum_{bus=1}^{B} Demand_{bus,t} \quad \forall t \tag{3.56}$$

The spinning reserve was modeled through the eq. (3.57). As presented, this constraint imposes that the summation of the capacity of the thermal and hydro with reservoir units that are in ON state at a given time (generation units which binary variables $U_{j,t}$ or $Vh_{hd,t}$ are equal to 1) needs to be higher than the liquid demand[8] by the

[8] In the context of spinning reserve analysis, the liquid demand is the resulting demand after subtracting nuclear, run-of-river hydro, wind and non-dispatchable generation at a given time.

percentage established by the $spin$ variable. In other words, this restriction can lead to a solution with more dispatched units that for the case without spinning reserve. However, this measure can give protection against to power variations in the system, as shown in Section 5.2.

$$\sum_{j=1}^{J}\left[Pcap_j * U_{j,t}\right] + \sum_{hd=1}^{Hd}\left[PhdMax_{hd} * Vh_{hd,t}\right] + \sum_{pen=1}^{Pen} GenPen_{pen,t} \geq (1+spin) * \left(\sum_{bus=1}^{B} Demand_{bus,t} - \sum_{ncl=1}^{NCL} Pncl_{ncl,t} - \sum_{hr=1}^{Hr} Pror_{hr,t} - \sum_{bus=1}^{B} \left(PwindEq_{bus,t} + Psolar_{bus,t} + Ppch_{bus,t} + Pstm_{bus,t}\right)\right) \forall t \quad (3.57)$$

3.2.6. Wind power generation constraints

Wind energy is a priority in the developed model because, unlike thermal and hydropower plants which have variable cost defined according to their fuel cost or water value, its variable generation cost is null. However, in this model the generation of wind energy is not treated as an uncontrollable generation that must be injected into the grid. Instead, it is individually modeled at its connection point, being subject to curtailment by the UC model if required to reach optimality. This means that wind generation is a priority source to meet the demand, but not a mandatory source to be directly subtracted from the load. The flexibility provided by modeling wind generation as a priority source subject to curtailment can lead to a reduction in operating costs [130]. This restriction is represented in eq.(3.60).

$$PwindFcast_{busWind,t} = \sum_{wn \in \Lambda_{wn-busW}}^{WN} WindCao_{wn} * PwindPU_{wn,t} \quad \forall t, \forall busWind \quad (3.58)$$

$$PwindTemp_{busWind,t} = PwindFcast_{busWind,t} \quad \forall t, \forall busWind \tag{3.59}$$

$$PwindEq_{busWind,t} \leq PwindTemp_{busWind,t} \quad \forall t, \forall busWind \tag{3.60}$$

3.2.7. Non dispatchable power plants

The solar PV generation and the generation from small thermal and small hydro power plants are considered Non Individually Simulated Plants (NISP) [137]. These plants are represented as hourly energy blocks to be withdrawn from the bus load at which each NISP is connected. The NISP generation is defined by its installed power capacity multiplied by the availability of the resource.

a. Solar PV Generation

The solar PV data are provided as a normalized hourly profile for each hotspot, the total generation is obtained by multiplying the installed capacity of each hotspot by the hourly profile. The total solar PV generation by bus is calculated as a sum of all equivalent solar hotspots generation in each bus as presented in eq. (3.61).

$$PsolarFcast_{bus,t} = \sum_{sr \in \Lambda_{sr-b}}^{SR} PVCap_{sr} * PsolarPU_{sr,t} \quad \forall t, \forall bus \tag{3.61}$$

b. Small generation plants

In this group there are two types of generation plants: Small thermal power plants (*stm*) composed mainly by biomass thermal power plants and small hydro power plants (*pch*) (power plants with nominal power below 30MW). The generation of each plant in this category is obtained by multiplying its installed capacity by the seasonal generation profile. The small power plants' generation by bus is calculated as the sum of the power generation of the small plants connected to each bus as presented in (3.62).

$$Psu_{bus,t} = \sum_{sm \in \Lambda_{sm-b}}^{SM} SmUnCap_{sm} * PsmPU_{sm,t} \quad su: \{stm, pch\}, \forall t, \forall bus \tag{3.62}$$

Chapter 4

Robust Unit Commitment Model

In this section, a two-stage robust UC optimization problem with wind power uncertainty is presented. To do so, the definition of [20] "*A UC decision is called robust, if when the real wind power deviates from the forecast value and remains in a certain region, there will always be a corrective action that recovers all the operating constraints without changing the given UC decision*" is considered. In the first stage of the optimization problem, UC decisions are defined with the objective of minimizing the system-wide power generation cost; i.e. unit commitment cost and dispatch cost under the worst-case scenario. The worst-case scenario is defined in the second stage problem.

4.1. Mathematical Formulation for the Adaptive Robust Approach

The mathematical formulation of a two-stage adaptative robust optimization model suited to deal with uncertain events, here called as R-STORM, was based on the model proposed by Jiang et al. [34], [35]. However, in addition with the restrictions considered in that model, the formulation of R-STORM also takes into account the detailed characteristics of hydropower units with reservoir and allows wind power curtailment. This last feature allows a more cost-efficient system operation, as presented by [152], and reduces from three to one the number of blocks of bilinear terms of the dual objective function. The solution methodology considers Benders decomposition [62]. The uncertainty set was defined as a box set [70] with uncertainty budgets, as proposed by [68]. Due to the fact that the worst-case scenarios were found on the extreme level of the resultant polyhedral uncertainty set, the uncertainty budget was defined as a cardinality budget [36], [35].

4.1.1. Uncertainty set definition

This thesis uses a static uncertainty set to capture the randomness nature of wind energy. The uncertainty set used in this thesis is defined from a box type uncertainty set (as defined by eq. (2.1)) which is transformed into a polyhedral set by considering temporal uncertainty budget (as described in Section 2.2.2), in order to avoid over-conservative UC decisions. Furthermore, since the probability that the worst-cases scenarios are located at the vertex of the polyhedral uncertainty set is high under the model of data uncertainty [153], [68], the implemented uncertainty budget is a cardinality budget (presented in eq. (2.4)). This approach restricts the number of time periods in which the wind power generation deviates from its forecasted value at power system bus *bus*.

To define the upper and lower levels of the initial uncertainty set (Box type) two statistical analysis were performed. The analyzes considers the hotspots presented in Table II-10. In the first one, the homoscedasticity of the wind speed data was tested using the F-test. Results in Table 4-1 present, for each hotspot, the cases were the null hypothesis was rejected, i.e. the months with different wind speed variances. It can be deduced that for all hotspots considered the wind speed showed homoscedasticity within the first and the second semester. Therefore, it could be possible to use two variance values (for each hotspot) to describe the wind speed behavior through the year. It is highlighted, nonetheless, that the hourly data available are from the year 2015. Therefore, this analysis does not consider the possibility of variance variations over a longer time frame.

Table 4-1. F-test Results for Wind energy hotspots.

Hotspot Name	Months with different variance	Hotspot Name	Months with different variance
HS-1-Parnaíba	6-9	HS-16-São Paulo -Congonhas	6-9
	6-10		6-11
	6-11		6-12
	6-12	HS-17-Chapecó	6-9
HS-13-Diamantina	6-9	HS-21-Torres	4-9
	6-10		6-9

HS-14-Paranaíba	6-9	HS-24-Pelotas	6-9
	6-10		6-12
	6-11	HS-25-Santa Vitoria do Palmar	6-9
	6-12		6-12

In the second statistical analysis, the use of quantiles was analyzed as an alternative to establish the variation range for wind speed and wind power output. Figure 4.1 and Figure 4.2 present an illustrative example using real data in which the interval for the wind power output is defined using: i) the 5^{th} -quantile (Q(0.05)) and 95^{th} - quantile (Q(0.95)) and ii) ± one standard deviation. It was chosen to work with quantiles and with wind power output data. Thus, the upper and lower bounds of the variation modeled by the uncertainty set are presented in eq. (4.1) and eq.(4.2), respectively.

$$\begin{aligned} PwindUP_{busWind,t} \\ &= PwindCap_{busWind} * Q(0.95) \\ &- PwindFcast_{busWind,t} \ \forall t, \forall busWind \end{aligned} \tag{4.1}$$

$$\begin{aligned} PwindDW_{busWind,t} \\ &= -PwindCap_{busWind} * Q(0.05) \\ &+ PwindFcast_{busWind,t} \ \forall t, \forall busWind \end{aligned} \tag{4.2}$$

Therefore, the model of data uncertainty considers the following possible values for the uncertain parameter i.e. wind power generation of each *busWind* at each time:

$$\begin{Bmatrix} PwindFcast_{busWind,t} - PwindDW_{busWind,t}; \\ PwindFcast_{busWind,t}; \\ PwindFcast_{busWind,t} + PwindUP_{busWind,t} \end{Bmatrix} \tag{4.3}$$

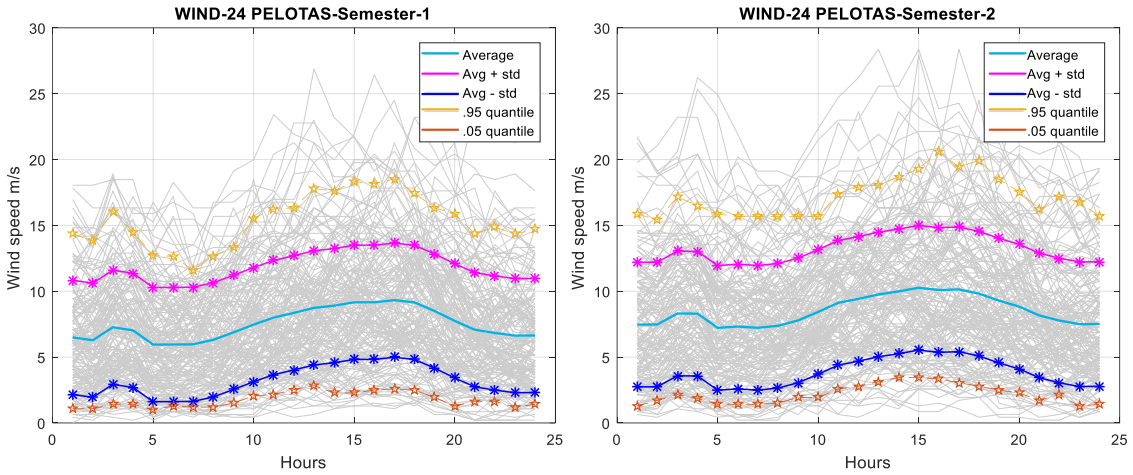

Figure 4.1 Statistical data for wind speed of Hotspot H24-Pelotas.

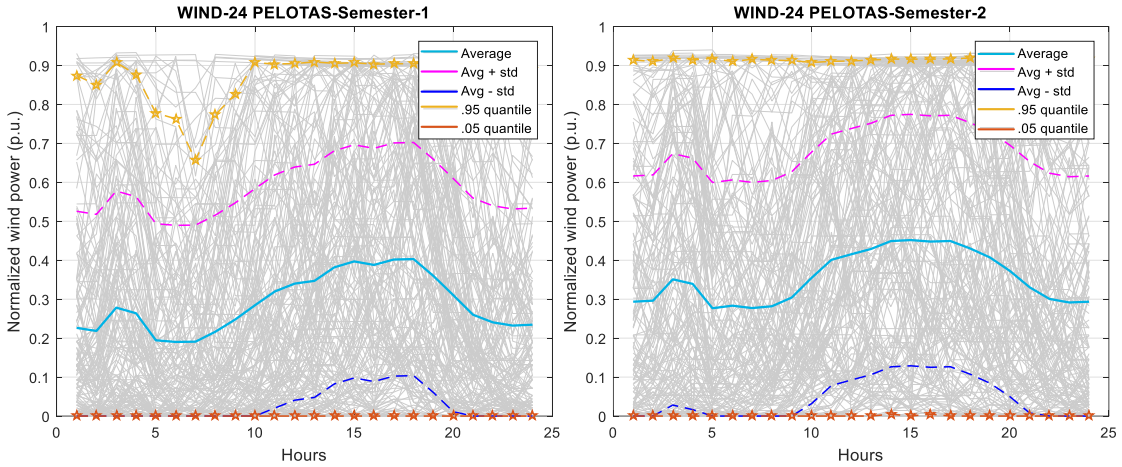

Figure 4.2 Statistical data for wind power of Hotspot H24-Pelotas.

It is important to highlight that the numerical definition of upper and lower level done in this thesis was made considering the hourly wind speed variability due to data availability. It could be interesting and, perhaps less conservative, to define the uncertainty set using wind power prediction error. Nonetheless, the upper and lower bound definition is an exogenous data of the R-STORM and can be adjusted based on the user requirements and available data.

From de definitions above, a cardinality uncertainty budget ($Bgt_{busWind}$) is used to adjust the level of conservatism [35], as stated by (4.4) and (4.5).

$$\sum_{t=1}^{T} Zpos_{busWind,t} + Zneg_{busWind,t} \leq Bgt_{busWind} \; \forall busWind \tag{4.4}$$

$$PwindTemp_{busWind,t} = PwindFcast_{busWind,t} + Zpos_{busWind,t} * PwindUP_{busWind,t} - Zneg_{busWind,t} * PwindDW_{busWind,t} \quad \forall t, \forall busWind \tag{4.5}$$

In other words, if $Bgt_{busWind} = 0$, then $PwindTemp_{busWind,t}$ will be equal to be forecasted value assuming that small deviations can be balanced by the online conventional generation and, therefore, this is the less conservative case; if $1 \leq Bgt_{busWind} \leq T$, the model will allow $PwindTemp_{busWind,t}$ to highly deviate from the forecasted value, within the uncertainty set, for $Bgt_{busWind}$ or less periods. In this sense, the case with $Bgt_{busWind} =$ T is the most conservative. The uncertainty budget presented in eq.(4.4) can be defined for each bus with wind generation. The binary variables $Zpos$ and $Zneg$ indicate when the wind power in bus $buswind$ and hour t deviates to the upper or lower level of the uncertainty set.

Considering the uncertainty set defined by eq. (4.4)- (4.5) the definition of wind power for the Robust UC is presented in eq. (4.5). As mentioned in 3.2.6, wind energy is subject to curtailment by the UC model, as shown by eq. (4.6).

$$PwindEq_{busWind,t} \leq PwindTemp_{busWind,t} \quad \forall t, \forall busWind \tag{4.6}$$

4.1.2. Objective Function and constrains

The objective function of the Robust UC model is presented in eq. (4.7).

$$\begin{aligned}
&\underset{U}{\text{Min}} \sum_{t=1}^{T}\sum_{j=1}^{J}\left\{CSd_j * UOff_{j,t} + ColdS_j * UOn_{j,t} + U_{j,t} * IndB_j\right\} \\
&\quad + \underset{\text{PwindEq} \in W}{\text{Max}} \; \underset{\text{Pt, TurbWat, TurbROR, Pncl, GenPen}}{\text{Min}} \sum_{t=1}^{T}\left\{\sum_{j=1}^{J} Pt_{j,t} \right. \\
&\quad * \left(IndA_j + CVOMt_j\right) \\
&\quad + \sum_{hd=1}^{Hd}\left\{-DeltaVol_{hd} * CWater_{hd} + Phd_{hd,t} * CVOMdEq\right\} \\
&\quad + \sum_{hr=1}^{Hr}\left\{TurbROR_{hr,t} * RoRCost_{hr}\right\} \\
&\quad \left. + \sum_{pen=1}^{Pen} GenPen_{pen,t} * CPen + \sum_{ncl=1}^{Ncl} Pncl_{ncl,t} * COVF\right\}
\end{aligned} \tag{4.7}$$

The robust UC model considers most of the restrictions of STORM model, presented in Section 3.2. However, in order to simplify the model, start up and shut down ramps are not considered for thermal power plants, only online ramps; i.e. ramp constraints (3.18) - (3.19) are replaced by eqs. (4.8) - (4.9). Nonetheless, it is important to highlight that for the Monte Carlo sampling analysis presented in Section 5.2 the deterministic equivalent model also only considers online ramps.

$$Pt_{j,t} - Pt_{j,t-1} \leq Ramp_j \quad \forall j, \forall t \tag{4.8}$$

$$Pt_{j,t-1} - Pt_{j,t} \leq Ramp_j \quad \forall j, \forall t \tag{4.9}$$

The two-stage robust UC formulation is divided in two sub-problems: the master and the slave problem. The separation scheme is embedded in the Benders' decomposition framework. The Robust UC master problem is defined as presented in eq. (4.10), the variable Θ and the Benders cut are defined in Section 4.2.

$$\begin{aligned}
&\underset{U, UOn, UOff}{\text{Min}} \sum_{t=1}^{T}\sum_{j=1}^{J}\left\{CSd_j * UOff_{j,t} + ColdS_j * UOn_{j,t} + U_{j,t} * IndB_j\right\} \\
&\quad + \Theta
\end{aligned} \tag{4.10}$$

s.t:

- Turn on eq. (3.11)
- Turn off eq. (3.12)
- Min time off eq. (3.14)
- Min time on eq. (3.15)
- Binary variables definition eq. (3.13)
- Benders' cuts

The slave problem is defined by the objection function in eq. (4.11) and subject to constraints in $\boldsymbol{X}(PwindEq)$, where π_x are the dual variables of the slave problem restrictions. In the slave problem formulation, the unit commitment decisions (output of the master problem) are considered constants or fixed binary parameters, for each Benders algorithm iteration.

$$\begin{aligned}\underset{\text{PwindEq} \in \text{W}}{\text{Max}} \; \underset{\substack{\text{Pt, TurbWat, TurbROR,}\\ \text{Pncl, GenPen}}}{\text{Min}} \; & \sum_{t=1}^{T}\left\{\sum_{j=1}^{J} Pt_{j,t} * \left(IndA_j + CVOMt_j\right)\right. \\ & + \sum_{hd=1}^{Hd}\left\{-DeltaVol_{hd} * CWater_{hd} + Phd_{hd,t} * CVOMdEq\right\} \\ & + \sum_{hr=1}^{Hr}\left\{TurbROR_{hr,t} * RoRCost_{hr}\right\} \\ & \left. + \sum_{pen=1}^{Pen} GenPen_{pen,t} * CPen + \sum_{ncl=1}^{Ncl} Pncl_{ncl,t} * COVF\right\}\end{aligned} \tag{4.11}$$

$\mathbf{X}(PwindEq)$:	
• Max. power output eq. (3.16) – π1 • Min. power output eq.(3.17) – π2 • Online ramp up eq.(4.8)– π4 • Online ramp down eq.(4.9) – π3 • Min. nuclear power output eq. (3.20) – π5 • Max. nuclear power output eq.(3.21) – π6 • Online ramp up nuclear eq. (3.22) – π7 • Online ramp down nuclear eq. (3.23) – π8	Thermal power units' restrictions (π - dual variables)
• Max. power output eq. (3.37) – π9 • Min. power output eq. (3.41) – π10 • Max. turbinated outflow eq. (3.39) – π11 • Min. turbinated outflow eq. (3.42) – π12 • Max. reservoir level eq. (3.45) – π13 • Min. reservoir level eq. (3.46) – π14 • Spillage limit eq. (3.43) – π15 • Reservoir water balance eq. (3.49) – π16 • Reservoir Initial value eq. (3.47) • Inflow of unit hT (considering cascade) eq. (3.48) – π17 • RES- Hydropower production function eq.(3.35)– π18 • ROR- Hydropower production function eq. (3.36) – π19 • Max. turbinated outflow for ROR plants eq. (3.40) – π20 • Spillage definition for ROR plants eq. (3.44) – π21 • Delta between the initial and the final reservoir level eq.(3.10)	Hydro power plants' restrictions (π - dual variable)
• Demand balance eq. (3.56) – π23 • DC power flow (+), Transmission line capacity eq. (3.54) – π24 • DC power flow (-), Transmission line capacity eq. (3.55) – π25	Electrical grid' restrictions
• Dispatchable Wind power eq.(3.59) - (3.60) – π29	Wind power plants' restrictions
$Pt, Phd, TurbWat, Spil, Rsrv, Pror, TurbROR, SpilROR, Pncl, GenPen, VazaoInEq, \geq 0$	

4.2. Solution Methodology

The proposed formulation is a min-max-min problem (eq. (4.7)). This type of formulation cannot be solved directly by commercial software such as CPLEX. Therefore, the Benders' decomposition duality-based approach [28], [35] is employed as a solution methodology. The algorithm solves the master problem iteratively by adding new constraints to cut off the infeasible or non-optimal solutions defined through the solution of the slave problem. By dualizing the inner problem of the slave problem, which is a max-min problem, the slave problem is transformed into a maximization problem (max-max) only. The dual objective function of the slave problem is presented in eqs. (4.12) - (4.13) and it is subject to constraints (4.14) - (4.25).

$$\underset{\text{PwindEq}}{\text{Max}}\ \underset{\pi_x}{\text{Max}}\ \sum_{t=1}^{T}\sum_{j=1}^{J}\left[-Pcap_{(j)} * U.l_{(j,t)} * \pi 1_{(j,t)} + Pmin_{(j)} * U.l_{(j,t)} * \pi 2_{(j,t)} - \pi 3_{(j,t)} * Ramp_{(j)} - \pi 4_{(j,t)} * Ramp_{(j)}\right]$$

$$+ \sum_{t=1}^{T}\sum_{ncl=1}^{Ncl}\left[\pi 5_{(ncl,t)} * MinNcl_{(ncl)} - \pi 6_{(ncl,t)} * MaxNcl_{(ncl)} - \pi 7_{(ncl,t)} * RUNcl_{(ncl)} - \pi 8_{(ncl,t)} * RDNcl_{(ncl)}\right]$$

$$+ \sum_{t=1}^{T}\sum_{hd=1}^{Hd}\langle -\pi 9_{(hd,t)} * PhdMax_{(hd)} * Vh.l_{(hd,t)} + \pi 10_{(hd,t)} * PhdMin_{(hd)} * Vh.l_{(hd,t)} - \pi 11_{(hd,t)} * Qmax_{(hd)}$$

$$+ \pi 12_{(hd,t)} * Qmin_{(hd)} - \pi 13_{(hd,t)} * MaxLevel_{(hd)} + \pi 14_{(hd,t)} * MinLevel_{(hd)} - \pi 15_{(hd,t)} * SpilMax_{(hd)} \quad (4.12)$$

$$- \sum_{pln=1}^{K_{hd}} \gamma_o^{hd,pln} * \pi 18_{(hd,pln,t)}\rangle + \sum_{hd=1}^{Hd} \pi 16_{(hd,0)} * Initval_{(hd)} + \sum_{hd=1}^{Hd}\sum_{planes=1}^{P} \gamma_V^{hd,pln} * Initval_{(hd)} * \pi 18_{(hd,pln,0)}$$

$$+ \sum_{t=1}^{T}\sum_{hT=1}^{HT} \pi 17_{(hT,t)} * Inflowht_{hT,t} + \sum_{t=1}^{T}\sum_{hr=1}^{Hr}\langle \sum_{PlnR=1}^{K_{hr}}\left\{-\pi 19_{(hr,plnR,t)} * \gamma_o^{hr,plnR}\right\} - \pi 20_{(hr,t)} * QmaxROR_{hr}\rangle + \cdots$$

$$
\begin{aligned}
\ldots + \sum_{t=1}^{T} \pi 22_{(t)} \left\{ - \sum_{j=1}^{J} Pcap_{(j)} - \sum_{hd=1}^{Hd} PhdMax_{(hd)} \right\} \\
+ \sum_{t=1}^{T} \sum_{bus=1}^{B} \pi 23_{(t)} \langle -PsolarEq_{(bus,t)} - Ppch_{(t,bus)} - Pstm_{(t,bus)} + Demand_{(t,bus)} \rangle \\
+ \sum_{t=1}^{T} \sum_{line=1}^{L} \pi 24_{(t,line)} \langle -CapTx_{(line,"lim+")} \\
+ \sum_{bus=1}^{B} PTDF_{line,bus} \{ PsolarEq_{(bus,t)} + Ppch_{(bus,t)} + Pstm_{(bus,t)} - Demand_{bus,t} \} \rangle \qquad (4.13) \\
+ \sum_{t=1}^{T} \sum_{line=1}^{L} \pi 25_{(line,t)} \langle -CapTx_{(line,"lim-")} \\
+ \sum_{bus=1}^{B} PTDF_{line,bus} \{ -PsolarEq_{(bus,t)} - Ppch_{(t,bus)} - Pstm_{(t,bus)} + Demand_{bus,t} \} \rangle \\
+ \sum_{t=1}^{T} \sum_{bus=1}^{B} PwindTemp_{(busWind,t)} * \langle -\pi 29_{(busWind,t)} \rangle
\end{aligned}
$$

Subject to:

- Dual of $Pt_{(j,t)}$

$$-\pi 1_{(j,t)} + \pi 2_{(j,t)} - \pi 3_{(j,t)} + \pi 3_{(j,t+1)} + \pi 4_{(j,t)} - \pi 4_{(j,t+1)} - \pi 22_{(t)} + \pi 23_{(t)} + \sum_{line\ \epsilon\ Tx} \sum_{\forall bus \leftrightarrow GB(bus,j) \sim \emptyset} PTDF_{line,bus} * \{\pi 25_{(line,t)} - \pi 24_{(line,t)}\} \leq IndA_{(j)} + CVOMt_j \quad \forall t, \forall j \tag{4.14}$$

- Dual of $Pncl_{(ncl,t)}$

$$\pi 5_{(ncl,t)} - \pi 6_{(ncl,t)} - \pi 7_{(ncl,t)} + \pi 7_{(ncl,t++1)} + \pi 8_{(ncl,t)} - \pi 8_{(ncl,t++1)} + \pi 23_{(t)} + \sum_{line\ \epsilon\ Tx} \sum_{\forall bus \leftrightarrow GB(bus,ncl) \sim \emptyset} PTDF_{line,bus} * \{\pi 25_{(line,t)} - \pi 24_{(line,t)}\} \leq COVF \quad \forall t, \forall ncl \tag{4.15}$$

- Dual of $Phd_{(hd,t)}$

$$-\pi 9_{(hd,t)} + \pi 10_{(hd,t)} - \sum_{pln} \pi 18_{(hd,t,pln)} - \pi 22_{(t)} + \pi 23_{(t)} + \sum_{line\ \epsilon\ Tx} \sum_{\forall bus \leftrightarrow GB(bus,hd) \sim \emptyset} PTDF_{line,bus} * \{\pi 25_{(line,t)} - \pi 24_{(line,t)}\} \leq CVOMdEq \quad \forall hd, \forall t \tag{4.16}$$

- Dual of $TurbWat_{(hd,t)}$

$$-\pi 11_{(hd,t)} + \pi 12_{(hd,t)} + 0.0036 * \pi 16_{(hd,t)} - \sum_{\forall hT \rightarrow TblCasc(hT,hd) \sim \emptyset} \pi 17_{(hT,t+tviag(hT))} - \sum_{planes} \gamma_Q^{hd,pln} * \pi 18_{(pln,hd,t)} \leq 0 \quad \forall hd, \forall t \tag{4.17}$$

- Dual of $Spil_{(hd,t)}$

$$\pi 12_{(hd,t)} - \pi 15_{(hd,t)} + 0.0036 * \pi 16_{(hd,t)} - \sum_{\forall hT \rightarrow TblCasc(hT,hd) \sim \emptyset} \pi 17_{(hT,t+tviag(hT))} + \sum_{planes} \gamma_S^{hd,pln} * \pi 18_{(pln,hd,t)} \leq 0 \quad \forall hd, \forall t \tag{4.18}$$

- Dual of $Rsrv_{(hd,t)}$

$$-\pi 13_{(hd,t)} + \pi 14_{(hd,t)} + \pi 16_{(hd,t)} - \pi 16_{(hd,t+1)} - \sum_{planes} \gamma_V^{hd,pln} * \pi 18_{(pln,hd,t+1)} \leq \varphi \quad \forall hd, \forall t \tag{4.19}$$

$$\varphi := \begin{cases} 0 \leftrightarrow (t < T) \\ -CWater_{(hd)} \leftrightarrow (t = T) \end{cases}$$

- Dual of $VazaoInEq_{(hT,t)}$

$$\pi 17_{(hT,t)} - 0.0036 * \pi 16_{(hd,t)} - \pi 21_{(hr,t)} \leq 0 \quad \forall hd \rightarrow (hd = hT), \forall hr \rightarrow (hr = hT), \forall hT, \forall t \tag{4.20}$$

- Dual of $TurbROR(hr,t)$

$$-\sum_{\forall hT \rightarrow TblCasc(hT,hr) \sim \emptyset} \pi 17_{(hT,t+tviag(hT))} + \sum_{planesROR} \left\{\gamma_Q^{hr,plnR} * \pi 19_{(hr,plnR,t)}\right\} - \pi 20_{(hr,t)} + \pi 21_{(hr,t)} \leq RORCost \quad \forall hr, \forall t \tag{4.21}$$

- Dual of $SpillROR(hr,t)$

$$-\sum_{\forall hT \rightarrow TblCasc(hT,hr)\sim\emptyset} \pi 17_{(hT,t+tviag(hT))} + \sum_{planesROR} \left\{\gamma_S^{hr,plnR} * \pi 19_{(hr,plnR,t)}\right\} + \pi 21_{hr,t} \leq 0 \quad \forall hr, \forall t \tag{4.22}$$

- Dual of $Pror_{(hr,t)}$

$$-\sum_{plnR} \pi 19_{(hr,plnR,t)} + \pi 23_{(t)} + \sum_{line\ \epsilon\ Tx} \sum_{\forall bus \leftrightarrow GB(bus,hr)\sim\emptyset} PTDF_{line,bus} * \left\{\pi 25_{(line,t)} - \pi 24_{(line,t)}\right\} \leq 0 \quad \forall hr, \forall t \tag{4.23}$$

- Dual of $GenPen_{pen,t}$

$$\pi 23_{(t)} + \sum_{line\ \epsilon\ Tx} \sum_{\forall bus \leftrightarrow GB(bus,pen)\sim\emptyset} PTDF_{line,bus} * \left\{\pi 25_{(line,t)} - \pi 24_{(line,t)}\right\} \leq CPen \quad \forall pen, \forall t \tag{4.24}$$

- Dual of $PwindEq_{(busWind,t)}$

$$\pi 23_{(t)} + \sum_{line\ \epsilon\ Tx} PTDF_{line,bus} * \left\{\pi 25_{(line,t)} - \pi 24_{(line,t)}\right\} - \pi 29_{busWind,t} \leq 0 \quad \forall busWind, \forall t \tag{4.25}$$

For the dualization of the inner problem of the slave problem, wind power was considered as a known parameter. However, once the slave problem is transformed into a maximization problem, the variables $PwindTemp(busWind, t)$ and, consequently, $PwindEq(busWind, t)$ become decision variables of the outer problem of the slave problem. As a result, the objective function of the slave problem has a bilinear term (the last term in eq. (4.12)- (4.13)). To linearize this bilinear term, it is employed the big M-method (disjunctive constraints) [154] as follows:

H(...) is the rest of the objective function defined in (4.12) -(4.13)

$$Max\ \mathrm{H}(\dots) + \sum_{t=1}^{T}\sum_{bus=1}^{B} PwindTemp_{(busWind,t)} * \langle -\pi 29_{(busWind,t)} \rangle \tag{4.26}$$

Replacing (4.5) in (4.26):

$$\begin{aligned}\mathrm{Max\ H}(\dots) + \sum_{t=1}^{T}\sum_{bus=1}^{B} \big(&PwindFcast_{(buswind,t)} + Zpos_{(buswind,t)} \\ &* PwindUP_{(busWind,t)} - Zneg_{(buswind,t)} \\ &* PwindDW_{(busWind,t)}\big) * -\pi 29_{(busWind,t)}\end{aligned} \tag{4.27}$$

$Zpos_{(buswind,t)}, Zneg_{(buswind,t)} \in \{0,1\}$

The variables $\pi 29^{+}_{(buswind,t)}$ and $\pi 29^{-}_{(buswind,t)}$ are defined as:

$$\begin{aligned}\pi 29^{+}_{(buswind,t)} &= Zpos_{(buswind,t)} * -\pi 29_{(busWind,t)} \\ \pi 29^{-}_{(buswind,t)} &= Zneg_{(buswind,t)} * -\pi 29_{(busWind,t)}\end{aligned} \tag{4.28}$$

Finally, by replacing (4.28) in (4.27) and employing the big M method, the bilinear term in the objective function is translated as eq. (4.29) subject to constraints (4.30) - (4.33).

$$\begin{aligned}\mathrm{Max\ H}(\dots) + \sum_{t=1}^{T}\sum_{bus=1}^{B} \big(&-\pi 29_{(buswind,t)} * PwindFcast_{(buswind,t)} \\ &+ \pi 29^{+}_{(buswind,t)} * PwindUP_{(busWind,t)} + \pi 29^{-}_{(buswind,t)} \\ &* PwindDW_{(busWind,t)}\big)\end{aligned} \tag{4.29}$$

$$\pi 29^{+}_{(buswind,t)} \leq \mathrm{M} * Zpos_{(buswind,t)} \quad \forall busWind, \forall t \tag{4.30}$$

$$\pi 29^{+}_{(buswind,t)} \leq -\pi 29_{(buswind,t)} + \mathrm{M}\,(1 - Zpos_{(buswind,t)}) \quad \forall busWind, \forall t \tag{4.31}$$

$$\pi 29^{-}_{(buswind,t)} \leq \mathrm{M} * Zneg_{(buswind,t)} \quad \forall busWind, \forall t \tag{4.32}$$

$$\pi 29^{-}_{(buswind,t)} \leq \pi 29_{(buswind,t)} + \mathrm{M}\,(1 - Zneg_{(buswind,t)}) \quad \forall busWind, \forall t \tag{4.33}$$

The final form of the dual slave problem is established as follow:

$$\text{Max H}(\dots) + \sum_{t=1}^{T}\sum_{bus=1}^{B} -\pi 29_{(buswind,t)} * PwindFcast_{(buswind,t)} + \pi 29^{+}_{(buswind,t)} * PwindUP_{(busWind,t)} + \pi 29^{-}_{(buswind,t)} * PwindDW_{(busWind,t)} \quad (4.34)$$

Subject to:

Equations (4.1) - (4.2) , (4.4)

(4.14) - (4.25)

(4.30) - (4.33)

With:

$$\pi 29_{(buswind,t)}, \pi 22_{(t)}, \pi 23_{(t)}, \pi 24_{(t,line)}, \pi 25_{(t,line)}, \pi 20_{(t,hr)}, \pi 19_{(t,hr,plnR)}, \pi 18_{(t,hd,pln)}, \pi 15_{(t,hd)}, \pi 14_{(hd,t)}, \pi 13_{(t,hd)}, \pi 12_{(hd,t)}, \pi 11_{(t,hd)}, \pi 10_{(t,hd)}, \pi 9_{(t,hd)}, \pi 8_{(t,ncl)}, \quad (4.35)$$

$$\pi 7_{(t,ncl)}, \pi 6_{(t,ncl)}, \pi 5_{(t,ncl)}, \pi 4_{(t,j)}, \pi 3_{(t,j)}, \pi 2_{(t,j)}, \pi 1_{(t,j)} \geq 0$$

$$\pi 17_{(hT,t)}, \pi 16_{(t,hd)}, \pi 21_{(t,hr)} \text{ are free}$$

As mentioned, the solution methodology is based in the Benders' decomposition framework, in which the master problem is solved iteratively by adding new constraints to cut off the infeasible or non-optimal solutions [91]. Within this method, the exact separation requires the reformulation of the bilinear sub-problem as a mixed-integer linear program. It is important to highlight that this approach is challenging due to the use of a large amount of integer decision variables. The definition of the Benders's non-optimal cuts (cuts that restrict the possible unit commitment solutions in order to avoid non-optimal outcomes) performed in this work is presented in eq. (4.36) - (4.38). Since the UC model use penalty power plants there is no need for the infeasible cuts. In eq. (4.36), $z.l$ is the value of the objective function of the slave problem for each iteration.

$$
\begin{aligned}
cutconst_{(iter)} &= z.l \\
&- \sum_{j=1}^{J}\sum_{t=1}^{T} -Pcap_{(j)} * U.l_{(j,t)} * \pi 1.l_{(j,t)} + Pmin_{(j)} * U.l_{(j,t)} \\
&* \pi 2.l_{(j,t)} \\
&- \sum_{hd=1}^{Hd}\sum_{t=1}^{T} -\pi 9.l_{(hd,t)} * PhdMax_{(hd)} * Vh.l_{(hd,t)} \\
&+ \pi 10.l_{(hd,t)} * Phdmin_{(hd)} * Vh.l_{(hd,t)}
\end{aligned} \tag{4.36}
$$

$$
cutcoeffU_{(iter,j,t)} = -Pcap_{(j)} * \pi 1.l_{(j,t)} + Pmin_{(j)} * \pi 2.l_{(j,t)} \tag{4.37}
$$

$$
\begin{aligned}
cutcoeffVh_{(iter,hd,t)} &= -\pi 9.l_{(hd,t)} * PhdMax_{(hd)} + \pi 10.l_{(hd,t)} * Phdmin_{(hd)}
\end{aligned} \tag{4.38}
$$

The final form of the master problem, considering the non-optimal cuts, is shown in eqs.(4.39) - (4.40).

Min Θ

Subject to:

- Turn on eq. (3.11)
- Turn off eq. (3.12)
- Min time off eq. (3.14)
- Min time on eq. (3.15)
- Binary variables eq. (3.13)

(4.39)

$$\Theta \geq \sum_{t=1}^{T}\sum_{j=1}^{J} CSd_{(j)} * UOff_{(j,t)} + ColdS_{(j)} * UOn_{(j,t)} + U_{(j,t)} * IndB_{(j)}$$
$$+ cutconst_{(cutset)} + \sum_{t=1}^{T}\sum_{j=1}^{J} cutcoeffU_{(cutset,j,t)} * U_{(j,t)} \qquad (4.40)$$
$$+ \sum_{t=1}^{T}\sum_{hd=1}^{Hd} cutcoeffVh_{(cutset,hd,t)} * Vh_{(hd,t)}$$

Finally, the presence of non-convex terms in the slave problem can prevent Benders decomposition from guaranteeing the attainment of global optimality. Therefore, a Monte Carlo sampling approach is used to assess the quality of the solutions achieved. A schematic diagram of the solution methodology is presented in Figure 4.3, and the problem formulation and solution algorithm are implemented in GAMS.

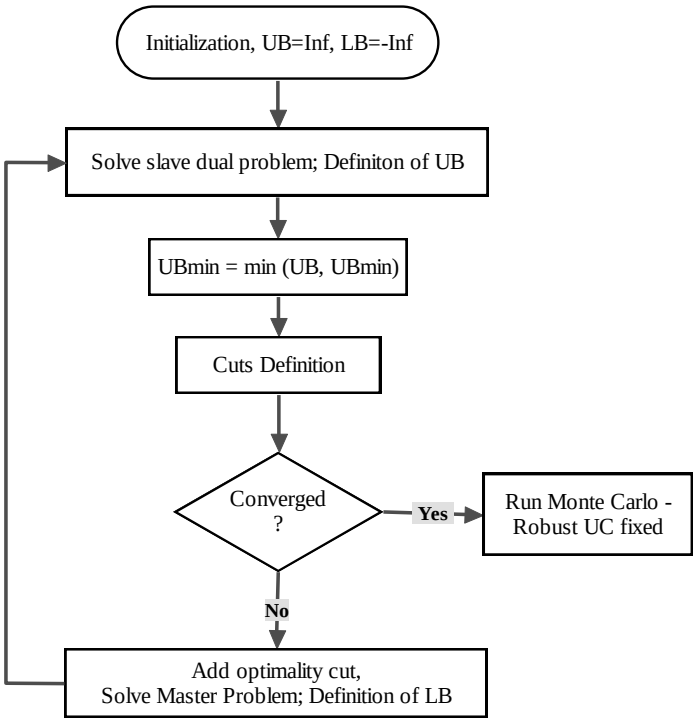

Figure 4.3 Solution methodology -Benders' decomposition Framework.

Chapter 5

Case Studies

This chapter presents the simulation results for the two models developed in this thesis: STORM and R-STORM. In the case of the deterministic UC Model (STORM), the analysis focused on validating the dispatch results of STORM considering the Brazilian power system. This validation was performed through numerical comparisons between the STORM dispatch and the power system dispatch made by the Brazilian power system operator (ONS). On the other hand, in the case of the Robust UC Model (R-STORM), two fictional systems were created in order to test the model's ability to hedge against wind power uncertainty. The R-STORM performance was compared against its equivalent deterministic model (STORM) using a Monte Carlo sampling method. It is worth mention that STORM handles energy uncertainty by imposing levels of spinning reserve.

5.1. Deterministic UC Model (STORM) Validation Analysis

In the context of sustainable development, it is essential to ensure energy security while reducing GHG emissions and increasing resilience to both climate variability and climate change. Traditionally, the term energy security has been related to easy access of energy carriers like oil and/or gas, for example. However, in a low-carbon development pathway, where variable renewable energy resources become more relevant in the electrical power mix, taking a major role in energy security, it is crucial to improve the representation of renewable energy uncertainty and variability in both long- and short-term models. In this context, the STORM model contributes to ongoing efforts to develop a soft-link between the BLUES[9] Model, COPPE's national integrated assessment model (IAM) and a short-term model for the power sector. The STORM

[9] BLUES is a linear optimization energy model developed at CENERGIA Lab of the Energy Planning Program, Universidade Federal do Rio de Janeiro, for the Brazilian energy system using the MESSAGE (Model for Energy Supply Strategy Alternatives and Their General Environmental Impacts) platform developed by IIASA (International Institute for Applied System Analysis) [161].

model can represent, in a simplified but representative way, the characteristics of the Brazilian power system. Therefore, this model can be used as a tool to analyze potential system limitations for the integration of high levels of renewable energy and/or to assess the technical viability of renewable energy penetration pledges produced by integrated energy models. In other words, the link of a dispatch model with a national IAM offers the possibility of evaluating how likely transformation pathways, proposed by energy models, are indeed technically achievable.

In order to validate the STORM model, a comparative analysis was performed between the actual dispatch made by the Brazilian power system operator (ONS) and some of the STORM's results for the Brazilian power system. To perform this, a day for each trimester of 2019 was chosen. The selected dates were: January 15th, April 15th, July 15th and October 4th[10]. The main exogenous input data considered to build this economic dispatch model are described in Section 5.1.1 and in the Appendices. However, in order to perform a fair comparison, the input deck for wind power generation, solar PV generation, power demand and reservoirs initial volume were updated based on the data reported by ONS [155] for the scheduled days.

5.1.1. Inputs and assumptions

The main Exogenous input data considered to build the short-term model are briefly described in the following subsections.

a. Electricity Demand

The hourly demand curve for each grid bus was based on [139][11]. The future demand scenarios are a by-product of the iNoPa project [140], in which the MESSAGE v.1.3 (MSB-300) model was used. The Brazilian demand data was update considered an annual growth for 2015-2020 of 2.65%. This study considered the scenario for the year 2019. Finally, the Brazilian aggregated demand was divided by bus based on [141].

b. Characteristics of electricity generation technologies

Existing capacities were implemented based on [142], [143]. In the case of new power plants and power line projects, they were defined according to [129], [134] and

[10] The data for the comparative analysis was gathered on October 6th of 2019, this is the reason for not had not choose October 15th as the fourth day.
[11] Personal communication

[144]. The installed capacity for the considered technologies is summarized in Table 5-1 and Table 5-2.

Table 5-1. Installed Capacity by bus for the Brazilian Power System (MW) – Scenario for 2019.

	Installed Capacity (MW)								
Power Plant*	**Bus-1**	**Bus-2**	**Bus-3**	**Bus-4**	**Bus-5**	**Bus-6**	**Bus-7-8**	**Bus-9**	**Bus-10**
ST-BIO	-	254.8	22.5	-	-	-	235.2	-	334
ST-COAL	1080	360.1	-	-	-	-	-	-	1388.2
OGT-GAS	594.5	907.4	863.6	-	-	-	1829.2	-	1279.3
CCGT-GAS	4280	499.2	932.9	-	-	529.2	4448.2	-	1758.4
ICG	2684.2	331.8	407.5	-	-	426.4	664.6	-	8.0
Hydro-RES	2927.3	1727	8650	-	216.5	-	21570.3	-	8457.7
Hydro-ROR	7891.6	14088.9	2588.4	11233.1	7324.7	1820	12691.8	10800	7561.8
SU-Hydro	209.6	359.2	-	-	134.6	-	4962.8	-	2659.7
SU-Thermal	1388.1	110.1	551.2	-	82.2	1081.4	9216.6	-	964.9
NUC-UR	-	-	-	-	-	-	1990	-	-
Wind Pwr	12613.6	-	-	-	-	-	127.8	-	2242.3
PV Solar Pwr	1979	-	-	-	-	210	570	-	-

* The full thermal power plant names are divided in two parts: technology + fuel. The technologies are combined cycle – CC, Open cycle – OGT, Steam turbine –ST, Internal combustion generator –IC, Nuclear power -NUC. Hydro-RES stands for hydropower units with reservoir, Hydro-ROR for run-of-river hydropower units and SU for small units.

Table 5-2 Installed capacity by technology for the 2019 scenario*.

Power Source**	#Units	Installed Capacity (MW)	% of total installed capacity
ST-BIO	5	846.5	0,5%
ST-COAL	12	2828.3	1,5%
OGT-GAS	23	5474	2,9%
CCGT-GAS	24	12447.9	6,7%
ICG	41	4522.5	2,4%
Hydro-RES	61	43548.8	23,3%
Hydro-ROR	102	76000.3	40,6%
SU-Hydro	-	8325.9	4,4%
SU-Thermal	-	13394.5	7,2%
NUC-UR	2	1990	1,1%
Wind Pwr	-	14983.7	8,0%
PV Solar Pwr	-	2759	1,5%

*[129],[142].

**The thermal power plant names are divided in two parts: technology + fuel. The technologies are combined cycle – CC, Open cycle – OGT, Steam turbine –ST, Internal combustion generator –IC, Nuclear power -NUC. Hydro-RES stands for hydropower units with reservoir, Hydro-ROR for run-of-river hydropower units and SU for small units.

Typical costs and parameters for the operational restrictions of thermal power technologies such as: ramp-up, ramp-down, minimum up-time, minimum down-time, minimum and maximum load rate; required for the unit commitment optimization model are provided by Table 5-3 and Table 5-4. More specific technical parameters for the development of STORM applied to the Brazilian power system are presented in the Appendices.

Table 5-3. Thermal Power Plant Technical Parameters.

Power Plant Technical Parameters**								
Type of thermal unit	**Min Stable level (%)**	**Max. Ramp Up/down (%/h)**	**Start-up Ramp (%/min)**	**Efficiency at 100% of Capacity (%)***	**Efficiency at 75% of Capacity (%)***	**Efficiency at 50% of Capacity (%)***	**Min. Up Time (h)**	**Min. Down Time (h)**
ST-BIO	40	25	40	36.2	35.4	33	6	4
ST-COAL	40	25	40	36.2	35.4	33	6	4
OGT-GAS	50	60	50	38	33.6	28.7	0-1	0-1
CCGT-GAS	35	30	35	54.5	49.7	47.1	4	2
ICG	50	60	50	46	44	42	1-2	1-2
NUC-UR	60	12	-	-	-	-	-	-

*Efficiency curve based on [32].
** data based on [145].

Table 5-4. Power Plant Economical Parameters.

Power Plant Economical Parameters**				
Type of thermal unit	**Startup cost ($/MW)**	**O &M Variable Cost ($/MWh)**	**Shut-down cost ($/MW)**	**Fuel price (USD$/MMBTU)***
ST-BIO	8.63	12	8.63	1.47
ST-COAL	8.63	6.3	8.63	2.76
OGT-GAS	1.04	5.8	1.04	8.02
CCGT-GAS	2.07	4.9	2.07	8.02
ICG	1.04	14.2	1.04	35.59
Hydro-RES	-	5.94	-	-
Hydro-ROR	-	6.02	-	-
NUC-UR	16.16	31.66	16.16	7.92

*Based on[134].
**Based on [146], [147].

c. Reservoir information and hydropower generation

To accurately represent hydropower reservoirs the following parameters were considered: i) maximum and minimum reservoir volume levels, ii) minimum flow requirement, iii) maximum flow discharge, and iv) cascaded configuration and time travel. The data for each reservoir was taken from [148], [127], [149], [150] and is presented in Appendix B. The inflow of the hydropower plants was computed using the average monthly natural inflow from ONS [151]. Technical and economic parameters for hydropower plants with reservoir are presented in Appendix B and for run-of-river plants in Appendix C.

d. Transmission System characteristics

To describe the Brazilian transmission system, a simplified and equivalent electric grid between the major energy markets is considered. The power grid, based on [129], has twelve equivalent nodes and it is presented in Figure 5.1. Operational restrictions to existing and new transmission capacities between regions were implemented based on [129] and presented in Appendix E.

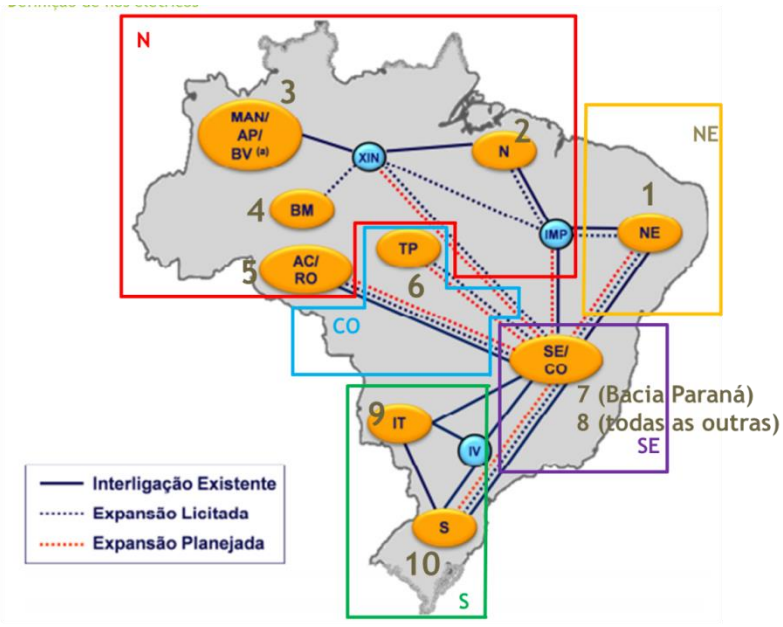

Figure 5.1 Equivalent Brazilian transmission system [129]

The single line diagram of the transmission grid is presented in Figure 5.2.

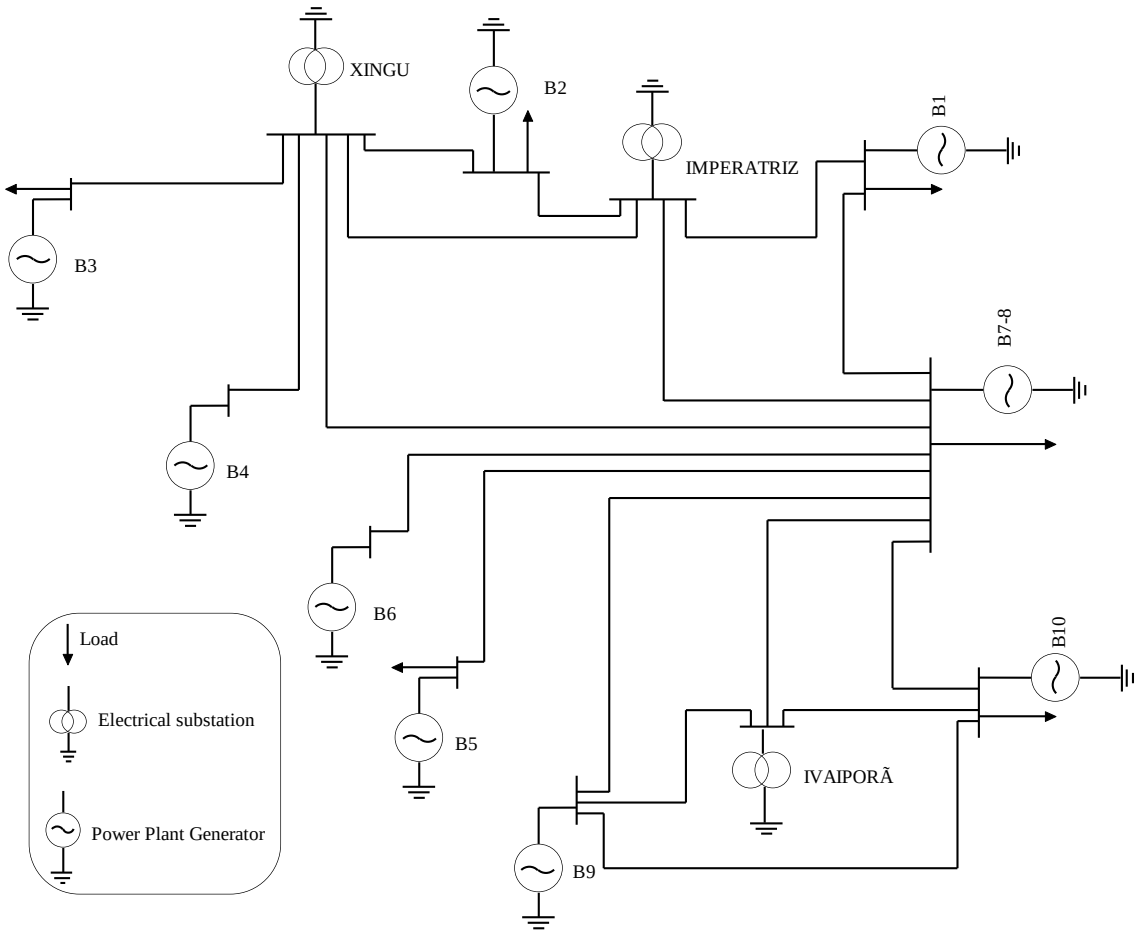

Figure 5.2 Equivalent transmission system – Single line diagram.

e. Wind Energy

The wind energy data used in this work are a by-product of [133] and [134]. These studies used time series of wind speeds, ambient temperature and pressure from Meteonorm [135] and SWERA/NREL [136]. It was used the power curve of a 2.3MW wind turbine. The parameter $PwindPU_{wn,t}$ is the normalized hourly profile for 25 wind hotspots (show in Table II-10). The hourly wind forecasted generation of each hotspot is obtained by multiplying its installed capacity ($WindCao_{wn}$) by the hourly profile. The total forecasted wind energy for each bus ($PwindFcast$) is the sum of all wind energy hotspots connected to bus *b* as shown in eq.(3.58). The used data are showed in Appendix F.

Since the UC model considers an equivalent transmission grid (Figure 5.2), the 25 hotspot of Table II-10 were aggregated in six equivalent wind hotspots according to their geographic location and seasonality. The equivalent wind hotspots are defined as follow: i) three equivalent hotspots in the Brazilian North East associated with Bus B1,

ii) one equivalent hotspot in the Brazilian South East associated with Bus B7-8 and iii) two equivalent hotspots in the south associated with bus B10.

f. Solar PV Generation

The solar PV energy data used in this work are a by-product of [133] - [134]. Similarly to the pre-processing done for wind energy, the 22 solar hotspots of these references were grouped into six equivalent hot spots: i) one equivalent hotspot representing the North East region (linked to bus B1), ii) two equivalent hotspots for the North region (linked to bus B3 & B5), iii) one equivalent for South East region (linked to bus B7-8), iv) one equivalent hotspot for the Midwest region (linked to B6) and v) one equivalent hotspot for the South (linked to B10). The used data are show in Appendix F.

g. Small generation plants

The generation of each plant in this category is obtained by multiplying its installed capacity by the seasonal generation profile given by [138]. The used data are show in Appendix F.

5.1.2. Case Study Results

Results presented in Figure 5.3 correspond to the aggregated energy generation of the dispatch defined by STORM for each day. It is important to highlight that STORM offers as results hourly power generation of each one of the considered power generation plants, and that an aggregation was made by type of energy source in order to allow for a straight forward comparison with the available public data reported by ONS[12].

[12] The available public data of the hourly historical generation is presented grouped by type of source.

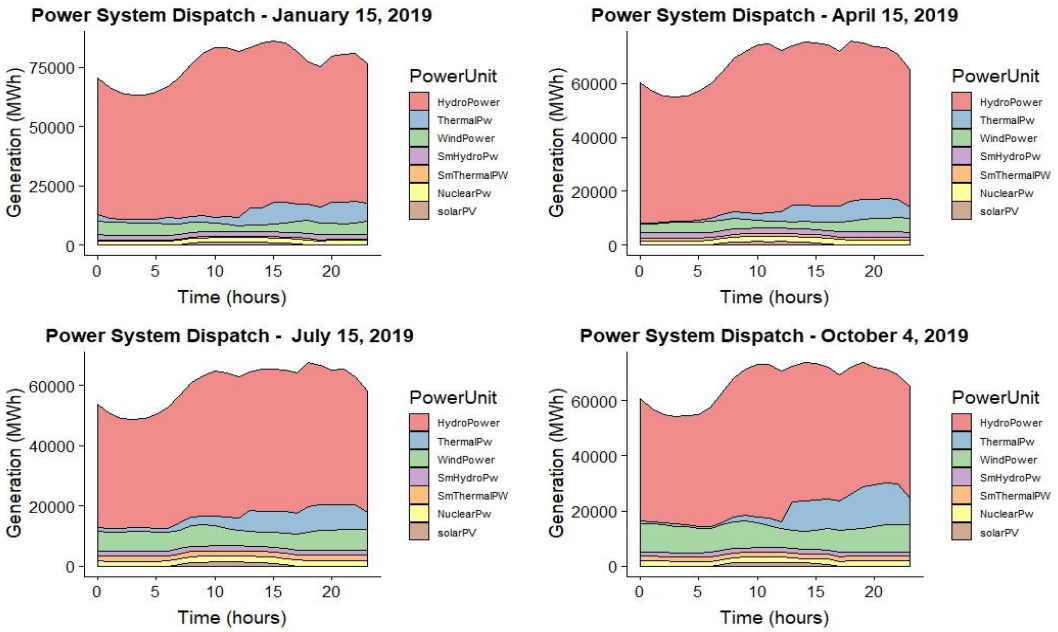

Figure 5.3 STORM model Dispatch for the 4 representative days considered in the validation analysis.

The first comparison between the STORM results and the ONS operative dispatch was made considering the daily cumulative dispatched energy. This comparison is presented in Table 5-5. As can be seen, the average difference between the two sets of dispatch results was less than 5% for all the generation technologies. Differences between the two sets were expected. However, the fact that they are not so large attests that the model results are reasonably close to real-life dispatch. One reason for the differences could be the fact that STORM considers an equivalent transmission grid topology and not the detailed Brazilian transmission grid. Moreover, as can be seen in the weekly planning of power system operation presented by ONS, for the analyzed days, an important parcel of the operative dispatched thermal power generation was defined based on non-economic dispatch decisions for system reliability purposes (electrical grid[13] and/or GenCos[14] restrictions). In this sense, the ratio between non-economic thermal power energy dispatched and the total thermal power energy dispatched by the ONS is presented in Table 5-6. Therefore, even though variable operating costs are the primary driver of the dispatch decisions made by an electric power system operator, real-life factors can lead to deviations from the economic optimal dispatch curve.

[13] Operative limitation on equipment, installations or systems that must be considered in a given period.
[14] Mandatory dispatch amount asked from the power generation company (GenCos) in order to meet the requirements solicited by the system operator.

Table 5-5. Daily accumulative results of the Brazilian power dispatch.

	Source	Hydro Pwr	Thermal Pwr	Wind Pwr	Nuclear Pwr	Solar Pwr
Day1- Energy dispatched (%)	ONS	82.88	8.09	5.79	2.65	0.60
	STORM	83.97	7.19	5.79	2.44	0.60
	|Delta|	1.09	0.9	0	0.21	0
Day2- Energy dispatched (%)	ONS	81.54	9.65	5.45	2.70	0.66
	STORM	84.08	7.08	5.45	2.73	0.66
	|Delta|	2.54	2.57	0	0.03	0
Day3- Energy dispatched (%)	ONS	68.72	17.20	9.94	3.33	0.81
	STORM	75.32	10.81	9.94	3.12	0.81
	|Delta|	6.60	6.39	0	0.21	0
Day4- Energy dispatched (%)	ONS	64.87	18.02	13.18	2.99	0.94
	STORM	71.14	11.96	13.18	2.79	0.94
	|Delta|	6.27	6.06	0	0.20	0
|Delta| Average (%)		4.12	3.98	0.00	0.16	0.00

Table 5-6 also shows the evaluation of Δgen, as defined by (5.1), for each of the days considered for STORM validation. Once Δgen determines the ratio between the thermal energy generation difference and the total thermal energy dispatched by ONS, a straightforward comparison among the two sets of percentage values can be performed. As can be concluded from this comparison, it is likely that the divergence between the STORM and ONS dispatches is lower than the non-economic operative dispatch.

$$\Delta gen = \frac{ThermalONS\ (MWh) - ThermalSTORM(MWh)}{ThermalONS(MWh)} \tag{5.1}$$

Table 5-6. Non-economic thermal energy (nuclear energy included) dispatched*.

Operational week	Ratio between Non-economic thermal energy and Total thermal energy	Simulated day	Δgen
12/01/2019-18/01/2019	24.5%	15/01/2019	8.5%
13/04/2019-19/04/2019	14%	15/04/2019	20.6%
13/07/2019-19/07/2019	40.2%	15/07/2019	32.5%
28/09/2019-04/10/2019	45.7%	04/10/2019	28.9%

*Data took from [156].

From this analysis it can be argued that STORM properly represents the Brazilian power system for the proposed goal of being a tool to assess the technical viability of the renewable energy penetration pledges produced by long-term energy models.

The differences between the two power dispatches can be seen with more detail in the second comparison, presented in Figure 5.4, in which the hourly profile of the dispatched hydro, nuclear and thermal power resources are examined. As can be seen, the nuclear generation follows the profile of the real dispatched curve. In the case of the hydropower generation, some hydropower energy is displaced as a result of the thermal power energy profile. For instance, it is noted that for days 1 and 2, which have low or medium levels of non-economic thermal power energy due system reliability purposes, STORM' results have a better match with the ONS dispatch. However, for day 3 and day 4 the dispatch is quite influenced by the high levels of non-economic thermal power energy that, according to Table 5-6, are about 40% and 45%, respectively.

One way to improve the STORM model in order to approximate its hourly results with the real dispatch of ONS is to adjust the model by adding a constraint that indicates, based on historical non-economic thermal generation data, which thermal power plants should be kept online based on stability requirements. This constraint is sometimes called as "special electrical restrictions" and can be adjusted by the user. Nonetheless, this kind of adjustment is outside the focus of this thesis. Then, considering the discussion presented in this section, it is argued that the STORM model can represent the main characteristics of the Brazilian power system, in such a way that it can be used as a tool to analyze and better understand market interactions, electricity costs and possible impacts of national energy policy/regulatory initiatives.

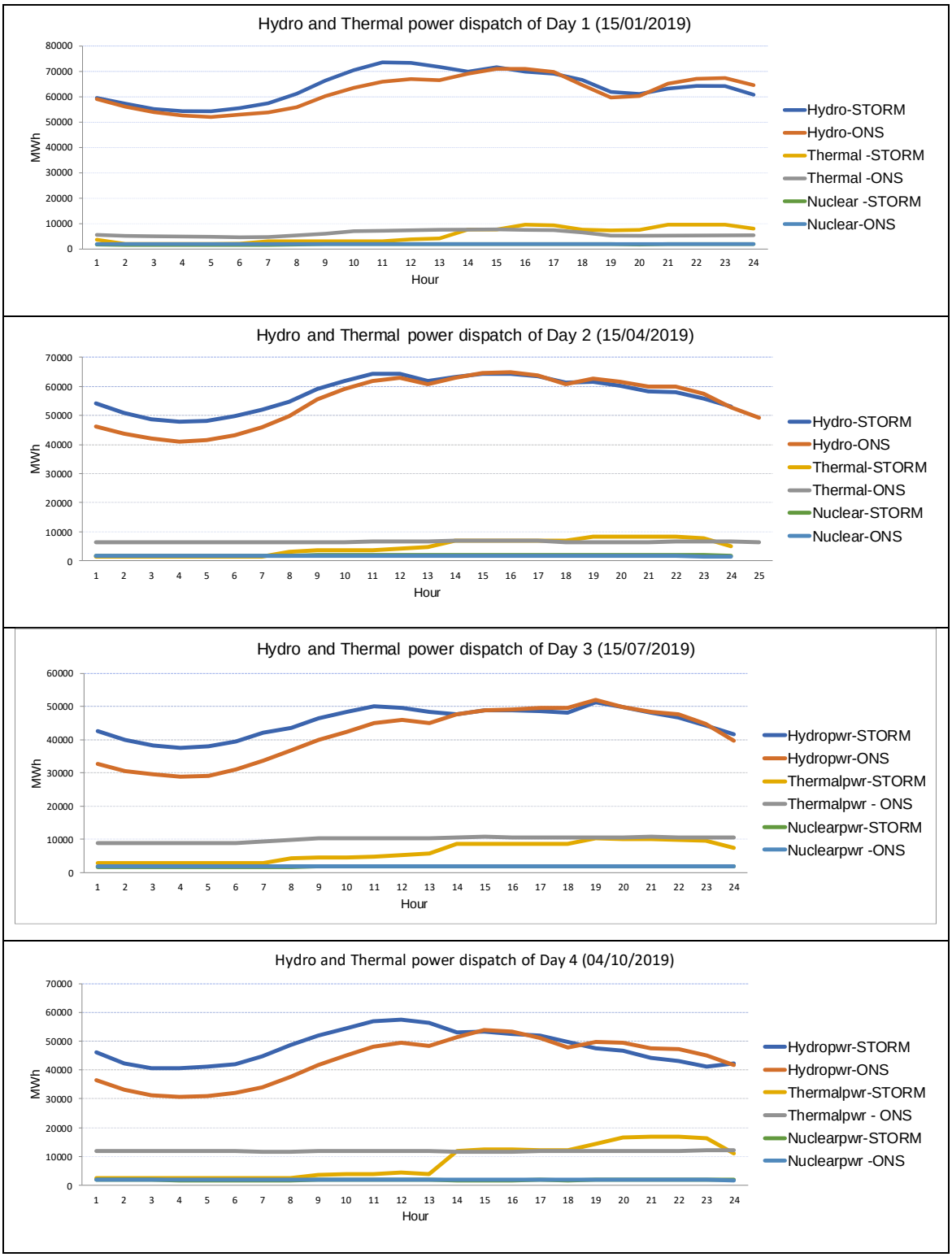

Figure 5.4 Hourly profile of the dispatch of hydro and thermal power resources.

The next section focuses on the validation of R-STORM model. In this context, it is worth highlight that due to the high computational complexity of the Robust approach and a limited access of a high-performance cluster computation unit, it was decided to employ two fictional case-study systems for this analysis, rather than the Brazilian

system representation used in this section. A computational performance analysis of R-STORM is presented in Section 5.2.3.

5.2. Robust UC Model (R-STORM) simulation analysis

This section presents the numerical results of the application of the R-STORM model (detailed in Chapter 4) for the simulation of two Case Study Systems (system A and system B), described next. Both cases correspond to hydrothermal power systems with cascade configuration; however, system B imposes a greater number of variables and restriction, which allows to obtain insights about the computational performance of R-STORM. The capability of R-STORM to determinate robust unit commitment decisions, considering wind power uncertainty and variability, was evaluated using a Monte Carlo sampling approach. For comparison reasons, the same Monte Carlo sampling approach was applied to the unit commitment results of a deterministic optimization model that takes into account all the restrictions of R-STORM and an additional restriction related to spinning reserve capability but disregards wind power generation uncertainty. All the experiments were implemented using CPLEX at IBM / Lenovo NextScale Cluster (2015) from the Potsdam Institute for Climate Impact Research (PIK).

The thermal power generators for system A are the first seven plants listed in Table 5-7, while for System B, all plants listed in the same table are considered; additional characteristics are presented in Section 0. The considered hydropower plants are listed in Table 5-8. The selection of the hydropower plants was made so all generation buses of the electrical grid have at least one power plant. Additional technical data are presented in Section 0 and Appendices B to D. The Installed capacity of Belomonte-Mod and Itaipu 60Hz-Mod is 5% of the installed capacity of Belomonte and Itaipu 60Hz, respectively. The electrical grid data are the same considered for the deterministic model presented in 3.2.4 and 3.2.5, which considers the same 12-bus electrical power system.

Table 5-7. Technical and economic data of thermal generation plants*.

Power Plant**	Upper (MW)	Lower (MW)	Min-up (h)	Min-down (h)	Ramp (MW/h)
TEPE-CC-GAS	533.0	186.5	4	2	159.9
CAMA-GT-GAS	346.5	173.2	0	0	207.9

MAR-CC-GAS	529.2	185.2	4	2	158.7
BAR-GT-GAS	385.6	192.8	0	0	231.3
VIA-IC-HFO	174.6	87.3	1	1	104.7
CAN-ST-COAL	350.0	140.0	6	4	87.5
ANG1-NUC-UR	640.0	384.0	48	48	76.80
PECEM1-ST-COAL	720.0	288.0	6	4	180.0
PERN-IC-HFO	201.0	100.5	0	0	120.6
GERI-IC-HFO	165.9	82.9	1	1	99.5
MARIV-GT-GAS	337.6	168.8	0	0	202.5
POR-ST-COAL	360.1	144.0	6	4	90.0
APA-GT-GAS	251.5	125.7	0	0	150.9
CRI-IC-GAS	85.5	42.7	2	2	51.3
MAU-CC-GAS	583.0	204.0	4	2	174.9
BRA-IC-HFO	10.0	5.0	1	1	6.0
AUR-CC-GAS	226.0	79.1	4	2	67.8
IPA-ST-BIO	76.0	30.4	6	4	19.0
ARA-CC-GAS	484.1	169.4	4	2	145.2
KLA-ST-BIO	330.0	132.0	6	4	82.5
ARJ-GT-GAS	41.2	20.6	0	0	24.7

* Cells with orange background color refer to generation plants of system A; all the generation plants are considered in system B.
** The full power plant name is divided in three parts: name + technology + fuel. The technologies are combined cycle – CC, Open cycle – GT, Steam turbine –ST, Instant combustion –IC.

Table 5-8.Hydropower plants (hd- with reservoir and hr – run-of-river).

Power plant*	type	Installed Cap. (MW)	Power plant*	type	Installed Cap. (MW)
BALBINA	hd	250	CANA BRAVA	hr	450
SERRA DA MESA	hd	1275	BELO MONTE-Mod	hr	550
BARRA GRANDE	hd	698	ITAIPU 60 HZ-Mod	hr	540
I. SOLT. EQV	hd	4251	14 DE JULHO	hr	100
TRÊS MARIAS	hd	396	BEM QUERER	hr	708
QUEIMADO	hd	105	ITAPEBI	hr	450
SOBRADINHO	hd	1050	AIMORÉS	hr	330
SAMUEL	hd	250	SÃO SALVADOR	hr	243
PEIXE ANGICAL	hd	452	--		

*Cells with orange background color refer to generation plants of system A; all the generation plants are considered in system B.

The seasonal data, i.e. demand, biomass generation and wind power generation data for systems A and B, used in this thesis are by-products of technical works [133] and [134]. More specifically, a typical day of July of 2015 was selected as the time reference for the hourly data. Concerning wind power generation, three equivalent wind

hotspots (NE1, NE2 and NE3) were defined based on the wind hotspots from the Brazilian Northeast region, established in Table II-10. In this context, NE1 equivalent hotspot considers the HS1-HS4 hotspots; equivalent hotspot NE2 considers the HS5-HS10 hotspots; and equivalent hotspot NE3 consider the HS11-HS12 hotspots.

As shown in Section 4.1.1, the generation data of all wind hotspots showed homoscedasticity within the first and the second semester. Therefore, the definition of upper and lower bounds of the wind power uncertainty set was based on data for the second semester of 2015. Figure 5.5 shows that the 95th and 5th quantiles for the wind power of the Brazilian Northeast were almost fixed values. This analysis was also made for each one of the hotspots H1-HS10 individually and the results were very similar. Based on this, the upper and lower bound were defined for both data sets as presented in Figure 5.6.

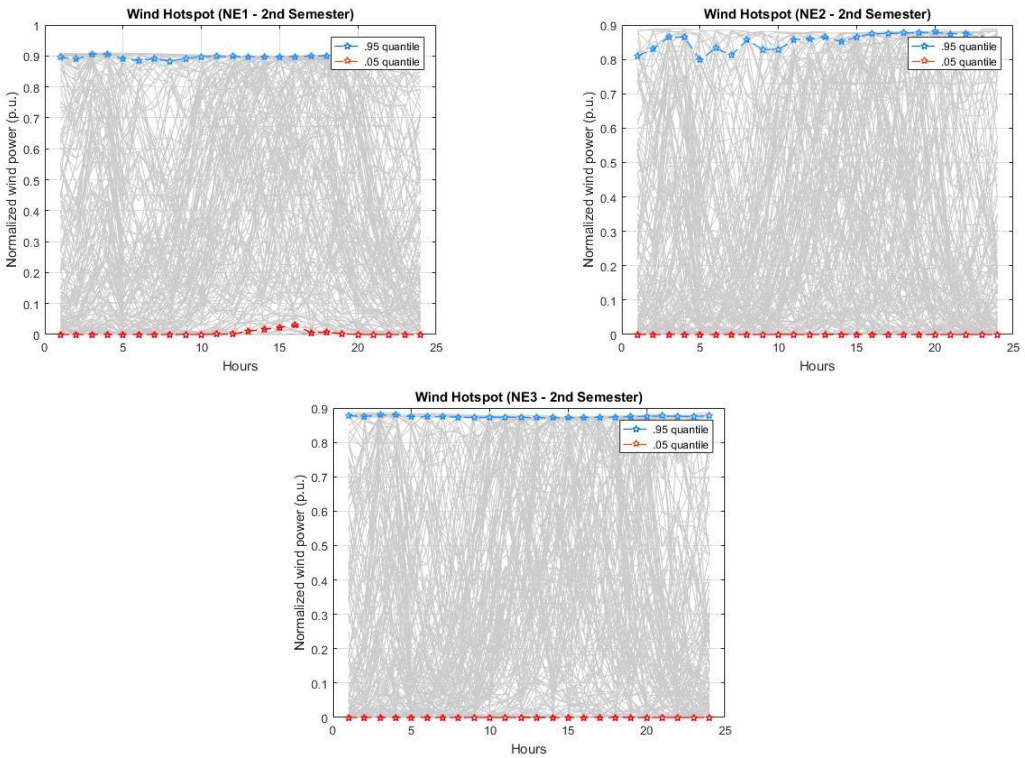

Figure 5.5 Equivalent hotspots for the Brazilian Northeast.

All the equivalent hotspots (NE-1, NE-2 and NE-3) were integrated into the modeled power system at bus B1 for both case studies. Therefore, $busWind = B1$. In this sense, the corresponding total energy injection was defined as the sum of the energy generated by the three equivalent wind hotspots presented in Figure 5.5. The wind power installed capacity varies according to the system: for system A it is 1,261 MW and for system B it is 6,307 MW. Considering the uncertainty set presented in Figure 5.6, the level of

conservatism was adjusted with the uncertainty budget ($Bgt_{busWind}$), a parameter that defines the number of periods in which wind power deviates from its forecasted value to the upper or lower level. In this context, six uncertainty budgets ($Bgt_{busWind} = 0$, 2, 4, 6, 8, and 10) were considered for the simulation studies carried out for both systems.

Based on the mathematical analysis presented by [68] and equation (2.6), the probability of non-constraint violation given an uncertainty budget ($Bgt_{busWind}$), i.e. the probability that a Robust UC solution obtained by using $Bgt_{busWind}$ is feasible for all possible wind power realizations within the upper and lower bounds of the uncertainty set, for the case of 24 uncertain variables (the hourly wind power profile over a day period) is shown in Table 5-9. It is important to highlight that, as described by (4.3), to set the uncertainty budget to zero is equivalent to consider no variation in the wind energy profile. Therefore, this operation mode of R-STORM ($Bgt_{busWind} = 0$) is equivalent to a deterministic UC solution without spinning reserve.

Table 5-9.Probability of NON constraint violation for different uncertainty budgets.

Budget	2	4	6	8	10
Probability	68.4%	79.1%	88.8%	94.8%	97.9%

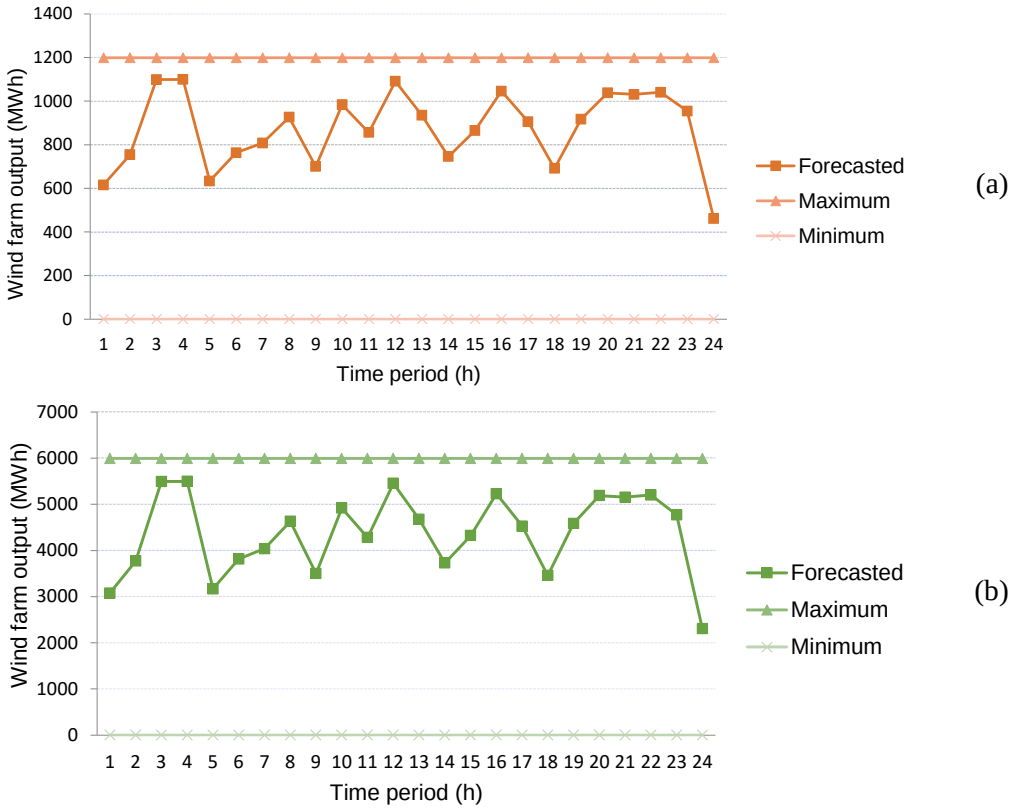

Figure 5.6 Wind energy output – (a) System A; (b) System B.

Monte Carlo sampling approach

As mentioned at the beginning of this chapter, the validation of the robustness of R-STORM UC solutions was performed through a Monte Carlo (MC) sampling approach. This MC sampling aims to create thousand (1000) random scenarios for each uncertainty budget and wind forecasted generation profile, under the model of wind power generation uncertainty. Therefore, considering the upper and lower levels of the uncertainty set defined by Figure 5.6, it can be argued that the scenarios covered by this MC sampling are highly demanding, once a variation in almost the entire range of wind generation is allowed.

The methodology of this analysis is presented in Figure 5.7. As can be seen, the methodology consists in, once the status of the binary variables that indicate the thermal and hydropower plants that are online at a given time period ($U_{j,t}$ and $Vh_{hd,t}$, respectively, also known as first stage solution) are maintain fixed, determinate the dispatch solutions (i.e. second stage solutions) considering a set of random wind generation scenarios, created considering uncertainty budget parameter ($Bgt_{busWind}$).

The generation of the Monte Carlo sampling wind generation scenarios follows the formulation of (5.2), previously used [35]. In (5.2) a random variable $rm_{busWind,t,MCs}$ is generated for each *Windbus*, time period and random scenario, using a uniform distribution over [0, 1]. According to the value of $rm_{busWind,t}$, the binary variables that indicate if the wind power deviates to the upper or lower level of the uncertainty ($Zpos_{busWind,t}$ and $Zneg_{busWind,t}$) are stablished. Once (5.2) was applied to all the time instants over the analysis period (T), the inequation $\sum_{t=1}^{T} Zpos_{busWind,t} + Zneg_{busWind,t} \leq Bgt_{busWind}$ is verified. If this inequation is true, then binary $Zpos_{busWind,t}$, $Zneg_{busWind,t}$ set is valid and used to calculate the dispatch solution; if the inequation is false, (5.2) is reevaluated for each time instant.

$$\begin{aligned} &Zpos_{busWind,t} = 0;\ Zneg_{busWind,t} = 1,\ \text{if}\ rm_{busWind,t} \leq Bgt_{busWind}/2T\ ; \\ &Zpos_{busWind,t} = 1;\ Zneg_{busWind,t} = 0,\ \text{if}\ rm_{busWind,t} \geq (1 - Bgt_{busWind}/2T)\ ; \\ &Zpos_{busWind,t} = 0;\ Zneg_{busWind,t} = 0,\ \text{otherwise.} \end{aligned} \qquad (5.2)$$

The second stage solution, i.e. the dispatch solution, varies based on the values of $Zpos_{busWind,t}$ and $Zneg_{busWind,t}$ generated by the Monte Carlo sampling.

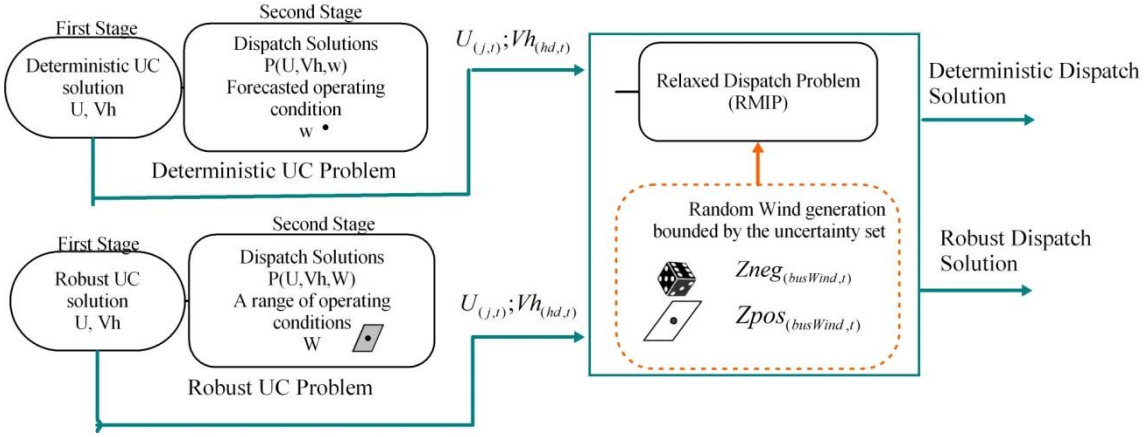

Figure 5.7 Monte Carlo sampling methodology.

For comparison reasons, the described Monte Carlo sampling approach was applied to two optimization models:

a) STORM model with the data base of Systems A and B, as it corresponds (deterministic approach with spinning reserve).
b) R-STORM with uncertainty budget zero (deterministic approach without spinning reserve); and with uncertainty budgets 2, 4, 6, 8 and 10 (robust approach);

The uncertainty budget definition for Monte Carlo sampling analysis follows the value used by the R-STORM model that is 2, 4, 6, 8 or 10 as it corresponds for each simulation case.

5.2.1. Case Study-System A

System Description

The first case study considers the power system shown in Table 5-10 and Figure 5.8. This case study includes six thermal power plants distributed between buses B1, B6, B7-8 and B10, one nuclear power plant at B7-8, one wind farm at B1 and 5 hydropower plants distributed between buses B2, B3, B4 and B9, wherein the two hydropower plants at B2 operate in cascaded mode. The operation of small hydro and thermal power plants is considered seasonally and, therefore, remains constant during the simulation time. In order to avoid infeasibilities, flexible and expensive thermal plants, called

Penalty plants, are considered at B1-B3, B6, B7-8 and B10. The simulation time horizon (T) is 24 hours.

Table 5-10 Power mix for system A.

Power Source*	#Units	Installed Capacity (MW)	% of total installed capacity
ST-COAL	1	350	4.2%
OGT-GAS	2	732.1	8.7%
CCGT-GAS	2	1062.2	12.7%
IC-HFO	1	174.6	2.1%
Hydro-RES	2	1525	18.2%
Hydro-ROR	3	1540	18.4%
SU-Hydro	-	416.295	5.0%
SU-Thermal	-	669.725	8.0%
NUC-UR	1	640	7.6%
Wind Pwr	1	1261	15.1%

*The thermal power plant names are divided in two parts: technology + fuel. The technologies are combined cycle – CC, Open cycle – OGT, Steam turbine –ST, Internal combustion generator –IC, Nuclear power -NUC. Hydro-RES stands for hydropower units with reservoir, Hydro-ROR for run-of-river hydropower units and SU for small units.

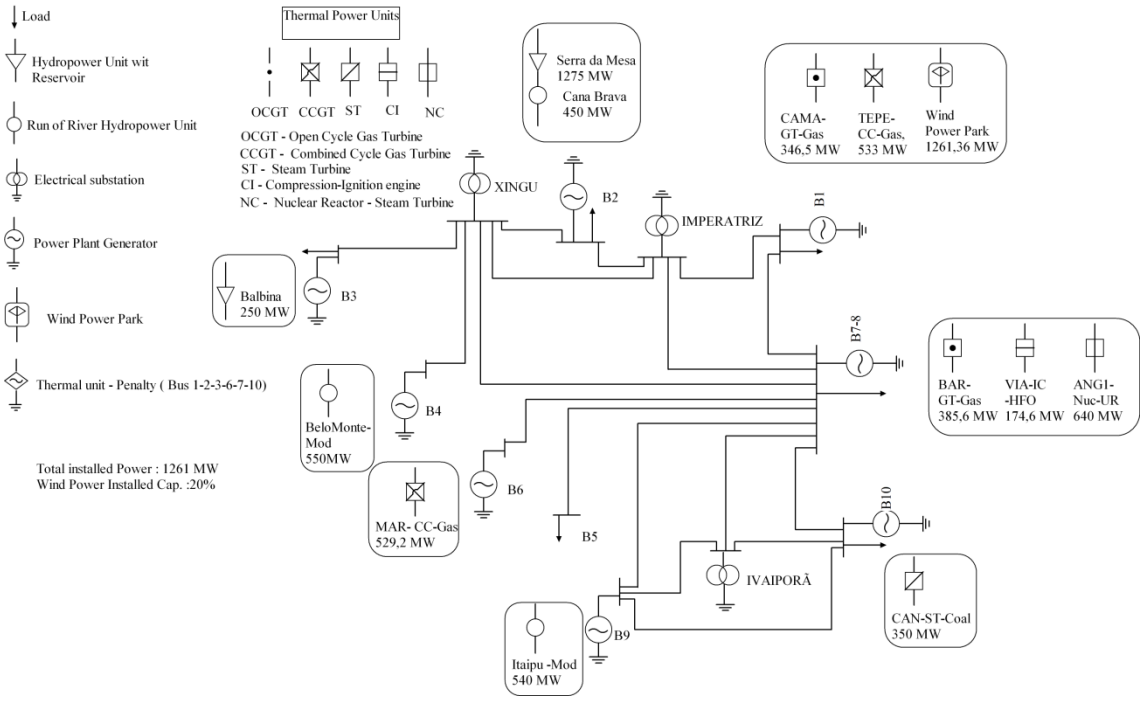

Figure 5.8 Case study – System A.

The demand profile is showed in Figure 5.9.

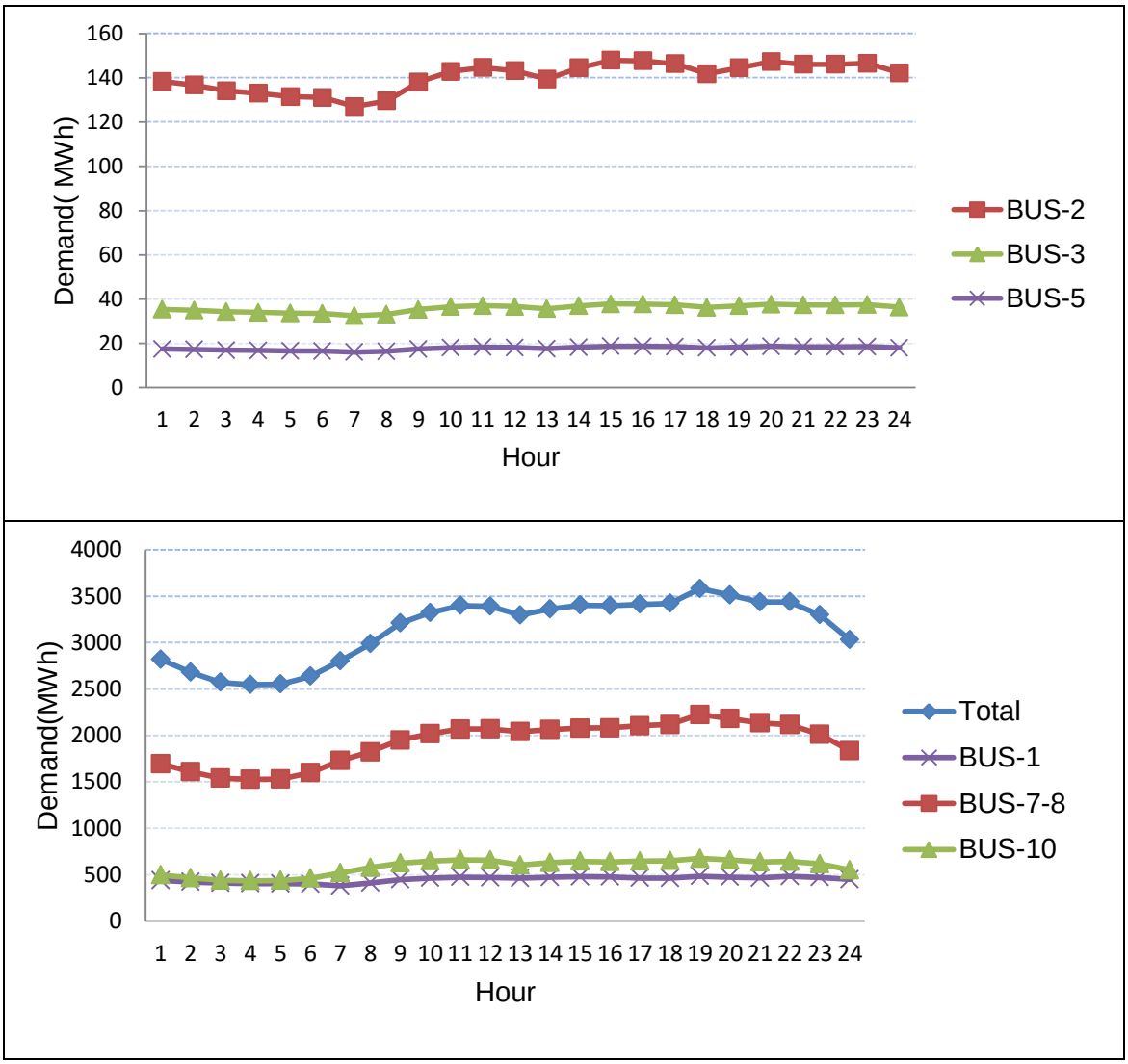

Figure 5.9 Hourly demand for System A.

Simulation Results

Table 5-11 shows the R-STORM UC optimal solution for two uncertainty budgets, $Bgt_{busWind} = 0$ (deterministic approach without spinning reserve) and $Bgt_{busWind} = 10$. In other words, Table 5-11 shows the status of the binary variables $U_{j,t}$ and $Vh_{hd,t}$ which define if thermal power plant j and hydropower plant hd are online for the simulation time t. As shown, the UC solution for budget $Bgt_{busWind} = 10$ demanded a higher number of online thermal generator plants than the UC solution for budget $Bgt_{busWind} = 0$ for the same load profile. Even though this result implies a higher operation cost, this extra-cost translates into a more flexible system.

Table 5-11 Robust UC solution for System A.

Period	Robust UC solution - Budget =0			Robust UC solution - Budget =10				
	Therm. Gen.	Hydro Generators		Thermal Generators			Hydro Generators	
	CAN-ST-COAL	SERRA DA MESA	BALBINA	TEPE-CC-GAS	MAR-CC-GAS	CAN-ST-COAL	SERRA DA MESA	BALBINA
0	0	1	1	0	0	1	1	1
1	0	1	1	0	0	1	1	1
2	0	1	1	0	0	1	1	1
3	0	1	1	0	0	1	1	1
4	0	1	1	0	0	1	1	1
5	0	1	1	0	0	1	1	1
6	0	1	1	0	0	1	1	1
7	0	1	1	0	0	1	1	1
8	1	1	1	0	1	1	1	1
9	1	1	1	0	1	1	1	1
10	1	1	1	0	1	1	1	1
11	1	1	1	0	1	1	1	1
12	1	1	1	1	0	1	1	1
13	1	1	1	1	0	1	1	1
14	1	1	1	1	0	1	1	1
15	1	1	1	1	0	1	1	1
16	1	1	1	1	0	1	1	1
17	1	1	1	1	0	1	1	1
18	1	1	1	1	0	1	1	1
19	1	1	1	1	0	1	1	1
20	1	1	1	1	0	1	1	1
21	1	1	1	1	0	1	1	1
22	1	1	1	1	0	1	1	1
23	1	1	1	0	0	1	1	1

Figure 5.10 compares the operation cost of R-STORM UC solutions, as the uncertainty budget increases, against the Deterministic UC solution for the ideal situation in which the wind energy forecasted profile actually happens. As expected, this increased participation of thermal plants in the UC solution implies in operational cost rise. More specifically, as illustrated in Figure 5.10 in the robust solution the thermal operation cost can increase up to 27%. However, this additional thermal power generation means less hydropower energy used to meet the demand; which translates in more stored water in the reservoirs. An increment on the reservoir volumes represents a negative cost in the objective function (see eq. (4.7)). Therefore, the higher thermal operation cost is partially compensated with this negative hydropower cost and the increase in the total operation cost is lower. For example, in the case of the conservative approach ($Bgt_{busWind} = 10$) the increase in the system operation cost is less than 10%.

$Bgt_{busWind} = 10$ is a conservative approach once, as presented in Section 2.2.2, represents a UC Robust optimal solution with probability of constraint violation lower than 2%.

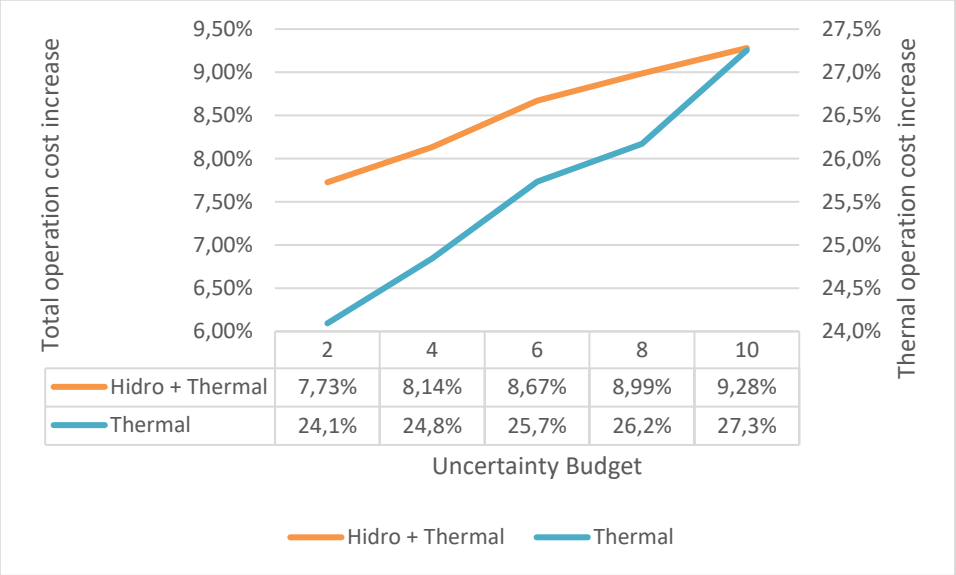

Figure 5.10 Percentage increase of Robust UC cost vs Deterministic approach cost with NO spinning reserve for wind power equal to the forecasted wind profile.

The temporal distribution of variables $Zpos_{busWind,t}$ and $Zneg_{busWind,t}$ that defines the worst- case scenario for wind power output in the case of $Bgt = 10$ is shown in Figure 5.11. As shown, all values of $Zpos_{busWind,t}$ are calculated as zero. This can be explained due to the fact that the forecasted value is closer to the upper bound than to the lower bound, as can be seen in Figure 5.6. Therefore, the system is more stressed by making the wind power output deviated to the lower bound, given that the resulting worst-case scenario will present higher ramp requirements.

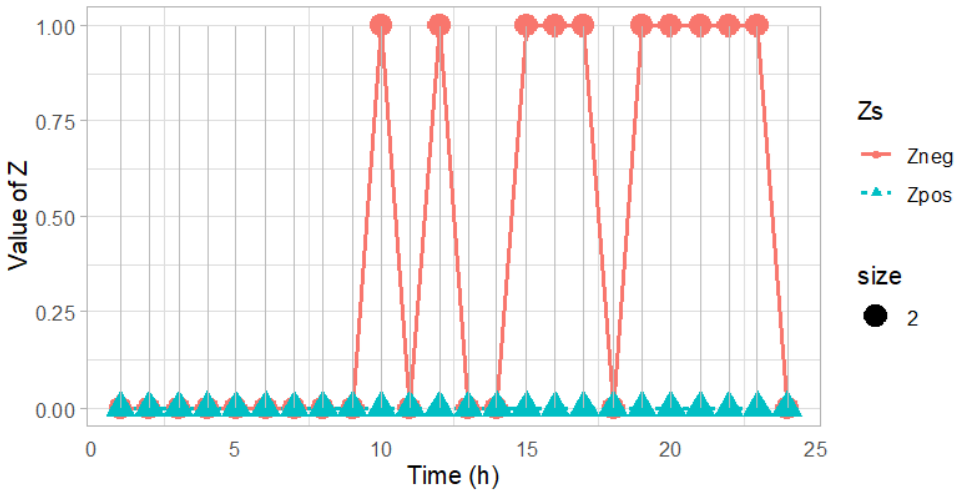

Figure 5.11 Distribution of $Zpos_{B1,t}$ and $Zneg_{B1,t}$ for the worst case scenario.

Figure 5.12 shows the results of the Monte Carlo sampling analysis for all the uncertainty budgets previously indicated (2, 4, 6, 8 and 10). As it can be seen, the R-STORM UC solutions were able to handle satisfactorily the wind energy variability without the use of penalty plants in all the thousand Monte Carlo scenarios for each uncertainty budget. On the other hand, it could be observed that the UC solutions obtained by the deterministic model without spinning reserve were infeasible (i.e. penalty plants were turn on) for many Monte Carlo sampling cases in each uncertainty budget. These results show the superiority of the robust approach over the deterministic one regarding system reliability. This observation indicates that it could be shortsighted to rely on forecasted values overlooking the uncertainty of wind energy. For power system operations, which tend to be risk-averse, Robust optimization can be an interesting approach to tackle uncertainty and maintain system stability.

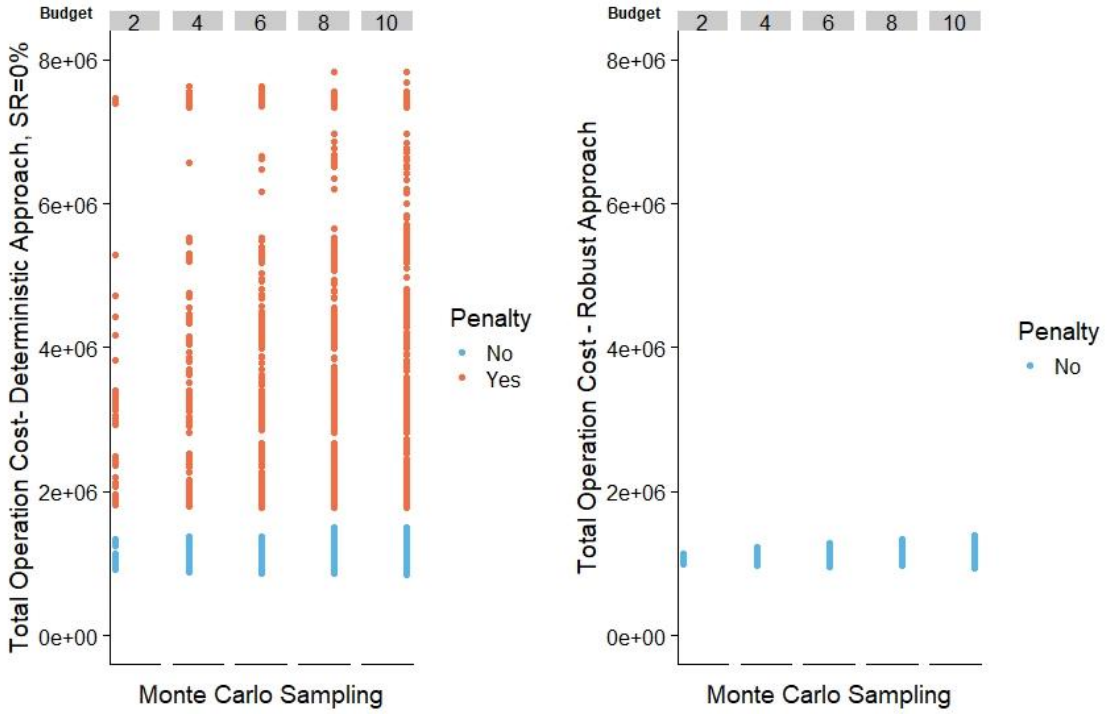

Figure 5.12 Monte Carlo sampling results for deterministic and robust approaches considering different uncertainty budgets – System A.

It can be derived from Figure 5.12 that the higher operational costs that the described robust optimization approach could cause are satisfactorily compensated by more flexibility. Furthermore, in the case of wind power deviations from the foreseen, the R-STORM UC decisions are in fact more economically appropriate that the ones obtained by the deterministic approach. Nonetheless, this economical comparison could be considered as unfair since it does not consider any spinning reserve for the deterministic

model, which is a typical resource to deal with power balance uncertainties in power system operations. Therefore, additional comparisons in which different values of spinning reserve are established for a deterministic model were performed. For this analysis, the STORM model described in Chapter 3 with the data base of System A is employed. The spinning reserve definition of this model is done by eq. (3.57) in Section 3.2.5

The results of this analysis, showed in Figure 5.13, indicate that only when a spinning reserve (variable *spin* in the formulation of (3.57)) of 32% was set for the deterministic model this was feasible; i.e. no penalty plants were used in all Monte Carlo sampling events.

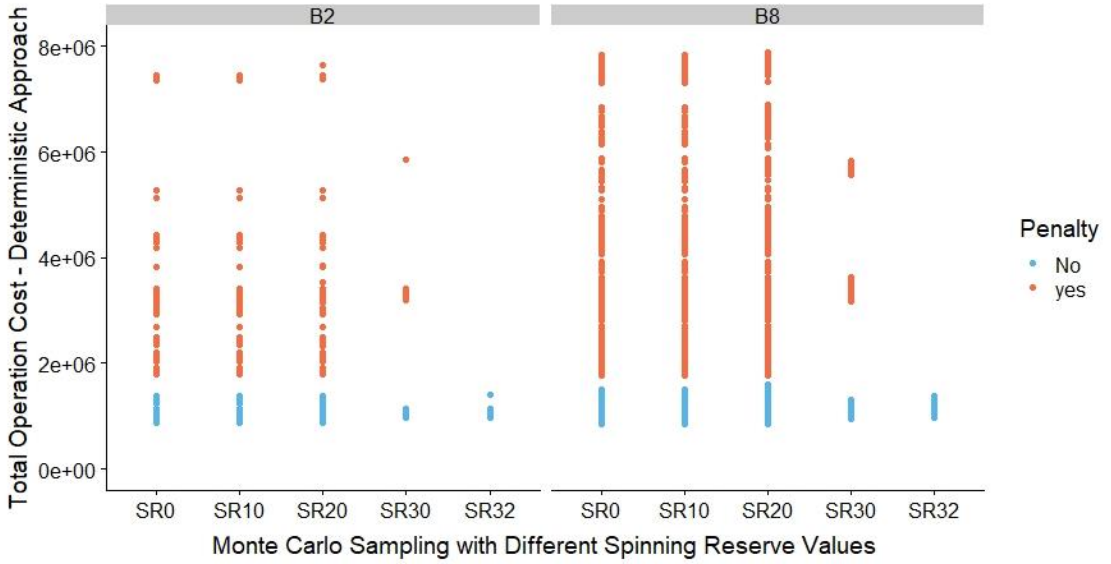

Figure 5.13 Monte Carlo sampling sensibility analysis of required spinning reserve for the deterministic approach.

Even though a spinning reserve level of 32% may seem as a high number, it is important to highlight that, as it can be seen in Figure 5.14, for some time periods of the day the wind energy at bus B-1 is responsible for meeting up to 43% of the total demand. Therefore, since the Monte Carlo sampling was focused in finding a spinning level that will be able to handle any variation of wind power, it was expected a significant amount of spinning reserve. Additionally, the definition of spinning reserve, showed in eq. (3.57), considers only the fraction of net load[15] supplied by the following dispatchable power sources: thermal power plants (without considering nuclear power)

[15] Net load is defined as the total load minus the power energy not supply by thermal power and hydropower units with reservoir.

and hydro power plants with reservoirs; different from other approaches where it is defined as a percentage of the total load. Another difference of the spinning reserve indicator considered in this work in contrast with other methodologies is that it is constant over the analyzed period. For future works it could be interesting to define a dynamic spinning reserve that varies through time.

Although the introduction of spinning reserve in the deterministic model can allow feasible unit commitment decisions, considering the variability and uncertainty of wind generation, it is important to highlight that in the case of Robust optimization the power system operator would not have to define reserve requirements based on deterministic criteria, this because the Robust approach already considers the uncertain data and delivers the appropriate UC solution without spinning reserve constraints.

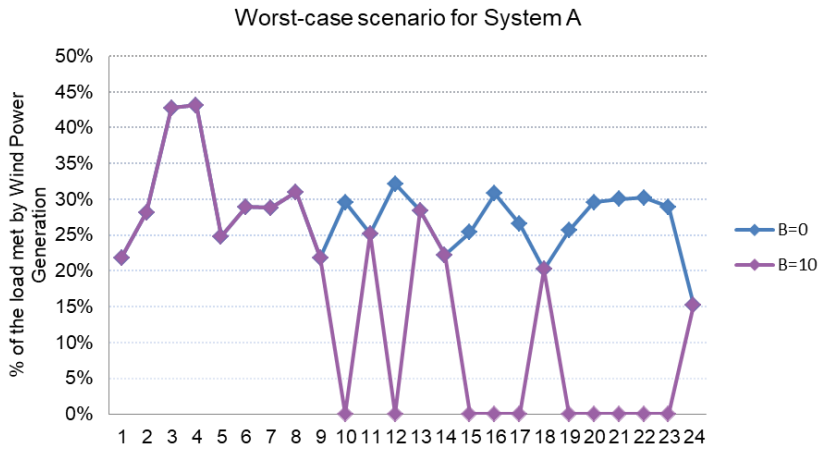

Figure 5.14 Percentage of the load met by wind generation for $Bgt = 0$ and by the worst-case scenario with $Bgt = 10$.

Finally, Figure 5.15 presents the system operation cost for the Monte Carlo sampling analysis for both Robust and Deterministic with spinning reserve of 32% optimization approaches. The difference between the total cost of the Deterministic approach and the total cost of the Robust approach is presented in Figure 5.16. As observed, the mean cost of the Monte Carlo events for all uncertainty budgets are lower using the Robust optimization method, which makes this approach a more cost-efficient solution. Even though some of the overcost of the deterministic approach could be originated by using a static value for the spinning reserve, this result also can be seen as a confirmation that defining the reserve requirement by some *a priori* system-wide rule can lead to an economically inefficient or even infeasible way to handle uncertainty.

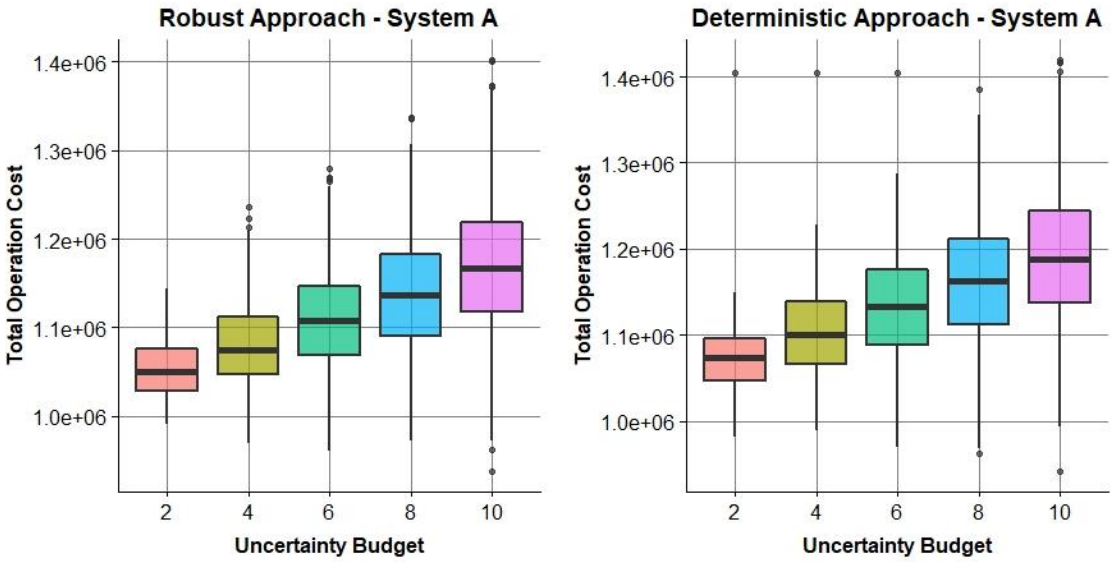

Figure 5.15 Box plot Analysis for the Monte Carlo sampling results (Deterministic approach with spinning reserve of 32%).

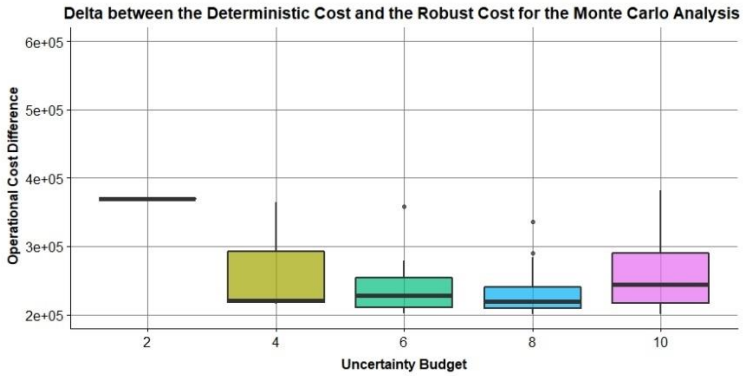

Figure 5.16 Box plot Analysis for the Monte Carlo sampling results (Deterministic approach minus Robust approach).

5.2.2. Case study-System B

Description

The second case study is show in Table 5-12 and Figure 5.17. In contrast with the system A, this case considers twenty thermal power plants distributed along buses B1-3, B6, B7-8 and B10, a nuclear power plant at B7-8, a wind farm at B1 and seventeen hydropower plants at B1-5, B7-10 as power system generation plants. Two different configurations of cascade mode were included. The first one is at Bus B-2 considering

four hydropower plants and the second one at Bus7-8 considering three hydropower plants. The simulation time horizon is 24 hours.

Table 5-12 Power mix for system B.

Power Source*	#Units	Installed Capacity (MW)	% of total installed capacity
ST-COAL/BIO	5	1836,1	7,3%
OGT-GAS	5	1362,48	5,4%
CCGT-GAS	5	2355,3	9,3%
IC-HFO	5	637	2,5%
Hydro-RES	9	8694,2	34,5%
Hydro-ROR	8	3371,7	13,4%
NUC-UR	1	640	2,5%
Wind Pwr	1	6307	25,0%

*The thermal power plant names are divided in two parts: technology + fuel. The technologies are combined cycle – CC, Open cycle – OGT, Steam turbine –ST, Internal combustion generator –IC, Nuclear power -NUC. Hydro-RES stands for hydropower units with reservoir, Hydro-ROR for run-of-river hydropower units and SU for small units.

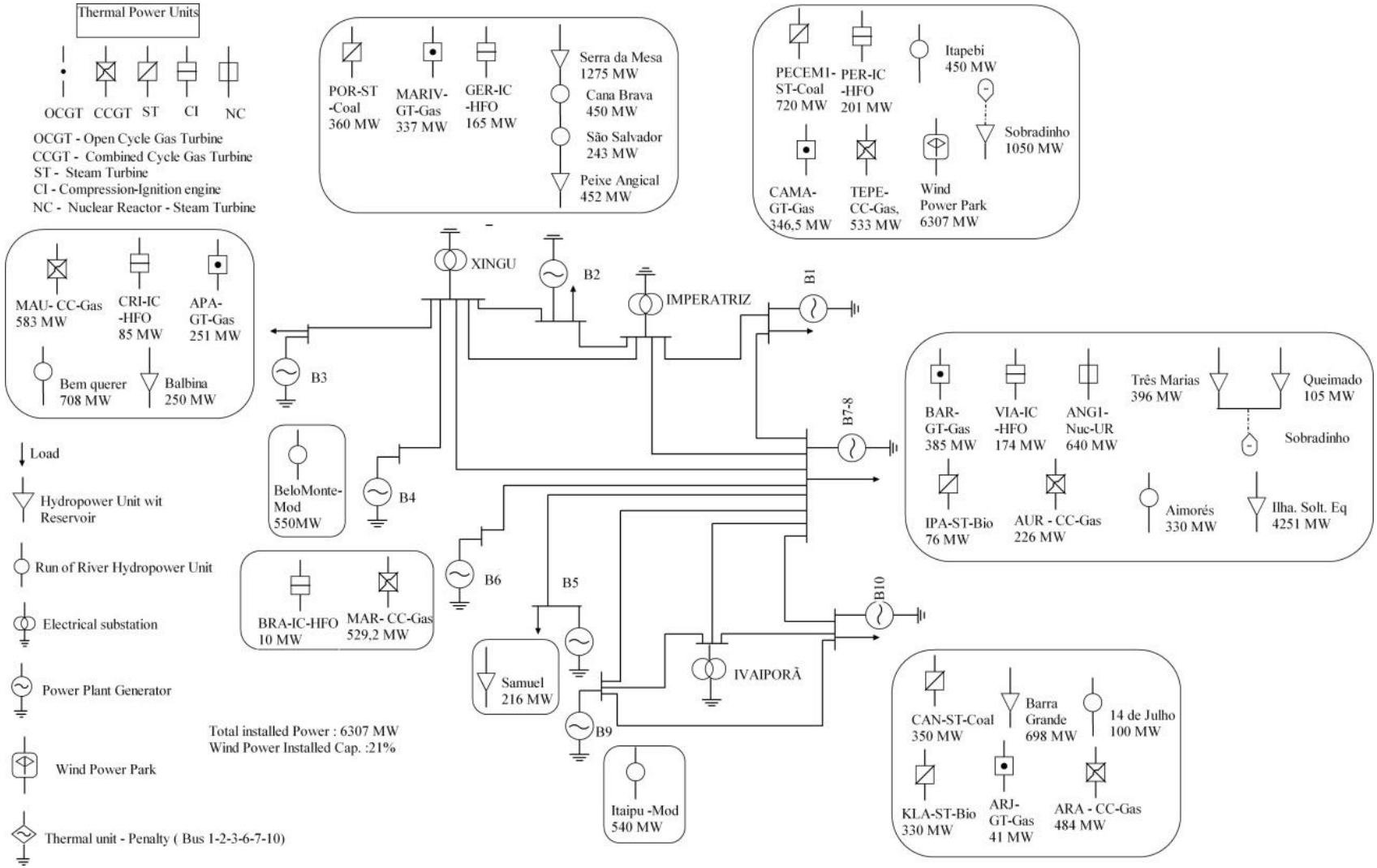

Figure 5.17 Case study System B schematic description.

The total demand profile is shown in Figure 5.18. The hourly profile was maintained but the demand was increase five times compared with that of system A.

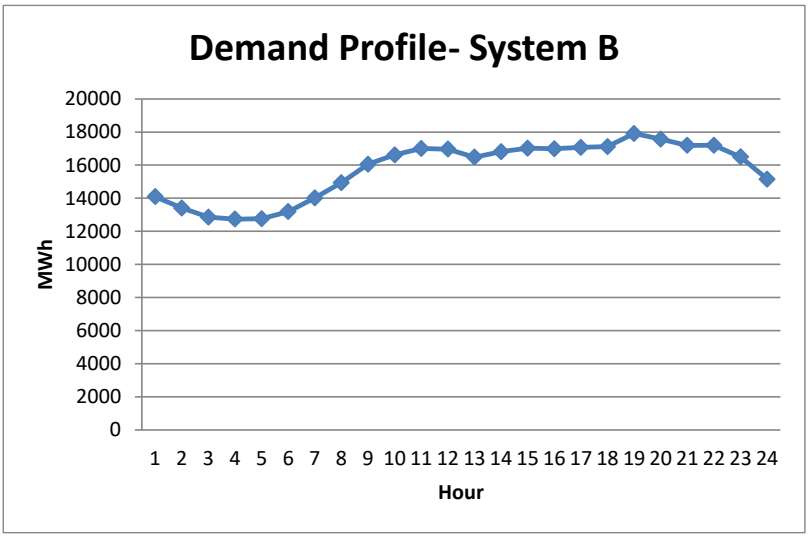

Figure 5.18 Hourly demand for System B.

Results

As presented for the results of system A, Table 5-13 shows the Robust UC optimal solution for two uncertainty budgets ($Bgt_{busWind}$ = 0 and $Bgt_{busWind}$=10). It can be observed that the UC solution for budget $Bgt_{busWind} = 10$ demanded, once again, a higher number of online generator plants than the UC solution for budget $Bgt_{busWind} = 0$.

Table 5-13 Robust UC solution for System B.

Period	Robust UC solution - Budget =0														Robust UC solution - Budget =10														
	Thermal Generators					Hydro Generators									Thermal Generators										Hydro Generators						
	PECEM1-ST-COAL	POR-ST-COAL	IPA-ST-BIO	CAN-ST-COAL	KLA-ST-BIO	BARRA GRANDE	I. SOLT. EQV	TRÊS MARIAS	QUEIMADO	SERRA DA MESA	SOBRADINHO	BALBINA	SAMUEL	PEIXE ANGICAL	TEPE-CC-GAS	PECEM1-ST-COAL	POR-ST-COAL	MAU-CC-GAS	MAR-CC-GAS	AUR-CC-GAS	IPA-ST-BIO	ARA-CC-GAS	CAN-ST-COAL	KLA-ST-BIO	BARRA GRANDE	I. SOLT. EQV	TRÊS MARIAS	QUEIMADO	SERRA DA MESA	SOBRADINHO	BALBINA	SAMUEL	PEIXE ANGICAL
0	0	0	0	0	0	1	1	1	1	1	1	1	1	1	0	0	1	0	0	0	0	0	0	0	1	1	1	1	1	1	1	1
1	0	0	0	0	0	1	1	1	1	1	1	1	1	1	0	0	1	0	0	0	0	0	0	0	0	1	1	1	1	1	1	1
2	0	0	0	0	0	0	1	0	1	1	1	0	0	1	0	0	1	0	0	0	0	0	0	0	1	1	1	1	0	1	1	1
3	0	0	0	0	0	0	1	0	1	1	1	1	1	1	0	0	1	0	0	0	0	0	0	0	0	1	1	1	0	1	1	1
4	1	0	0	0	0	1	1	1	1	1	1	1	1	1	0	0	1	0	0	0	0	0	0	0	0	1	1	1	1	1	1	1
5	1	0	0	0	0	1	1	1	1	1	1	1	1	1	0	0	1	0	0	0	0	0	0	0	0	1	1	1	1	1	1	1
6	1	1	0	1	0	1	1	1	1	1	1	1	1	1	0	0	1	0	0	0	0	0	1	0	0	1	1	1	1	1	1	1
7	1	1	0	1	1	1	1	1	1	1	1	1	1	1	0	1	1	0	0	0	0	0	1	0	0	1	1	1	1	1	1	1
8	1	1	1	1	1	1	1	1	1	1	1	1	1	1	0	1	1	0	0	0	0	1	1	1	1	1	1	1	1	1	1	1
9	1	1	1	1	1	1	1	1	1	1	1	1	1	1	0	1	1	0	0	0	1	1	1	1	1	1	1	1	1	1	1	1
10	1	1	1	1	1	1	1	1	1	1	1	1	1	1	0	1	1	0	0	0	1	1	1	1	1	1	1	1	1	1	1	1
11	1	1	1	1	1	1	1	1	1	1	1	1	1	1	0	1	1	0	0	0	1	1	1	1	1	1	1	1	1	1	1	1
12	1	1	1	1	1	1	1	1	1	1	1	1	1	1	0	1	1	0	0	0	1	0	1	1	1	1	1	1	1	1	1	1
13	1	1	1	1	1	1	1	1	1	1	1	1	1	1	0	1	1	0	0	0	1	0	1	1	1	1	1	1	1	1	1	1
14	1	1	1	1	1	1	1	1	1	1	1	1	1	1	1	1	1	0	0	0	1	0	1	1	1	1	1	1	1	1	1	1
15	1	1	1	1	1	1	1	1	1	1	1	1	1	1	1	1	1	0	0	0	1	0	1	1	1	1	1	1	1	1	1	1
16	1	1	1	1	1	1	1	1	1	1	1	1	1	1	1	1	1	1	1	0	1	0	1	1	1	1	1	1	1	1	1	1
17	1	1	1	1	1	1	1	1	1	1	1	1	1	1	1	1	1	1	1	0	1	0	1	1	1	1	1	1	1	1	1	1
18	1	1	1	1	1	1	1	1	1	1	1	1	1	1	0	1	1	1	1	1	1	1	1	1	1	1	1	1	1	1	1	1
19	1	1	1	1	1	1	1	1	1	1	1	1	1	1	0	1	1	1	1	1	1	1	1	1	1	1	1	1	1	1	1	1
20	1	1	1	1	1	1	1	1	1	1	1	1	1	1	0	1	1	0	0	1	1	1	1	1	1	1	1	1	1	1	1	1
21	1	1	1	1	1	1	1	1	1	1	1	1	1	1	0	1	1	0	0	1	1	1	1	1	1	1	1	1	1	1	1	1
22	1	1	1	1	1	1	1	1	1	1	1	1	1	1	0	1	1	0	0	0	1	0	1	1	1	1	1	1	1	1	1	1
23	1	1	1	1	1	1	1	1	1	1	1	1	1	1	0	1	1	0	0	0	1	0	1	1	1	1	1	1	1	1	1	1

The temporal distribution of variables $Zpos_{busWind,t}$ and $Zneg_{busWind,t}$ that defined the worst- case scenario for wind power output in the case of $Bgt_{busWind}$=10 is shown in Figure 5.19. Since the wind profile was maintained, the behaviour of the variables $Z_{busWind,t}$ over the time is similar to those obtained for system A. In other words, the wind power output is also deviated to the lower bound in order to challenge the system operation. It is important to highlight, however, that the exact curve over the time differs from the one obtained in the case analysis A because of the introduction of new power sources with different power slope characteristics.

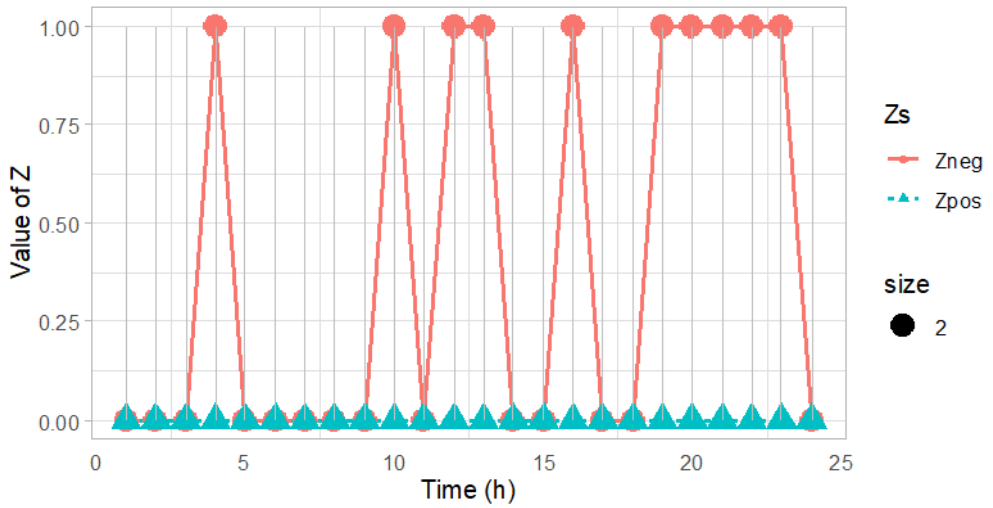

Figure 5.19 Distribution of $Zpos_{B1,t}$ and $Zneg_{B1,t}$ for System B worst-case scenario with Bgt_{busWind}=10.

The Monte Carlo sampling analysis results for this case system are shown in Figure 5.20. As can be seen, the Robust UC solution was again able to handle the wind energy variability and uncertainty without using penalty plants. In other words, it provides feasible solutions for all the Monte Carlo sampling scenarios of each uncertainty budget. The deterministic optimal solutions, on the other hand, had to turn on penalty plants in many sampling scenarios for all the uncertainty budgets considered.

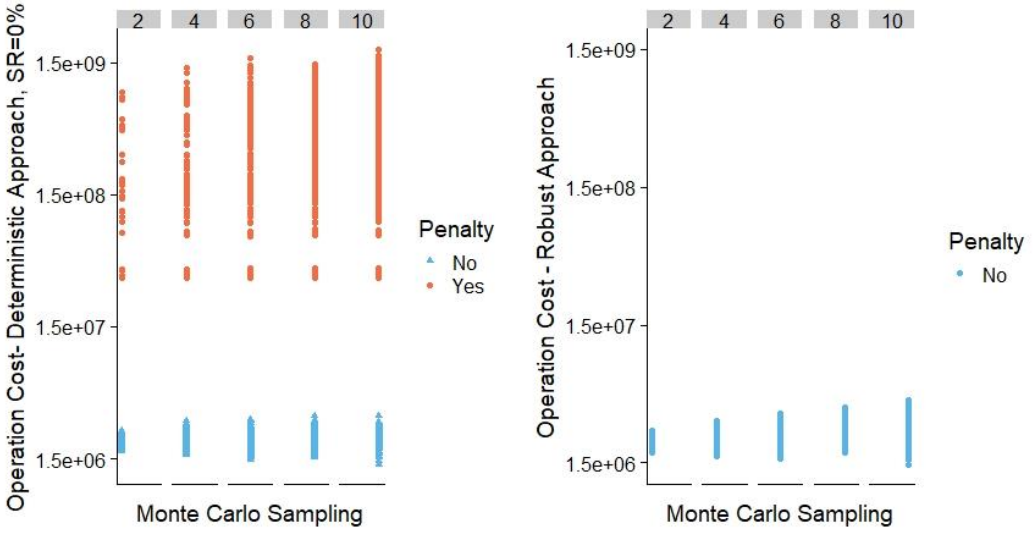

Figure 5.20 Monte Carlo sampling sensibility analysis for different uncertainty budgets – System B.

As performed for the case study A, a spinning reserve analysis, considering the deterministic model (STORM with system B database) was also performed, maintaining the same methodology. The result of this analysis indicated that the value of spinning reserve required to make the deterministic model feasible for all considered levels of uncertainty (i.e. uncertainty budgets 2, 4, 6, 8 and 10) is of 43%; this means that, according to eq. (3.57), the available generation by dispatchable thermal (without considering nuclear) and hydro generation plants should be 43% higher than the net load.

In this analysis, wind energy also represents an important source to meet the demand. As shown in Figure 5.21, in some time periods of the day the wind energy at bus B-1 is responsible of meeting up to 43% of the total demand.

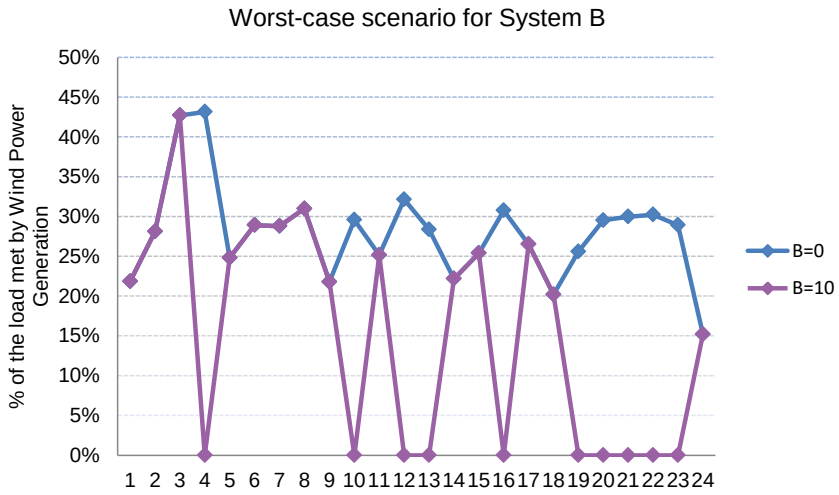

Figure 5.21 Worst-case scenario for Budget $Bgt_{busWind}$ =10 – System B.

The results of the Monte Carlo sampling analysis for the system operation cost are shown in are Figure 5.22 and Figure 5.23. It is observed that, once again, the Robust optimization model delivered the most cost-efficient solution (from an average perspective) for all considered levels of uncertainty.

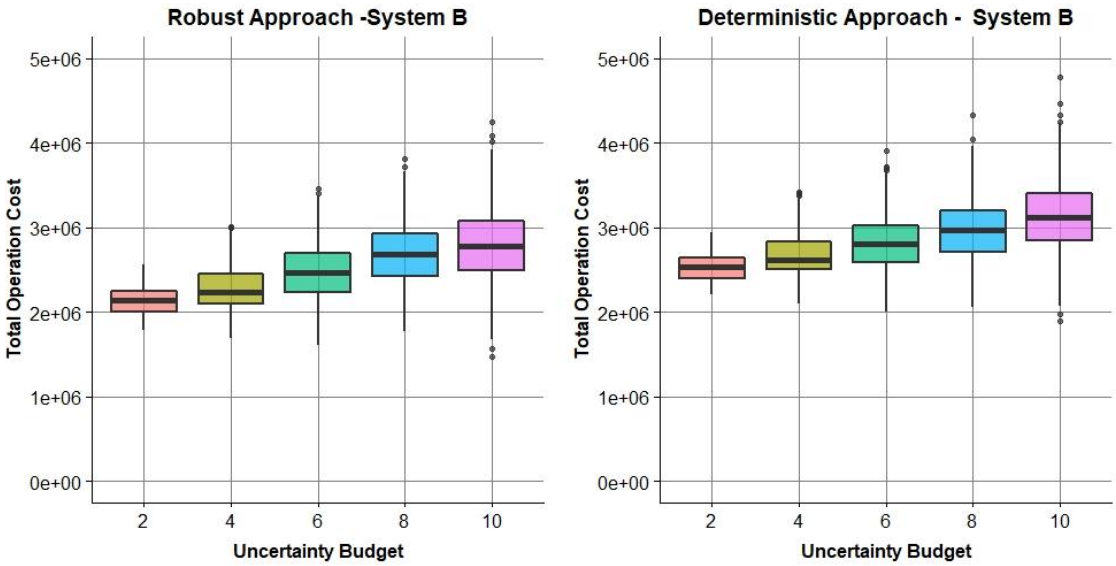

Figure 5.22 Box Analysis for the Monte Carlo sampling results (Deterministic approach with spinning reserve of 43%).

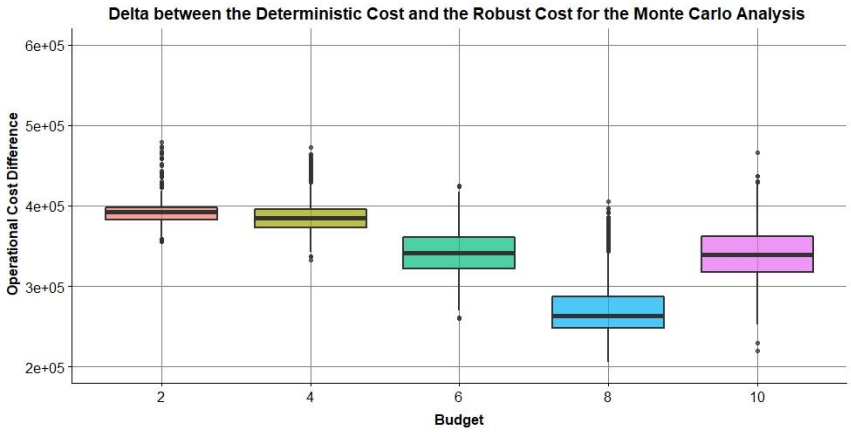

Figure 5.23 Box plot Analysis for the Monte Carlo sampling results (Deterministic approach minus Robust approach).

5.2.3. Computational performance

In this section the computational performance of the R-STORM was tested for different uncertainty budgets. The computational time required for the simulation of each of the uncertainty budget considered in this study, for both case systems, is shown

in Figure 5.24. As can be seen, the computational time increases exponentially as the budget uncertainty increases. This can be explained, based on the experiments, by two main reasons: i) Even though the size of the slave problem remains the same for different uncertainty budgets, this problem needs more time to solve since its complexity is higher due to the larger number of combinatorial options for the binary variables $Z_{busWind,t}$ and ii) more Benders' cuts are added to the master problem in order to solve the model as the uncertainty budget increases.

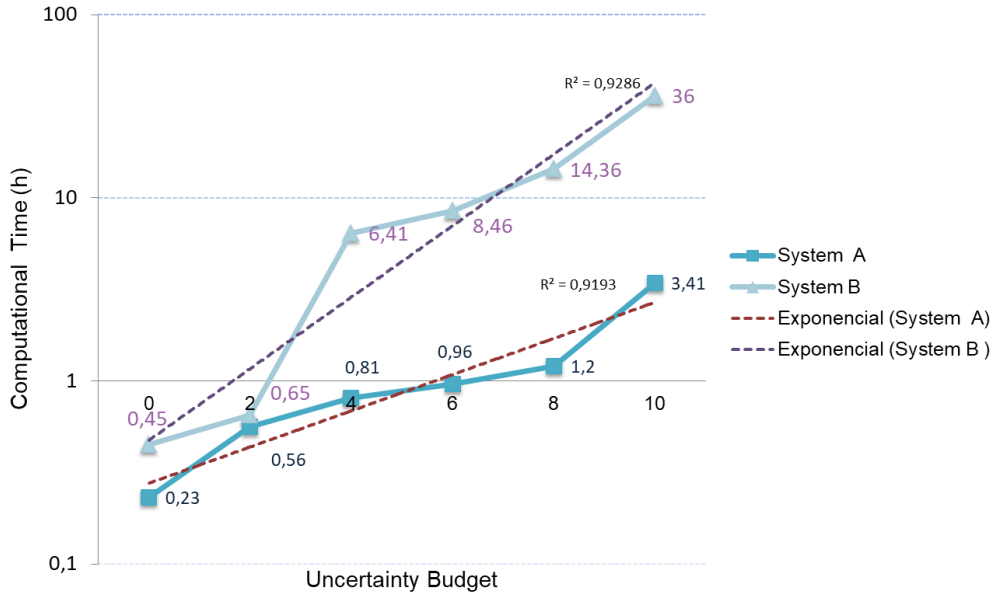

Figure 5.24 Budget Sensibility analysis for both System A and B considering the time period simulation of 24 hours.

Table 5-14 presents the model statistics for both case systems (A and B) with uncertainty budget equal to eight. As can be seen, the size of system B is some 3 times as high as that of system A, which explains the higher computational time difference between these two case studies.

Table 5-14 Model Statistics considering $Bgt_{busWind}$=*8* and time period simulation *T=24*.

	Type of prob.	Block of eq.	Block of var.	Non zero elements	Single eq.	Single var.	Discrete var.
System A	Master Problem	7	6	128,739	1.145	471	469
	Slave Problem	18	31	12,179	962	2,977	48
System B	Master Problem	7	6	490,703	3.415	1,541	1,539
	Slave Problem	18	31	34,869	2.618	8,017	48

As shown, even though the results presented in Sections 5.2.1 and 5.2.2 show that Robust optimization for hydrothermal UC problems can guarantee stability and feasibility for systems with wind power uncertainty, it can require significant computation effort, especially since both master and slave problems have binary decision variables. For future works, it could be interesting to implement an acceleration technique for Benders decomposition in order to facilitate the model application to large-scale power systems such as the Brazilian power system.

Chapter 6

Conclusions and Future Work

Demand for energy and associated services, to meet social and economic development and improve human welfare and health, is increasing. All societies require energy services to meet basic human needs such as lighting, cooking, space comfort, mobility, communication among others. At the same time, power sectors are evolving into low-carbon energy mix, with higher shares of renewable energy technologies. These intermittent technologies, however, bring operational challenges that must be addressed in order to maintain power system reliability. In this sense, energy modelers should take a deeper look at improving ways to better represent the variability and uncertainty of renewable generation. The ongoing energy transition can be the perfect scenario for policy makers and stakeholders to take action and deliver a more sustainable agenda. However, this agenda must be grounded on comprehensive data and advanced modelling techniques that portray the most critical power system characteristics.

To decarbonise an economy is not a simple subtraction, it requires a completely overhaul, after all, the system grew up through the massive use of fossil fuels. The great challenge of the 21st century is to reverse the increase in emissions that the 20th century set in train and at twice the speed, without shrinking the economy in ways that compromise the system ability to meet the population needs. The damage that climate change will end up doing will depend on the human response over the next decade. We must be willing to transform the machinery of the world economy. The inclusion of sustainable investment products can help to manage exposure to climate change and reduce risk.

In this sense, renewable energy deployment can play and important role within a portfolio of mitigation options. Renewable energy has a large potential to mitigate climate change, but also it can provide wider benefits to the population such as contribute to social and economic development, increase energy access, secure energy

supply, and reduce negative impacts on the environment and health. Integrating renewable energy into most existing energy supply systems and end-use sectors at an accelerated rate can be technologically feasible, though will result in several additional challenges. An option to reduce complexity and risk is to include the development of complementary flexible generation and flexible operation of existing schemes; improve short-term forecasting, system operation and planning tools. Therefore, in order to accommodate high renewable energy shares, energy systems will need to evolve and to be adapted.

This thesis described the formulation and development of two power dispatch models: i) a deterministic hydrothermal economic dispatch model formulated as a large-scale mixed-integer linear problem, called STORM, and ii) a Robust hydrothermal unit commitment model that considers wind power energy as an uncertainty parameter, called R-STORM.

The STORM model represents with high detail the characteristics of the Brazilian generation system. Among this, an important feature of STORM is that it considers the hydraulic configuration of the Brazilian hydropower system i.e. the production function of hydro power plants and the flow balance including the cascade effect. The hydropower production function was model as a four-dimensional piecewise linear model that considers head variation in a single multivariate linear function of turbinated outflow, storage, and spillage. Additionally, the model does not impose that all wind power energy must be injected in the grid. That is, it allows wind curtailment in the case its use would represent a higher operation cost. In this model, the transmission system considers a DC power flow between the major Brazilian power markets.

A validation of the STORM model was performed by comparing its proposed economic dispatch for four days (each one for a different trimester) against the actual dispatch made by the power system operator. As shown by the obtained results, the model provides a good approximation to the actual dispatch, where the main difference was observed for the dispatched thermal power generation. As discussed in Chapter 5, this can be explained based on the dispatch decisions of thermal power plants, on account of system reliability requirements, by the Brazilian system operator and also due to the simplified transmission system of STORM. As a matter of fact, for the days in which the non-economic dispatch of thermal generations reported by ONS was low (Day 1 and Day 2 in the comparison analysis), the difference between the energy

dispatched by STORM and the ONS dispatch, from hydro and thermal power, was lower than 2.5% and for Day 3 and Day 4, which had higher levels of non-economic thermal dispatch, the difference was less than 7%. Therefore, it is possible to affirm that the STORM model, in a simplified and yet adequate way, represents the Brazilian power system characteristics and can be a tool to reach a deeper understanding of the impacts of renewable energy integration in the Brazilian electricity system and to analyze supply reliability and the impacts of energy policies, such as feed-in-tariffs, quotas, carbon pricing mechanisms, incorporation of external costs for environmental impact assessment, and technology pathways like demand response programs.

Future research, related to the STORM model, includes: i) better specify thermal power units for the case study of the Brazilian power system, since most of the exogenous data for thermal power units was based on data available in the literature, ii) the improvement of the transmission grid representation by considering a more detailed electrical grid and iii) the development of a soft-link with the BLUES Model, COPPE's national IAM (Integrated Assessment Model). This link will allow exploring national low-carbon development pathways, in order to ensure their technical feasibility. In other words, this link can facilitate the assessment of transformation pathways focused on accomplish GHG emissions reductions. A combined tool as the one mentioned has much importance in a low-carbon development pathway, where variable renewable energy resources become more relevant in the electrical power system. It is important to mentioned that STORM can be adapted for any power system, and it can be extremely useful to represent systems with high shares of hydropower.

The R-STORM model, in turn, was formulated as a two-stage hydrothermal UC problem that deals with wind energy uncertainty using a Robust Optimization approach. This model has the objective of minimize the total operational cost under the worst wind power output scenario, while ensuring feasible solutions for all possible wind energy realizations within the model of data uncertainty, defined as a polyhedral set with a cardinality budget.

To the author's better knowledge, there is no literature related to Robust Optimization approaches applied to hydrothermal UC problems that considers the detailed operation of large water reservoirs for hydropower generation. This thesis tackled this gap by formulating and implementing a Robust UC model (R-STORM) that takes into account the main hydro power characteristics i.e. water balance with the

cascaded effect and a production function that considers variable net head and spillage effects.

The methodology solution for the R-STORM model was based on scientific literature that employs Benders' decomposition algorithm as a technique to obtain a robust UC solution for the day-ahead market. One of the difficulties to solve this robust problem stems from the bilinear block term presented in the dual slave problem, whose linearization was done using the big-M method, which translates the bilinear problem into a MIP problem. A Monte Carlo sampling approach was developed to evaluate the R-STORM performance under the model of data uncertainty and to compare the deterministic and Robust UC solutions.

The presented results showed that the model provides robust optimal solutions that are feasible under wind power output uncertainty, which increase the power system flexibility. Furthermore, these results validated the robust operation of the R-STORM dispatch and showed that overlooking the uncertainty of wind power can lead to unfeasible situations which could translate into economical-inefficient solutions such as high levels of spinning reserve, use of expensive plants or load sheading. Additionally, it was shown that the R-STORM UC solution is economically attractive even in the ideal situation of exact correspondence between the forecasted and actual wind generation, in other words a situation in which the wind generation is certain. This work provides an excellent starting point for further studies on the use of Robust UC to hydrothermal systems like the Brazilian.

A disadvantage of the R-STORM execution, on the other hand, is that its formulation represents much higher computational effort than its equivalent deterministic approach. It was showed that increasing the level of uncertainty causes exponential system complexity and higher computational requirements. In this sense, future research should include: i) implementation of a technique to accelerate the Benders' decomposition algorithm, ii) improvement of the approach for linearization of the bilinear terms, in order to avoid that the slave problem becomes a MIP formulation, iii) to update and extend the wind data information, perhaps using the forecasted error instead of wind energy as decision variable, in order better define the upper and lower bounds of the uncertainty set, iv) to analyze ways to model the correlations in wind power to better define the uncertainty set and v) to perform a deeper scalability analysis by adding more wind power farms connected at different buses. Additionally, comparisons using others

computational algorithms as solution methodologies, like Column and Constraint generation [85], are recommended as upcoming research efforts.

References

[1] IRENA, *Innovation Landscape for a Renewable-Powered Future : Solutions To Integrate Variable Renewables*. Bonn, Germany: International Renewable Energy Agency, 2019.

[2] S. Y. Abujarad, M. W. Mustafa, and J. J. Jamian, "Recent approaches of unit commitment in the presence of intermittent renewable energy resources: A review," *Renew. Sustain. Energy Rev.*, vol. 70, pp. 215–223, 2017.

[3] International Renewable Energy Agency, *Planning for the Renewable Future: Long-term modelling and tools to expand variable renewable power in emerging economices*. 2017.

[4] J. C. Smith, M. R. Milligan, E. A. DeMeo, and B. Parsons, "Utility wind integration and operating impact state of the art," *IEEE Trans. Power Syst.*, vol. 22, no. 3, pp. 900–908, 2007.

[5] F. A. Diuana, C. Viviescas, and R. Schaeffer, "an Analysis of the Impacts of Wind Power Penetration in the Power System of Southern Brazil," *Energy*, vol. 186, no. 2019, p. 115869, 2019.

[6] M. H. Albadi and E. F. El-Saadany, "Overview of wind power intermittency impacts on power systems," *Electr. Power Syst. Res.*, vol. 80, no. 6, pp. 627–632, 2010.

[7] GE Energy, "The Effects of Integrating Wind Power on Transmission System Planning, Reliability, and Operations," New York, 2005.

[8] H. Nosair and F. Bouffard, "Flexibility envelopes for power system operational planning," *IEEE Trans. Sustain. Energy*, vol. 6, no. 3, pp. 800–809, 2015.

[9] V. Oree and S. Z. S. Hassen, "A composite metric for assessing flexibility available in conventional generators of power systems," *Appl. Energy*, vol. 177, pp. 683–691, 2016.

[10] M. L. Kubik, P. J. Coker, and J. F. Barlow, "Increasing thermal plant flexibility in a high renewables power system," *Appl. Energy*, vol. 154, pp. 102–111, 2015.

[11] N. Menemenlis, M. Huneault, and A. Robitaille, "Thoughts on power system flexibility quantification for the short-term horizon," in *2011 IEEE power and energy society general meeting*, 2011, pp. 1–8.

[12] G. Morales-España, L. Ramírez-Elizondo, and B. F. Hobbs, “Hidden power system inflexibilities imposed by traditional unit commitment formulations,” *Appl. Energy*, vol. 191, pp. 223–238, 2017.

[13] EnerNex Corporation and Wind Logics Inc., “Wind Integration Study - Final Report.” Xcel Energy and Minnesota Department of, 2004.

[14] G. E. I. Inc., “Ontario Wind Integration Study - a report prepared for Ontario Power Authority (OPA) Independent Electricity System Operator and the Canadian Wind Energy Association (CanWEA).” New York, 2006.

[15] ILEX Energy Consulting and UMIST, “Quantifying the system costs of additional renewables in 2020.” a report to the Department of Trade & Industry, 2002.

[16] H. Zheng, J. Jian, L. Yang, and R. Quan, “A deterministic method for the unit commitment problem in power systems,” *Comput. Oper. Res.*, vol. 66, pp. 241–247, 2016.

[17] L. Lakshminarasimman and S. Subramanian, “A modified hybrid differential evolution for short-term scheduling of hydrothermal power systems with cascaded reservoirs,” *Energy Convers. Manag.*, vol. 49, no. 10, pp. 2513–2521, 2008.

[18] M. V. F. Pereira and L. M. V. G. Pinto, “Application of Decomposition Techniques to the MID - And Short - Term Scheduling of Hydrothermal Systems,” *IEEE Trans. Power Appar. Syst.*, vol. PAS-102, no. 11, pp. 3611–3618, 1983.

[19] R. Miranda, R. Soria, R. Schaeffer, A. Szklo, and L. Saporta, “Contributions to the analysis of ‘Integrating large scale wind power into the electricity grid in the Northeast of Brazil’[Energy 100 (2016) 401--415],” *Energy*, vol. 118, pp. 1198–1209, 2017.

[20] Y. Chen, F. Liu, W. Wei, S. Mei, and N. Chang, “Robust unit commitment for large-scale wind generation and run-off-river hydropower,” *CSEE J. Power Energy Syst.*, vol. 2, no. 4, pp. 66–75, 2016.

[21] K. K. Mandal and N. Chakraborty, “Differential evolution technique-based short-term economic generation scheduling of hydrothermal systems,” *Electr. Power Syst. Res.*, vol. 78, no. 11, pp. 1972–1979, 2008.

[22] M. V. F. Pereira, “Optimal stochastic operations scheduling of large hydroelectric systems,” *Int. J. Electr. Power Energy Syst.*, vol. 11, no. 3, pp.

161–169, 1989.

[23] S. Pereira, P. Ferreira, and A. I. F. Vaz, “Short-term electricity planning with increase wind capacity,” *Energy*, vol. 69, pp. 12–22, 2014.

[24] A. L. Diniz and M. E. P. Maceira, “A four-dimensional model of hydro generation for the short-term hydrothermal dispatch problem considering head and spillage effects,” *IEEE Trans. power Syst.*, vol. 23, no. 3, pp. 1298–1308, 2008.

[25] C. De Jonghe, B. F. Hobbs, and R. Belmans, “Optimal generation mix with short-term demand response and wind penetration,” *IEEE Trans. Power Syst.*, vol. 27, no. 2, pp. 830–839, 2012.

[26] N. Troy, E. Denny, and M. O’Malley, “Base-load cycling on a system with significant wind penetration,” *IEEE Trans. Power Syst.*, vol. 25, no. 2, pp. 1088–1097, 2010.

[27] T. Ackermann and others, *Wind power in power systems*, vol. 140. Wiley Online Library, 2005.

[28] D. Bertsimas, E. Litvinov, X. A. Sun, J. Zhao, and T. Zheng, “Adaptive Robust Optimization for the Security Constrained Unit Commitment Problem,” *IEEE Trans. Power Syst.*, vol. 28, no. 1, pp. 52–63, 2013.

[29] Long Zhao and Bo Zeng, “Robust unit commitment problem with demand response and wind energy,” *2012 IEEE Power Energy Soc. Gen. Meet.*, pp. 1–8, 2012.

[30] N. G. Cobos *et al.*, “Network-constrained unit commitment under significant wind penetration : A multistage robust approach with non-fixed recourse,” *Appl. Energy*, vol. 232, no. September, pp. 489–503, 2018.

[31] S. Pereira, P. Ferreira, and A. I. F. Vaz, “A simplified optimization model to short-term electricity planning,” *Energy*, vol. 93, pp. 2126–2135, 2015.

[32] R. Miranda, P. Ferreira, R. Schaeffer, and A. Szklo, “Limitations of thermal power plants to solar and wind development in Brazil,” *ECOS 2016-The 29th Int. Conf. Effic. Cost, Optim. Simul. Environ. Impact Energy Syst.*, no. June, pp. 1–21, 2016.

[33] R. Soria *et al.*, “The role of CSP in Brazil: A multi-model analysis,” in *AIP Conference Proceedings, V 1734*, 2016.

[34] R. Jiang, M. Zhang, G. Li, and Y. Guan, “Two-stage robust power grid optimization problem,” *Submitt. to J. Oper. Res.*, pp. 1–34, 2010.

[35] R. Jiang, J. Wang, and Y. Guan, “Robust unit commitment with wind power and pumped storage hydro,” *IEEE Trans. Power Syst.*, vol. 27, no. 2, pp. 800–810, 2012.

[36] A. Street, F. Oliveira, and J. M. Arroyo, “Contingency-constrained unit commitment with $ n-k $ security criterion: A robust optimization approach,” *IEEE Trans. Power Syst.*, vol. 26, no. 3, pp. 1581–1590, 2010.

[37] Y. Huang, P. M. Pardalos, and Q. P. Zheng, *Electrical power unit commitment: deterministic and two-stage stochastic programming models and algorithms*. Springer, 2017.

[38] X. Li, Q. Zhai, and X. Guan, “Robust Transmission Constrained Unit Commitment : A Column Merging Method,” *arXiv Prepr. arXiv1810.06215*, pp. 1–9, 2018.

[39] T. Senjyu, K. Shimabukuro, K. Uezato, and T. Funabashi, “A fast technique for unit commitment problem by extended priority list,” *IEEE Trans. Power Syst.*, vol. 18, no. 2, pp. 882–888, 2003.

[40] S. Salam, K. M. Nor, and A. R. Hamdan, “Hydrothermal scheduling based lagrangian relaxation approach to hydrothermal coordination,” *IEEE Trans. Power Syst.*, vol. 13, no. 1, pp. 226–235, 1998.

[41] T. Li and M. Shahidehpour, “Price-based unit commitment: A case of Lagrangian relaxation versus mixed integer programming,” *IEEE Trans. power Syst.*, vol. 20, no. 4, pp. 2015–2025, 2005.

[42] M. Carrión and J. M. Arroyo, “A computationally efficient mixed-integer linear formulation for the thermal unit commitment problem,” *IEEE Trans. power Syst.*, vol. 21, no. 3, pp. 1371–1378, 2006.

[43] W. van Ackooij, R. Henrion, A. Möller, and R. Zorgati, “Joint chance constrained programming for hydro reservoir management,” *Optim. Eng.*, vol. 15, no. 2, pp. 509–531, 2014.

[44] L. T. Anstine, R. E. Burke, J. E. Casey, R. Holgate, R. S. John, and H. G. Stewart, “Application of probability methods to the determination of spinning reserve requirements for the Pennsylvania-New Jersey-Maryland interconnection,” *IEEE Trans. Power Appar. Syst.*, vol. 82, no. 68, pp. 726–735, 1963.

[45] R. Billinton and R. Karki, “Capacity reserve assessment using system well-being analysis,” *IEEE Trans. Power Syst.*, vol. 14, no. 2, pp. 433–438, 1999.

[46] R. Billinton and M. Fotuhi-Firuzabad, “A reliability framework for generating unit commitment,” *Electr. Power Syst. Res.*, vol. 56, no. 1, pp. 81–88, 2000.

[47] H. B. Gooi, D. P. Mendes, K. R. W. Bell, and D. S. Kirschen, “Optimal scheduling of spinning reserve,” *IEEE Trans. Power Syst.*, vol. 14, no. 4, pp. 1485–1492, 1999.

[48] M. Shahidehpour, F. Tinney, and Y. Fu, “Impact of security on power systems operation,” *Proc. IEEE*, vol. 93, no. 11, pp. 2013–2025, 2005.

[49] F. D. Galiana, F. Bouffard, J. M. Arroyo, and J. F. Restrepo, “Scheduling and pricing of coupled energy and primary, secondary, and tertiary reserves,” *Proc. IEEE*, vol. 93, no. 11, pp. 1970–1983, 2005.

[50] J. M. Arroyo and F. D. Galiana, “Energy and reserve pricing in security and network-constrained electricity markets,” *IEEE Trans. power Syst.*, vol. 20, no. 2, pp. 634–643, 2005.

[51] J. M. Arroyo, “Bilevel programming applied to power system vulnerability analysis under multiple contingencies,” *IET Gener. Transm. Distrib.*, vol. 4, no. 2, pp. 178–190, 2010.

[52] L. Wu, M. Shahidehpour, and T. Li, “Stochastic security-constrained unit commitment,” *IEEE Trans. Power Syst.*, vol. 22, no. 2, pp. 800–811, 2007.

[53] A. Papavasiliou and S. S. Oren, “Multiarea stochastic unit commitment for high wind penetration in a transmission constrained network,” *Oper. Res.*, vol. 61, no. 3, pp. 578–592, 2013.

[54] H. Siahkali and M. Vakilian, “Stochastic unit commitment of wind farms integrated in power system,” *Electr. Power Syst. Res.*, vol. 80, no. 9, pp. 1006–1017, 2010.

[55] B. Zeng and L. Zhao, “Solving two-stage robust optimization problems using a column-and- constraint generation method,” *Oper. Res. Lett.*, vol. 41, no. 5, pp. 457–461, 2013.

[56] A. Moreira, A. Street, and J. M. Arroyo, “An Adjustable Robust Optimization Approach for Contingency-Constrained Transmission Expansion Planning,” *IEEE Trans. Power Syst.*, vol. 30, no. 4, pp. 2013–2022, 2015.

[57] U. A. Ozturk, M. Mazumdar, and B. A. Norman, “A solution to the stochastic unit commitment problem using chance constrained programming,” *IEEE Trans. Power Syst.*, vol. 19, no. 3, pp. 1589–1598, 2004.

[58] S. Takriti, J. R. Birge, and E. Long, “A stochastic model for the unit commitment

problem," *IEEE Trans. Power Syst.*, vol. 11, no. 3, pp. 1497–1508, 1996.

[59] P. Carpentier, G. Gohen, J.-C. Culioli, and A. Renaud, "Stochastic optimization of unit commitment: a new decomposition framework," *IEEE Trans. Power Syst.*, vol. 11, no. 2, pp. 1067–1073, 1996.

[60] H. Wu, M. Shahidehpour, Z. Li, and W. Tian, "Chance-constrained day-ahead scheduling in stochastic power system operation," *IEEE Trans. Power Syst.*, vol. 29, no. 4, pp. 1583–1591, 2014.

[61] W. Rmisch, "Scenario reduction in stochastic programming: an approach using probability metrics," 2000.

[62] R. Jiang, M. Zhang, G. Li, and Y. Guan, "Benders' decomposition for the two-stage security constrained robust unit commitment problem," in *IIE Annual Conference. Proceedings*, 2012, p. 1.

[63] A. Ben-Tal and A. Nemirovski, "Robust solutions of uncertain linear programs," *Oper. Res. Lett.*, vol. 25, no. 1, pp. 1–13, 1999.

[64] A. Ben-Tal and A. Nemirovski, "Robust convex optimization," *Math. Oper. Res.*, vol. 23, no. 4, pp. 769–805, 1998.

[65] A. Ben-Tal and A. Nemirovski, "Robust solutions of linear programming problems contaminated with uncertain data," *Math. Program.*, vol. 88, no. 3, pp. 411–424, 2000.

[66] L. El Ghaoui, F. Oustry, and H. Lebret, "Robust solutions to uncertain semidefinite programs," *SIAM J. Optim.*, vol. 9, no. 1, pp. 33–52, 1998.

[67] L. El Ghaoui and H. Lebret, "Robust solutions to least-squares problems with uncertain data," *SIAM J. matrix Anal. Appl.*, vol. 18, no. 4, pp. 1035–1064, 1997.

[68] D. Bertsimas and M. Sim, "The Price of Robustness," *Oper. Res.*, vol. 52, no. 1, pp. 35–53, 2004.

[69] D. Bertsimas and M. Sim, "Robust discrete optimization and network flows," *Math. Program.*, vol. 98, no. 1–3, pp. 49–71, 2003.

[70] Y. Guan and J. Wang, "Uncertainty sets for robust unit commitment," *IEEE Trans. Power Syst.*, vol. 29, no. 3, pp. 1439–1440, 2014.

[71] A. Ben-Tal and A. Nemirovski, "Robust optimization - Methodology and applications," *Math. Program. Ser. B*, vol. 92, no. 3, pp. 453–480, 2002.

[72] A. Ben-Tal, L. El Ghaoui, and A. Nemirovski, *Robust Optimization*, vol. 1. New Jersey: Princeton and Oxford, 2009.

[73] A. L. Soyster, "Convex programming with set-inclusive constraints and

applications to inexact linear programming," *Oper. Res.*, vol. 21, no. 5, pp. 1154–1157, 1973.

[74] A. H. Hajimiragha, C. A. Ca, M. W. Fowler, S. Moazeni, A. Elkamel, and M. Carlo, "A Robust Optimization Approach for Planning the Transition to Plug-in Hybrid Electric Vehicles," pp. 1–11.

[75] A. Moreira, S. Member, D. Pozo, and A. Street, "Reliable Renewable Generation and Transmission Expansion Planning : Co-Optimizing System ' s Resources for Meeting Renewable Targets," *IEEE Trans. Power Syst.*, vol. 32, no. 4, pp. 3246–3257, 2017.

[76] B. Fanzeres, S. Ahmed, and A. Street, "Robust strategic bidding in auction-based markets," *Eur. J. Oper. Res.*, vol. 272, no. 3, pp. 1158–1172, 2019.

[77] Y. An and B. Zeng, "Exploring the modeling capacity of two-stage robust optimization: Variants of robust unit commitment model," *IEEE Trans. Power Syst.*, vol. 30, no. 1, pp. 109–122, 2015.

[78] B. L. Gorissen, I. Yamkoglu, and D. den Hertog, "A Practical Guide to Robust Optimization," *Omega*, vol. 53, pp. 124–137, 2015.

[79] V. Gabrel, C. Murat, and A. Thiele, "Recent advances in robust optimization: An overview," *Eur. J. Oper. Res.*, vol. 235, no. 3, pp. 471–483, 2014.

[80] A. Lorca and X. A. Sun, "Multistage Robust Unit Commitment with Dynamic Uncertainty Sets and Energy Storage," *IEEE Trans. Power Syst.*, vol. 32, no. 3, pp. 1678–1688, 2017.

[81] Á. Lorca, X. A. Sun, E. Litvinov, and T. Zheng, "Multistage Adaptive Robust Optimization for the Unit Commitment Problem," *Oper. Res.*, vol. 64, no. 1, pp. 32–51, 2016.

[82] Q. Zhai, X. Li, X. Lei, and X. Guan, "Transmission Constrained UC With Wind Power : An All-Scenario- Feasible MILP Formulation with Strong Nonanticipativity," *IEEE Trans. Power Syst.*, vol. 32, no. 3, pp. 1805–1817, 2017.

[83] A. Ben-Tal, A. Goryashko, E. Guslitzer, and A. Nemirovski, "Adjustable robust solutions of uncertain linear programs," *Math. Program.*, vol. 99, no. 2, pp. 351–376, 2004.

[84] H. Ye and Z. Li, "Robust Security-Constrained Unit Commitment and Dispatch with Recourse Cost Requirement," *IEEE Trans. Power Syst.*, vol. 31, no. 5, pp. 3527–3536, 2016.

[85] B. Zeng, “Solving Two-stage Robust Optimization Problems Using a Column-and-Constraint Generation Method - Appendix.” pp. 1–5, 2013.

[86] A. M. da Silva, “Two-Stage Robust Optimization Models for Power System Operation and Planning under Joint Generation and Transmission Security Criteria,” PUC-Rio, 2014.

[87] C. Lee, C. Liu, S. Mehrotra, and M. Shahidehpour, “Modeling transmission line constraints in two-stage robust unit commitment problem,” *IEEE Trans. Power Syst.*, vol. 29, no. 3, pp. 1221–1231, 2014.

[88] A. Street, A. Moreira, and J. M. Arroyo, “Energy and reserve scheduling under a joint generation and transmission security criterion: An adjustable robust optimization approach,” *IEEE Trans. Power Syst.*, vol. 29, no. 1, pp. 3–14, 2013.

[89] A. Moreira, A. Street, and J. M. Arroyo, “Energy and Reserve Scheduling under Correlated Nodal Demand Uncertainty : An Adjustable Robust Optimization Approach,” in *18th Power Systems Computation Conference*, 2014, no. August 18-22.

[90] C. Ø. Naversen, H. Farahmand, and A. Helseth, “Procurement of Spinning Reserve Capacity in a Hydropower Dominated System Through Mixed Stochastic-Robust Optimization,” *arXiv Prepr. arXiv1903.04805*, pp. 1–8, 2019.

[91] R. Jiang, M. Zhang, G. Li, and Y. Guan, “Two-stage network constrained robust unit commitment problem,” *Eur. J. Oper. Res.*, vol. 234, no. 3, pp. 751–762, 2014.

[92] G. Liu and K. Tomsovic, “Robust unit commitment considering uncertain demand response,” *Electr. Power Syst. Res.*, vol. 119, no. 719, pp. 126–137, 2015.

[93] C. Duan, L. Jiang, W. Fang, and J. Liu, “Data-Driven Affinely Adjustable Distributionally Robust Unit Commitment,” *IEEE Trans. Power Syst.*, vol. 33, no. 2, pp. 1385–1398, 2018.

[94] W. Wei, F. Liu, and S. Mei, “Distributionally robust Co-optimization of energy and reserve dispatch,” *IEEE Trans. Sustain. Energy*, vol. 7, no. 1, pp. 289–300, 2016.

[95] G. Morales-España, Á. Lorca, and M. M. De Weerdt, “Robust unit commitment with dispatchable wind power,” *Electr. Power Syst. Res.*, vol. 155, pp. 58–66, 2018.

[96] D. Apostolopoulou, Z. De Greve, and M. Malcom, “Robust Optimisation for

Hydroelectric System Operation under Uncertainty," *IEEE Trans. Power Syst.*, vol. 33, no. 3, pp. 3337–3348, 2018.

[97] R. A. Jabr, "Robust transmission network expansion planning with uncertain renewable generation and loads," *IEEE Trans. Power Syst.*, vol. 28, no. 4, pp. 4558–4567, 2013.

[98] R. Jiang, J. Wang, M. Zhang, and Y. Guan, "Two-Stage Minimax Regret Robust Unit Commitment," *IEEE Trans. Power Syst.*, vol. 28, no. 3, pp. 2271–2282, 2013.

[99] H. Konno, "A cutting plane algorithm for solving bilinear programs," *Math. Program.*, vol. 11, no. 1, pp. 14–27, 1976.

[100] H. Ye, J. Wang, and Z. Li, "MIP Reformulation for Max-Min Problems in Two-Stage Robust SCUC," *IEEE Trans. Power Syst.*, vol. 32, no. 2, pp. 1237–1247, 2017.

[101] C. Peng, P. Xie, L. Pan, and R. Yu, "Flexible robust optimization dispatch for hybrid wind/photovoltaic/hydro/thermal power system," *IEEE Trans. Smart Grid*, vol. 7, no. 2, pp. 751–762, 2016.

[102] A. Soroudi, "Robust optimization based self scheduling of hydro-thermal Genco in smart grids," *Energy*, vol. 61, no. 21, pp. 262–271, 2013.

[103] Y. Chen, W. Wei, F. Liu, and S. Mei, "Distributionally robust hydro-thermal-wind economic dispatch," *Appl. Energy*, vol. 173, pp. 511–519, 2016.

[104] EPE -Empresa de Pesquisa Energética and MME - Ministério de Minas e Energia, "Plano Decenal de Expansão de Energia 2027." EPE, Rio de Janeiro, p. 345, 2018.

[105] C. Zhao and Y. Guan, "Unified stochastic and robust unit commitment," *IEEE Trans. Power Syst.*, vol. 28, no. 3, pp. 3353–3361, 2013.

[106] D. Bertsimas and V. Goyal, "On the Power of Robust Solutions in Two-Stage Stochastic and Adaptive Optimization Problems," *Math. Oper. Res.*, vol. 35, no. 2, pp. 284–305, 2010.

[107] P. Gögler, M. Dorfner, and T. Hamacher, "Hybrid Robust / Stochastic Unit Commitment With Iterative Partitions of the Continuous Uncertainty Set," *Front. Energy Res.*, vol. 6, no. July, pp. 1–17, 2018.

[108] C. Zhao, J. Wang, J. P. Watson, and Y. Guan, "Multi-stage robust unit commitment considering wind and demand response uncertainties," *IEEE Trans. Power Syst.*, vol. 28, no. 3, pp. 2708–2717, 2013.

[109] Z. Zhang, Y. Chen, X. Liu, and W. Wang, “Two-Stage Robust Security-Constrained Unit Commitment Model Considering Time Autocorrelation of Wind/Load Prediction Error and Outage Contingency Probability of Units,” *IEEE Access*, vol. 7, pp. 25398–25408, 2019.

[110] A. Lorca and X. A. Sun, “Adaptive robust optimization with dynamic uncertainty sets for multi-period economic dispatch under significant wind,” *IEEE Trans. Power Syst.*, vol. 30, no. 4, pp. 1702–1713, 2014.

[111] M. Minoux, “Two-stage robust optimization, state-space representable uncertainty and applications,” *RAIRO-Operations Res.*, vol. 48, no. 4, pp. 455–475, 2014.

[112] Z. Zhang, Y. Chen, J. Ma, X. Liu, and W. Wang, “Two-Stage Robust Security Constrained Unit Commitment Considering the Spatiotemporal Correlation of Uncertainty Prediction Error,” *IEEE Access*, vol. 7, pp. 22891–22901, 2019.

[113] Y. Cho, T. Ishizaki, and J.-I. Imura, “Hybrid Method of Two-Stage Stochastic and Robust Unit Commitment,” in *2019 18th European Control Conference (ECC)*, 2019, pp. 922–927.

[114] P. Xiong, P. Jirutitijaroen, and C. Singh, “A distributionally robust optimization model for unit commitment considering uncertain wind power generation,” *IEEE Trans. Power Syst.*, vol. 32, no. 1, pp. 39–49, 2016.

[115] C. Ning and F. You, “Data-driven adaptive robust unit commitment under wind power uncertainty: a bayesian nonparametric approach,” *IEEE Trans. Power Syst.*, vol. 34, no. 3, pp. 2409–2418, 2019.

[116] I. Blanco and J. M. Morales, “An Efficient Robust Solution to the Two-Stage Stochastic Unit Commitment Problem,” *IEEE Trans. Power Syst.*, vol. 32, no. 6, pp. 4477–4488, 2017.

[117] C. Liu, C. Lee, H. Chen, and S. Mehrotra, “Stochastic robust mathematical programming model for power system optimization,” *IEEE Trans. Power Syst.*, vol. 31, no. 1, pp. 821–822, 2016.

[118] I. A. De Oliveira, R. Schaeffer, and A. Szklo, “The impact of energy storage in power systems : The case of Brazil ’ s Northeastern grid,” *Energy*, vol. 122, pp. 50–61, 2017.

[119] M. E. P. Maceiral *et al.*, “Twenty Years of Application of Stochastic Dual Dynamic Programming in Official and Agent Studies in Brazil-Main Features and Improvements on the NEWAVE Model,” in *2018 Power Systems*

Computation Conference (PSCC), 2018, pp. 1–7.

[120] X. Guan, A. Svoboda, and C. Li, "Scheduling hydro power systems with restricted operating zones and discharge ramping constraints," *IEEE Trans. Power Syst.*, vol. 14, no. 1, pp. 126–131, 1999.

[121] G. W. Chang *et al.*, "Experiences with mixed integer linear programming based approaches on short-term hydro scheduling," *IEEE Trans. power Syst.*, vol. 16, no. 4, pp. 743–749, 2001.

[122] Z. K. Shawwash, T. K. Siu, and S. O. Russel, "The BC Hydro short term hydro scheduling optimization model," in *Proceedings of the 21st International Conference on Power Industry Computer Applications. Connecting Utilities. PICA 99. To the Millennium and Beyond (Cat. No. 99CH36351)*, 1999, pp. 183–189.

[123] H.--C. Chang and P.--H. Chen, "Hydrothermal generation scheduling package: a genetic based approach," *IEE Proceedings-Generation, Transm. Distrib.*, vol. 145, no. 4, pp. 451–457, 1998.

[124] R. A. Ponrajah and F. D. Galiana, "Systems to optimise conversion efficiencies at Ontario Hydro's hydroelectric plants," in *Proceedings of the 20th International Conference on Power Industry Computer Applications*, 1997, pp. 245–251.

[125] Oliver Paish, "Small hydro power: technology and current status," *Renew. Sustain. Energy Rev.*, vol. 6 (2002), no. 6 (2002), pp. 537–556, 2002.

[126] S. Soares and C. T. Salmazo, "Minimum loss predispatch model for hydroelectric power systems," *IEEE Trans. Power Syst.*, vol. 12, no. 3, pp. 1220–1228, 1997.

[127] HydroByte Software, "HydroExpert Software." 2019.

[128] EPE, "Arquivos do programa Newave," *Empresa de Pesquisa Energética*, 2015. [Online]. Available: http://www.epe.gov.br/pt/publicacoes-dados-abertos/publicacoes/arquivos-do-programa-newave. [Accessed: 07-Oct-2019].

[129] EPE-MME, "Plano Decenal de Energia 2024," *Empresa de Pesquisa Energética*. Ministerio de Minas e Energia, Rio de Janeiro, p. 467, 2015.

[130] K. den Bergh, E. Delarue, and W. D'haeseleer, "DC power flow in unit commitment models," *TME Work. Pap. - Energy Environ.*, vol. May, 2014.

[131] K. Purchala, "Modeling and analysis of techno-economic interactions in meshed high voltage grids exhibiting congestion," 2005.

[132] A. J. Monticelli, *Fluxo de carga em redes de energia elétrica*. E. Blucher, 1983.

[133] Greenpeace, "[R]evolução Energética," pp. 1–96, 2016.

[134] R. A. Soria Penãfiel, “Proposta Metodólogica para Formulação de uma Política de Desenvolvimento da Tecnologia Heliotérmica no Brasil,” Universidade Federal do Rio de Janeiro, 2016.

[135] METEONORM, “Meteonorm - Weather stations world-wide database.” 2014.

[136] SWERA/NREL, “Solar and Wind Energy Resource Assessment.” United States, 2007.

[137] ONS - Operador Nacional do Sistema Elétrico, “Definição da Modalidade de Operação de Usinas.” 2016.

[138] Agência Nacional de Energia Elétrica – ANEEL, “Análise de contribuições da audiência pública nº 21/2011 – estabelecimento dos critérios para a consideração de pequenas usinas nos modelos computacionais de planejamento da operação e formação de preço.” 2011.

[139] ONS, “Curva de carga horária do sistema elétrico Brasileiro, por sub-região, correspondente às usinas simuladas e despachadas individualmente pela ONS no ano 2013.” Operador Nacional do Sistema Elétrico, Rio de Janeiro, 2015.

[140] A. O. Menezes, A. L. Munzig Anja, D. P. Mohrmann, J. Ilona Daun, M. R. Dammann, and V. Kammertons, “The NoPa Case: new partnerships for innovation in sustainable developments.” Reflections and Achievements. New Partnerships for Innovation in Sustainable Development (NoPa), 2015.

[141] EPE, “Consumo Mensal de Energia Elétrica por Classe (regiões e subsistemas) 2004-2015,” 2015. [Online]. Available: http://www.epe.gov.br/pt/publicacoes-dados-abertos/publicacoes/Consumo-mensal-de-energia-eletrica-por-classe-regioes-e-subsistemas. [Accessed: 06-Jun-2019].

[142] ANEEL, “Banco de Informações da Geração Elétrica -BIG.,” 2014. [Online]. Available: http://www.aneel.gov.br/informacoes-tecnicas/-/asset_publisher/CegkWaVJWF5E/content/big-banco-de-informacoes-de-geracao/655808?inheritRedirect=false.

[143] CCEE, “Geral da Geração e Garantia Física de usinas em Operação Comercial.” 2014.

[144] CCEE, “Resultado consolidado dos leilões - Julho 2014.” Câmara de Comercialização de Energia Elétrica, 2014.

[145] A. Schröder, F. Kunz, J. Meiss, R. Mendelevitch, and C. Von Hirschhausen, “Current and Prospective Costs of Electricity Generation Until 2050,” 2013.

[146] R. Soria *et al.*, “Modelling concentrated solar power (CSP) in the Brazilian

energy system: A soft-linked model coupling approach," *Energy*, vol. 116, pp. 265–280, 2016.

[147] J. Portugal-Pereira, A. C. Köberle, R. Soria, A. F. P. Lucena, A. Szklo, and R. Schaeffer, "Overlooked impacts of electricity expansion optimisation modelling: The life cycle side of the story," *Energy*, vol. 115, pp. 1424–1435, 2016.

[148] ONS - Operador Nacional do Sistema Elétrico, "Hidroelétricas do SIN - Rede de Operação - Horizonte 2023." SINDAT - SISTEMA DE INFORMAÇÕES GEOGRÁFICAS CADASTRAIS DO SIN, 2019.

[149] ONS - Operador Nacional do Sistema Elétrico, "Invent_ario das restrições operativas hidr_aulicas dos aproveitamentos hidrel_etricos," 2016.

[150] EPE, "Arquivos do programa Newave," *Empresa de Pesquisa Energética*, 2015. .

[151] ONS - Operador Nacional do Sistema Elétrico, "Atualização de Séries Históricas de Vazões - Período 1931 a 2014 - Historicas de Vazões." 2014.

[152] B. P. Cotia, C. L. T. Borges, and A. L. Diniz, "Optimization of wind power generation to minimize operation costs in the daily scheduling of hydrothermal systems," *Int. J. Electr. Power Energy Syst.*, vol. 113, pp. 539–548, 2019.

[153] L. Sampath, M. Hotz, H. B. Gooi, and W. Utschick, "Network-Constrained Robust Unit Commitment for Hybrid AC/DC Transmission Grids," *arXiv Prepr. arXiv1811.08754*, 2018.

[154] C. Wang *et al.*, "Robust risk-constrained unit commitment with large-scale wind generation: An adjustable uncertainty set approach," *IEEE Trans. Power Syst.*, vol. 32, no. 1, pp. 723–733, 2016.

[155] ONS, "Histórico da Operação," *Operador Nacional do Sistema Elétrico*, 2019. [Online]. Available: www.http://www.ons.org.br/paginas/resultados-da-operacao/historico-da-operacao. [Accessed: 30-Oct-2019].

[156] ONS, "Informe do Programa Mensal da Operação," *Acervo Digital - Operador Nacional do Sistema Elétrico*, 2019. [Online]. Available: http://www.ons.org.br/paginas/conhecimento/acervo-digital/documentos-e-publicacoes?categoria=Relatório+PMO. [Accessed: 01-Nov-2019].

[157] CCEE, "Preços Médio da CCEE (R$/MWh)," *Câmara de Comercialização de Energia Elétrica -Biblioteca Virtual*, 2019. [Online]. Available: https://www.ccee.org.br/portal/faces/pages_publico/o-que-fazemos/como_ccee_atua/precos/precos_medios?_afrLoop=545397857075126&_adf.ctrl-

state=nltqgcbzg_1#!%40%40%3F_afrLoop%3D545397857075126%26_adf.ctrl-state%3Dnltqgcbzg_5. [Accessed: 22-Sep-2019].

[158] E. Ela, M. Milligan, and B. Kirby, “Operating Reserves and Variable Generation: A comprehensive review of current strategies, studies, and fundamental research on the impact that increased penetration of variable renewable generation has on power system operating reserves,” *NREL- Natl. Renew. Energy Labora*, no. August, pp. 1–103, 2011.

[159] B. J. Kirby, “Frequency Regulation Basics and Trends,” *U.S. Department of Energy (DOE)*, vol. December, no. 1. 2004.

[160] GAMS Development Corp., “The General Algebraic Modeling System (GAMS),” 2019. [Online]. Available: www.gams.com. [Accessed: 30-Oct-2019].

[161] A. de C. Köberle, “Implementation of Land Use in an Energy System Model to Study the Long-Term Impacts of Bioenergy in Brazil and its Sensitivity to the Choice of Agricultural Greenhouse Gas Emission Factors,” Universidade Federal do Rio de Janeiro, 2018.

Appendices

A. Fuel cost for thermal power plants

Table II-1. Coefficients for the fuel-cost curve*.

Power Plant	$IndA_j$ ($/Mwh)	$IndB_j$ ($)	Power Plant	$IndA_j$ ($/Mwh)	$IndB_j$ ($)
TEPE-CC-GAS	46.273	3251.673	URU-CC-GAS	46.273	3903.838
TEFO-CC-GAS	46.273	2116.943	ARJ-GT-GAS	53.367	869.8109
NOTE-CC-GNL	46.273	7552.667	ENE-ST-BIO	23.751	8.116
SERGI-CC-GAS	46.273	9242.561	RIO-GAS	46.273	7552.667
FACO-CC-CHP-GAS	46.273	841.8966	PAM-COAL	23.751	689.86
CELF-CC-CHP-GAS	46.273	1134.73	LUI-CC-GAS	46.273	2353.65
JESO-CC-CHP-GAS	46.273	1970.526	AUR-CC-GAS	46.273	1378.758
CAMA-GT-GAS	53.367	7301.102	BAI-CC-GAS	46.273	3233.371
TECE-GT-GAS	53.367	4635.62	BAR-GT-GAS	53.367	8124.978
PROSPE-GAS	53.367	589.988	DOA-IC-IR	236.09	13024.2
PECEM1-ST-COAL	23.751	1460.88	EUZ-CC-GAS	46.273	1524.565
PECEM2-ST-COAL	23.751	730.44	FER-CC-GAS	46.273	3533.22
PERN-IC-HFO	236.09	5342.58	LEO-CC-GAS	46.273	6456.371
CAMA_MI-IC-HFO	236.09	4040.16	IGA-ST-OIL	236.09	3481.98
CAMA_PI-IC-HFO	236.09	3987	IPA-ST-BIO	23.751	154.204
SUAP-IC-HFO	236.09	10126.98	JUI-GT-GAS	53.367	1833.177
TENE-IC-HFO	236.09	4545.18	LUI-GT-GAS	53.367	4298.484
TEPA-IC-HFO	236.09	4545.18	MAR-GT-GAS	53.367	19440.1
CAMP-IC-HFO	236.09	4492.02	NOR-CC-GAS	46.273	5300.898
MARA-IC-HFO	236.09	4465.44	PIR-GT-GAS	53.367	4214.2
TEMA-IC-LFO	236.09	3800.94	ROB-GT-GAS	53.367	632.13
GLOB1-IC-HFO	236.09	3960.42	SAN-CC-GAS	46.273	5710.255
GLOB2-IC-HFO	236.09	3960.42	VIA-IC-HFO	236.09	4640.868
PETR-IC_HFO	236.09	3614.88	COC-ST-BIO	23.751	57.2178
PAFE-IC_LFO	236.09	2498.52	BRA-IC-HFO	236.09	265.8
TEPO3-IC-LFO	236.09	1754.28	DAI-IC-HFO	236.09	1180.152
TEPO1-IC-LFO	236.09	1408.74	GOI-IC-HFO	236.09	3795.624
TECA-IC-HFO	236.09	1329	MAR-CC-GAS	46.273	3228.49
BAH-IC-HFO	236.09	850.56	PAL-IC-HFO	236.09	4667.448
ENCE1-IC-LFO	236.09	305.67	XAV-IC-HFO	236.09	1426.017
ENCE2-IC-LFO	236.09	305.67	APA-GT-GAS	53.367	5299.357
ENCE3-IC-LFO	236.09	393.384	CRI-IC-GAS	53.367	1801.571
ENCE4-IC-LFO	236.09	348.198	GERI-IC-HFO	236.09	4409.622

ENCE5-IC-LFO	236.09	393.384	GERII-IC-HFO	236.09	4409.622
ENCE6-IC-LFO	236.09	393.384	JAR-IC-GAS	53.367	1590.861
ENCE7-IC-LFO	236.09	393.384	MAN-IC-GAS	53.367	1801.571
ENPI1-IC-LFO	236.09	348.198	MARIII-CC-GAS	46.273	3045.469
ENPI2-IC-LFO	236.09	348.198	MARIV-GT-GAS	53.367	7113.57
ENPI3-IC-LFO	236.09	348.198	MARV-GT-GAS	53.367	7113.57
ENPI4-IC-LFO	236.09	348.198	MAUB3-GT-GAS	53.367	2528.52
ENBA1-IC-LFO	236.09	2698.933	MAUB4-GT-GAS	53.367	3160.65
ARA-CC-GAS	46.273	2953.349	MC2-GT-GAS	53.367	3712.71
CAN-ST-COAL	23.751	710.15	MAU-CC-GAS	46.273	3556.708
CHA-ST-COAL	23.751	36.522	PAR-GT-GAS	53.367	1179.976
FIG-ST-COAL	23.751	20.29	PON-IC-GAS	53.367	1801.571
LACA-ST-COAL	23.751	117.682	POR-ST-COAL	23.751	730.6429
LACB-ST-COAL	23.751	265.799	SAN-GT-GAS	53.367	3752.745
LACC-ST-COAL	23.751	736.527	SUZ-ST-BIO	23.751	517.0704
KLA-ST-BIO	23.751	669.57	TAM-IC-GAS	53.367	1590.861
NUT-IC-HFO	236.09	212.64	TER-CC-GAS	46.273	2134.94
MED-ST-COAL	23.751	226.2335	SAN-ST-BIO	236.09	598.05
JER-ST-COAL	23.751	13.52667	ACR-GAS	46.273	1000.515
SET-CC-GAS	46.273	1516.634			

*own calculation based on [32].

B. Technical and Economical parameters for hydropower plants with reservoir

Table II-2. RES - Hydro Power Plant Technical Parameters*.

Power Plant	$PhdMax_{hd}$ (MW)	$MaxLevel_{hd}$ (hm^3)	$MinLevel_{hd}$ (hm^3)	$Qmax_{hd}$ (m^3/s)	$Qmin_{hd}$ (m^3/s)	$tviag_{hd}(h)$
A. A. LAYDNER (Jurumirim)	97.7	7008	3843	355.1971	55	0
ÁGUA VERMELHA	1396.2	11025	5856	2445.635	484	6
AMADOR AGUIAR I (campim branco I)	240	241.13	228.27	491.2409	65	5
BALBINA	250	19959	9735	1289.84	19	0
BARRA BONITA	140	3135	569	733.3333	91	0
BARRA GRANDE	698.2	4904.45	2711.79	513.7546	19	0
BATALHA	53.6	1781.6	430	152.5862	16	0
BOA ESPERANÇA	237.3	5085	3173	605.3073	173	0
CACONDE	80.4	555	51	89.05817	8	0
CACU	65	231.77	197.27	276.2712	54	0
CAMARGOS	46	792	120	212.9534	34	0
CAMPOS NOVOS	879.9	1477	1320	548.1806	17	1
CAPIVARA (Escola Engenharia Mackenzie)	617.5	10540	4816	1654.645	192	3
CHAVANTES	414	8795	5754	628.8493	186	4
CORUMBÁ	375	1500	470	547.4178	74	16
CORUMBA III	95.4	972	709	275	27	1
CORUMBÁ IV	127	3624.4	2936.6	206.6884	22	0
CURUA-UNA	30	530	130	184.0764	35	0
EMBORCAÇÃO	1192	17725	4669	1010.145	73	1
ESPORA	31.8	209	71	68.30467	22	0
FUNIL	222	888	283	361.4943	51	81
FURNAS	1312	22950	5733	1666.452	204	23
GOV. BENTO MUNHOZ (Foz do Areia)	1676	5779	1974	1573.759	80	0
GOV. NEY BRAGA (Ex UHE Segredo)	1260	2950	2562	1237.685	94	1
GOV. PARIGOT SOUZA (Capivari-Cachoeira)	260	179	23	38.50688	7	0
I. SOLT. EQV	4251.5	34432	25467	11130.1	1552	9
IRAPÉ	399	5964	2268	257.563	8	0
ITAPARICA	1480	10782	7234	3248.705	501	1
ITUMBIARA	2280	17027	4573	2812.851	261	5
JAGUARI	27.6	1236	443	57.62712	7	0
MACHADINHO	1140	3340	2283	1294.849	44	1
MANSO	210	7337	4386	387.2	42	0
MARIMBONDO	1488	6150	890	2799.58	418	10
MASCARENHAS DE	478	4040	1540	1264.756	225	6

MORAES (Peixoto)						
MAUA	363.1	2137	1473	337.6923	27	1
MIRANDA	408	1120	974	660.6557	64	6
NOVA PONTE	510	12792	2412	526.3933	53	0
PARAIBUNA	85	4732	2096	126.1628	21	0
PASSO FUNDO	226	1589	185	98.50615	1	0
PASSO REAL	158	3646	289	461.8902	12	0
PEDRA DO CAVALO	160	3072	2192	174.026	1	0
PEIXE ANGICAL	452	2741	2212.7	2066.949	185	1
PICADA	50	7	6	43.66454	7	0
PORTO ESTRELA	112	89	56	247.032	25	2
PORTO PRIMAVERA	1540	20000	14400	8830.909	1881	24
PROMISSAO	264	7408	5280	1257.416	149	6
QUEBRA QUEIXO	121.5	137	111	113.7274	3	0
QUEIMADO	105	557	95.25	66.77116	9	0
RETIRO BAIXO	82	241.59	200.72	260.6452	24	0
SALTO SANTIAGO	1420	6775	2662	1528.118	116	1
SAMUEL	216.5	3493.44	943.23	824.4635	9	0
SANTA BRANCA	56	439	131	130.9333	23	6
SANTA CLARA - PR	120	431	169	160.3352	14	0
SÃO ROQUE	135	795.67	336.72	305.0808	14	0
SÃO SIMÃO	1710	12540	7000	2514.032	450	8
SERRA DA MESA	1275	54400	11150	1158.052	97	0
SERRA DO FACAO	212.6	5199	1752	304.8896	27	1
SINOP	400	3071.2	1012.4	1790.95	267	0
SOBRADINHO	1050	34116	5447	4151.337	506	1
TRÊS MARIAS	396	19528	4250	914.7126	58	1
TUCURUI	8370	50275	11293	13726.28	1269	1

* data taken from [148], [127], [149] [150]

Table II-3. Water Value for Hydro Power Plants with reservoir*.

Res –Hydro Power plant	$CWater_{hd,week1}$ ($/hm^3)	$CWater_{hd,week2}$ ($/hm^3)	$CWater_{hd,week3}$ ($/hm^3)	$CWater_{hd,week4}$ ($/hm^3)
A. A. LAYDNER (Jurumirim)	63255.32	57470.84	30578.46	28482.45
ÁGUA VERMELHA	25929.96	23558.76	12534.89	11675.68
AMADOR AGUIAR I (campim branco I)	58978.87	53585.46	28511.17	26556.86
BALBINA	3056.801	2777.267	865.258	864.505
BARRA BONITA	30985.26	28151.77	14978.69	13951.97
BARRA GRANDE	48488.9	46411.2	30259.72	25979.88
BATALHA	82143.19	74631.48	39709.11	36987.23
BOA ESPERANÇA	2150.921	1548.833	1079.662	1656.636
CACONDE	53226.51	48359.13	25730.4	23966.7
CACU	40984.36	37236.48	19812.38	18454.34

CAMARGOS	155515.5	141294.1	75178.24	70025.13
CAMPOS NOVOS	50645.71	48475.58	31605.68	27135.48
CAPIVARA (Escola Engenharia Mackenzie)	33557.41	30488.7	16222.1	15110.15
CHAVANTES	56059.29	50932.86	27099.8	25242.24
CORUMBÁ	58489.76	53141.08	28274.73	26336.63
CORUMBA III	64047.58	58190.65	30961.45	28839.19
CORUMBÁ IV	74068.01	67294.74	35805.46	33351.16
CURUA-UNA	2566.405	2331.716	726.446	725.814
EMBORCAÇÃO	66090.9	60047.11	31949.22	29759.25
ESPORA	24344.35	22118.14	11768.38	10961.71
FUNIL	85183.3	77393.58	41178.74	38356.13
FURNAS	144818.2	131575.1	70007.03	65208.37
GOV. BENTO MUNHOZ (Foz do Areia)	79462.53	76057.63	49588.95	42575.25
GOV. NEY BRAGA (Ex UHE Segredo)	66335.51	63493.1	41396.98	35541.92
GOV. PARIGOT SOUZA (Capivari-Cachoeira)	102673.1	98273.67	64073.63	55011.26
I. SOLT. EQV	17691.31	16073.5	8552.215	7966
IRAPÉ	24951.95	22670.18	12062.1	11235.3
ITAPARICA	10753.64	7743.468	5397.825	8282.434
ITUMBIARA	48044.33	43650.84	23225.27	21633.28
JAGUARI	92898.86	84403.58	44908.54	41830.27
MACHADINHO	27619.12	26435.67	17235.84	14798.06
MANSO	8173.264	7425.847	3951.064	3680.237
MARIMBONDO	33710.91	30628.16	16296.3	15179.27
MASCARENHAS DE MORAES (Peixoto)	132100.6	120020.4	63859.17	59481.92
MAUA	47990.82	45934.46	29948.89	25713.02
MIRANDA	68950.25	62644.99	33331.47	31046.75
NOVA PONTE	84495.8	76768.95	40846.39	38046.56
PARAIBUNA	102559.7	93180.93	49578.7	46180.31
PASSO FUNDO	48282.85	46213.98	30131.13	25869.48
PASSO REAL	39925.29	38214.52	24915.56	21391.58
PEDRA DO CAVALO	13652.09	9830.584	6852.714	10514.82
PEIXE ANGICAL	22800.12	20715.12	6453.797	6448.183
PICADA	96747.83	87900.57	46769.18	43563.37
PORTO ESTRELA	22063.55	20045.91	10665.81	9934.72
PORTO PRIMAVERA	8421.241	7651.148	4070.94	3791.896
PROMISSAO	24181.83	21970.48	11689.82	10888.53
QUEBRA QUEIXO	16276.88	15579.43	10157.66	8720.993
QUEIMADO	40035.51	36374.4	19353.69	18027.09

RETIRO BAIXO	26140.96	23750.46	12636.89	11770.69
SALTO SANTIAGO	50648.27	48478.03	31607.28	27136.85
SAMUEL	3808.741	3460.445	1078.102	1077.164
SANTA BRANCA	91313.25	82962.96	44142.03	41116.3
SANTA CLARA - PR	70114.87	67110.51	43755.5	37566.87
SÃO ROQUE	59534.95	56983.93	37153.06	31898.25
SÃO SIMÃO	28757.91	26128.1	13901.96	12949.04
SERRA DA MESA	46125.13	41907.15	22297.5	20769.11
SERRA DO FACAO	76454.6	69463.09	36959.17	34425.79
SINOP	64829.29	58900.88	31339.34	29191.17
SOBRADINHO	13767.73	9913.857	6910.762	10603.89
TRÊS MARIAS	21073.53	19146.43	10187.23	9488.938
TUCURUI	8271.344	7514.958	2341.285	2339.248

*own calculation based on PLD ($/MWh) [157] and productivity ($MW/(m^3/s)$) [127].

C. Technical and economical parameters for run-of-river hydropower plants

Table II-4. ROR - Hydro Power Plant Technical Parameters*

Hydropower Plant	$PmaxROR_{hr}$ (MM)	$QmaxROR_{hr}$ (m^3/s)	Qmin (m^3/s)	$tviag_{hr}$ (h)
14 DE JULHO	100	340	8	1
AIMORÉS	330	1296	205	1
ÁLVARO DE SOUZA LIMA (Bariri)	144	771	103	1
ALZIR DOS SANTOS ANTUNES (ex UHE Monjolinho)	74	134	2	1
AMADOR AGUIAR II (campim branco II)	210	537	68	1
APERTADOS	139	624	72	1
ARMANDO S. OLIVEIRA (Limoeiro)	32	178	12	3
BAGUARI	140	872	163	24
BAIXO IGUAÇU	350	2502	160	1
BARRA DO BRAÚNA	39	192	19	0
BARRA DOS COQUEIROS	90	278	56	1
BELO MONTE	11000	13950	-	0
BELO MONTE - Complemento	233.1	2466	380	0
BEM QUERER	708.5	4953	185	0
CACHOEIRA CALDEIRÃO	219	1641	25	0
CACHOEIRA DOURADA	658	2513	273	4
CANA BRAVA	450	1155	102	10
CANOAS I	82.5	567	98	1
CANOAS II	72	561	96	2
CASTRO ALVES	129.9	159	3	0
COARACY NUNES	78	399	25	1
COLIDER	300	1581	292	1
COMISSARIO	140	459	32	0
COMP. P.AFONSO/MOXOTO	4279.6	4199	501	1
COUTO MAGALHÃES	150	116	36	0
DARDANELOS	261	306	27	0
DONA FRANCISCA	125	376	21	1
ERCILANDIA	87	681	86	1
ESTREITO	1087.2	6280	585	144
EUCLIDES DA CUNHA	108.8	148	12	12
FERREIRA GOMES	252	1722	25	1
FONTES NOVA	132	51	-	0
FOZ DO CHAPECÓ	855.2	1888	79	1
FOZ PIQUIRI	96	762	97	1
FUNDAO	120	152	14	2
FUNIL GRANDE	180	585	68	12
GARIBALDI	174.9	480	17	1

GOV. JOSÉ RICHA (Ex Salto Caxias)	1240	2100	148	1
GUAPORE	120	84	19	0
GUILMAN AMORIM	140	136	21	0
HENRY BORDEN	889	152	-	0
IBITINGA	131.4	702	128	1
IGARAPAVA	210	1480	229	5
ILHA DOS POMBOS	187.1	724	166	1
ITÁ	1450	1590	49	2
ITAIPU 60 HZ	10800	9945	2839	46
ITAOCARA	150	668	183	1
ITAPEBI	450	660	24	60
ITAPIRANGA	735	2915	128	1
ITAUBA	500	620	15	1
ITIQUIRA I	60.8	80	25	0
ITIQUIRA II	95.2	78	25	1
ITUTINGA	52	236	34	1
JACUI	180	234	12	1
JAGUARA	424	1076	227	3
JATOBA	2338	16920	3356	1
JAURU	117.9	127	55	0
JIRAU	3750	26900	1386	1
JLM GODOY PEREIRA (Ex Foz do Rio Claro)	68.4	298	62	1
JUPIA	1551.2	8344	1649	1
L. E. MAGALHÃES (Ex UHE Lajeado)	902.5	3400	259	64
LUCAS N. GARCEZ (Salto Grande)	73.7	580	96	2
LUIZ CARLOS BARRETO (Estreito)	1104	2028	226	2
MASCARENHAS	198	1216	221	1
MONTE CLARO	130	372	8	1
NILO PEÇANHA	380	144	-	0
NOVA AVANHANDAVA	347.4	1431	153	6
OURINHOS	44.1	486	74	1
PARANHOS	62.6	236	8	0
PASSO SÃO JOÃO	77	326	21	1
PEREIRA PASSOS	99.9	318	-	1
PIRAJU	80	362	56	1
PONTE DE PEDRA	176.1	81	40	0
PORTO COLÔMBIA	328	1988	245	6
RISOLETA NEVES (Ex-Candonga)	140	318	43	0
RONDON II	73.5	138	33	0
ROSAL	55	32	3	0
ROSANA	354	2468	227	4
SÁ CARVALHO	78	83	23	4
SALTO	116	260	85	0
SALTO APIACÁS	45	204	3	0

SALTO GRANDE - MG	102	132	24	0
SALTO OSORIO	1078	1784	119	1
SALTO PILAO	191.8	110	10	0
SALTO RIO VERDINHO	93	254	92	1
SANTA CLARA - MG	60	132	5	0
SANTO ANTONIO	3151.2	25736	1407	1
SANTO ANTONIO JARI	369.9	1668	33	0
SÃO DOMINGOS	48	162	87	0
SÃO JOSE	51	288	20	0
SAO LUIZ TAPAJOS	7740	26676	3475	1
SÃO MANOEL	700	3805	316	1
SÃO SALVADOR	243.2	1206	107	5
SERRA QUEBRADA	1328	5232	406	1
SIMPLICIO	305.7	309	-	56
SOBRAGÍ	60	90	-	1
TABAJARA	350	1551	-	1
TAQUARUCU (Escola Politécnica)	525	2550	-	4
TELEMACO BORBA	109	252	-	0
TELES PIRES	1820	3860	-	1
VOLTA GRANDE	380	1584	-	3
XINGÓ	3162	2976	-	1

** data taken from [148], [127], [149] [150]

D. Production function coefficients for hydropower plants

Table II-5. Production function coefficients for hydropower plants with reservoir – Part 1*.

Planes	**1**	**1**	**1**	**1**	**2**	**2**	**2**	**2**	**3**	**3**	**3**	**3**	**4**	**4**	**4**	**4**
Coefficients	$\gamma_Q^{hT,pln}$	$\gamma_V^{hT,pln}$	$\gamma_o^{hT,pln}$	$\gamma_S^{hT,pln}$	$\gamma_Q^{hT,pln}$	$\gamma_V^{hT,pln}$	$\gamma_o^{hT,pln}$	$\gamma_S^{hT,pln}$	$\gamma_Q^{hT,pln}$	$\gamma_V^{hT,pln}$	$\gamma_o^{hT,pln}$	$\gamma_S^{hT,pln}$	$\gamma_Q^{hT,pln}$	$\gamma_V^{hT,pln}$	$\gamma_o^{hT,pln}$	$\gamma_S^{hT,pln}$
A. A. LAYDNER (Jurumirim)	-0.238	-0.008	-31.120	-0.005	-0.262	-0.004	-15.099	-0.005	-0.310	-0.001	-8.959	-0.003	-0.225	-0.009	-33.251	-0.006
ÁGUA VERMELHA	-0.431	-0.042	-244.530		-0.439	-0.036	-215.754		-0.514	-0.009	-93.254		-0.506	-0.011	-98.110	
AMADOR AGUIAR I (campim branco I)	-0.487	-0.146	-32.604		-0.487	-0.142	-31.543		-0.494	-0.034	-7.445		-0.471	-0.258	-53.829	
BALBINA	-0.175	-0.003	-30.610	-0.009	-0.181	-0.003	-24.155	-0.009	-0.220	0.000	-1.200	-0.006	-0.137	-0.007	-46.760	-0.014
BARRA BONITA	-0.095	-0.033	-18.557	-0.006	-0.118	-0.021	-14.110	-0.008	-0.195	-0.004	-11.406	-0.003	-0.177	-0.007	-11.066	-0.006
BARRA GRANDE	-1.203	-0.066	-180.239	-0.004	-1.302	-0.022	-60.652	-0.004	-1.471	-0.003	-12.089	-0.001	-1.073	-0.096	-225.157	-0.006
BATALHA	-0.254	-0.018	-7.448	-0.007	-0.315	-0.005	-3.128	-0.007	-0.381	-0.002	-2.746	-0.003	-0.232	-0.020	-6.558	-0.009
BOA ESPERANÇA	-0.329	-0.016	-48.467	-0.008	-0.379	-0.005	-23.838	-0.005	-0.371	-0.006	-25.290	-0.008	-0.277	-0.027	-64.937	-0.011
CACONDE	-0.601	-0.053	-2.440	-0.011	-0.672	-0.030	-1.847	-0.012	-0.837	-0.005	-1.891	-0.007	-0.818	-0.007	-1.818	-0.011
CACU	-0.228	-0.099	-19.096	-0.005	-0.229	-0.093	-17.913	-0.004	-0.228	-0.096	-18.614	-0.005	-0.247	-0.032	-6.956	-0.003
CAMARGOS	-0.105	-0.047	-5.649		-0.149	-0.024	-4.340		-0.213	-0.008	-4.567		-0.207	-0.008	-4.459	
CAMPOS NOVOS	-1.599	-0.081	-106.651		-1.599	-0.080	-104.727		-1.643	-0.005	-6.829		-1.569	-0.157	-198.872	
CAPIVARA (Escola Engenharia Mackenzie)	-0.294	-0.031	-149.119	-0.007	-0.328	-0.014	-71.355	-0.009	-0.399	-0.004	-38.218	-0.004	-0.334	-0.012	-65.583	-0.007
CHAVANTES	-0.595	-0.015	-85.331	-0.008	-0.673	-0.002	-16.630	-0.004	-0.659	-0.003	-23.285	-0.008	-0.528	-0.026	-125.145	-0.011
CORUMBÁ	-0.470	-0.129	-57.944	-0.010	-0.509	-0.093	-44.087	-0.011	-0.679	-0.020	-22.249	-0.007	-0.658	-0.025	-22.986	-0.010
CORUMBA III	-0.334	-0.024	-16.490	-0.007	-0.336	-0.020	-13.639	-0.007	-0.370	-0.004	-3.213	-0.004	-0.306	-0.050	-30.950	-0.009
CORUMBÁ IV	-0.589	-0.009	-26.338	-0.009	-0.593	-0.007	-20.564	-0.009	-0.640	-0.001	-5.107	-0.005	-0.548	-0.019	-50.376	-0.013

CURUA-UNA	-0.122	-0.023	-2.505	-0.008	-0.133	-0.015	-1.826	-0.008	-0.182	-0.006	-2.346	-0.005	-0.092	-0.034	-0.678	-0.011
EMBORCAÇÃO	-0.802	-0.036	-166.501		-0.897	-0.022	-109.947		-1.188	-0.003	-40.031		-1.150	-0.004	-43.613	
ESPORA	-0.358	-0.040	-2.454	-0.004	-0.391	-0.018	-1.606	-0.004	-0.403	-0.014	-1.586	-0.004	-0.297	-0.060	-1.145	-0.005
FUNIL	-0.389	-0.122	-33.630	-0.008	-0.419	-0.091	-26.408	-0.009	-0.562	-0.019	-13.368	-0.005	-0.557	-0.020	-13.481	-0.008
FURNAS	-0.654	-0.017	-97.534	-0.005	-0.707	-0.008	-57.148	-0.006	-0.800	-0.002	-41.262	-0.002	-0.757	-0.004	-42.957	-0.005
GOV. BENTO MUNHOZ (Foz do Areia)	-0.862	-0.099	-194.364	-0.009	-0.946	-0.066	-135.960	-0.009	-1.233	-0.010	-47.717	-0.005	-0.355	-0.220	-13.266	-0.029
GOV. NEY BRAGA (Ex UHE Segredo)	-0.996	-0.133	-341.378	-0.005	-1.008	-0.061	-156.065	-0.005	-1.042	-0.011	-33.495	-0.002	-0.990	-0.151	-382.436	-0.009
GOV. PARIGOT SOUZA (Capivari-Cachoeira)	-6.398	-0.068	-1.553		-6.484	-0.033	-1.357		-6.586	-0.012	-1.597		-6.398	-0.068	-1.553	
I. SOLT. EQV	-0.361	-0.040	-993.938	-0.008	-0.366	-0.028	-718.038	-0.008	-0.404	-0.008	-256.768	-0.004	-0.344	-0.057	-1339.63	-0.010
IRAPÉ	-1.227	-0.027	-61.998	-0.012	-1.304	-0.017	-38.903	-0.014	-1.576	-0.001	-4.702	-0.005	-1.507	-0.003	-9.404	-0.012
ITAPARICA	-0.413	-0.044	-318.289		-0.417	-0.038	-276.721	0.000	-0.457	-0.007	-72.046	0.000	-0.384	-0.066	-425.191	
ITUMBIARA	-0.515	-0.054	-243.185	-0.014	-0.551	-0.040	-185.062	-0.018	-0.725	-0.006	-75.844	-0.007	-0.707	-0.008	-79.533	-0.014
JAGUARI	-0.374	-0.013	-5.760		-0.440	-0.005	-2.488		-0.535	-0.002	-1.809		-0.355	-0.014	-5.683	
MACHADINHO	-0.802	-0.151	-344.478	-0.010	-0.839	-0.063	-144.590	-0.010	-0.935	-0.006	-18.915	-0.004	-0.728	-0.238	-493.992	-0.015
MANSO	-0.451	-0.010	-42.624	-0.007	-0.452	-0.010	-41.470	-0.009	-0.528	-0.001	-8.389	-0.003	-0.517	-0.002	-10.756	-0.007
MARIMBONDO	-0.350	-0.104	-84.486	-0.015	-0.391	-0.067	-68.696	-0.019	-0.504	-0.018	-72.211	-0.008	-0.495	-0.020	-70.264	-0.015
MASCARENHAS DE MORAES (Peixoto)	-0.267	-0.054	-81.541	-0.008	-0.273	-0.049	-75.182	-0.010	-0.369	-0.011	-37.666	-0.005	-0.361	-0.013	-38.442	-0.008
MAUA	-0.997	-0.035	-51.589	-0.008	-1.016	-0.017	-25.913	-0.008	-1.076	-0.003	-6.880	-0.004	-0.940	-0.062	-80.574	-0.011
MIRANDA	-0.603	-0.099	-95.836		-0.608	-0.058	-56.089		-0.630	-0.012	-13.373		-0.596	-0.127	-120.643	
NOVA PONTE	-0.715	-0.023	-53.070	-0.012	-0.896	-0.006	-22.884	-0.012	-1.057	-0.002	-22.562	-0.006	-0.656	-0.025	-42.370	-0.016
PARAIBUNA	-0.577	-0.009	-18.320		-0.647	-0.003	-8.185		-0.737	-0.002	-6.300		-0.465	-0.013	-19.453	
PASSO FUNDO	-2.199	-0.010	-1.904		-2.256	-0.002	-0.506		-2.323	0.000	-0.141		-2.193	-0.011	-1.669	
PASSO REAL	-0.185	-0.043	-12.318		-0.313	-0.009	-3.997		-0.429	-0.001	-3.136		-0.125	-0.051	-0.380	

PEDRA DO CAVALO	-0.878	-0.014	-29.966	-0.003	-0.901	-0.005	-10.562	-0.003	-0.949	0.000	-0.255	-0.001	-0.871	-0.015	-32.249	-0.004
PEIXE ANGICAL	-0.234	-0.040	-84.794	-0.008	-0.235	-0.038	-80.596	-0.008	-0.252	-0.007	-14.612	-0.005	-0.207	-0.087	-158.593	-0.014
PICADA	-1.093	-0.255	-1.502	-0.003	-1.101	-0.060	-0.391	-0.002	-1.095	-0.161	-0.955	-0.003	-1.081	-0.565	-3.066	-0.005
PORTO ESTRELA	-0.374	-0.587	-32.849	0.000	-0.456	-0.062	-5.475	0.000	-0.449	-0.083	-6.507		-0.347	-0.711	-36.141	
PORTO PRIMAVERA	-0.162	-0.019	-229.292		-0.165	-0.015	-178.060		-0.179	-0.007	-80.168		-0.133	-0.037	-331.670	
PROMISSAO	-0.185	-0.020	-105.506	-0.004	-0.195	-0.010	-54.405	-0.004	-0.223	-0.003	-19.824	-0.002	-0.180	-0.023	-116.997	-0.006
QUEBRA QUEIXO	-1.037	-0.192	-21.252	-0.002	-1.051	-0.074	-8.218	-0.002	-1.083	-0.006	-0.748	-0.001	-1.010	-0.308	-32.535	-0.002
QUEIMADO	-1.487	-0.030	-2.743		-1.576	-0.008	-1.436		-1.630	-0.004	-1.601		-1.479	-0.031	-2.512	
RETIRO BAIXO	-0.305	-0.076	-14.960	-0.006	-0.322	-0.011	-2.504	-0.003	-0.310	-0.046	-9.248	-0.006	-0.287	-0.148	-26.986	-0.010
SALTO SANTIAGO	-0.762	-0.088	-231.949	-0.013	-0.798	-0.063	-169.775	-0.016	-0.988	-0.007	-43.846	-0.006	-0.933	-0.017	-62.506	-0.013
SAMUEL	-0.211	-0.014	-13.233	-0.016	-0.233	-0.007	-6.846	-0.016	-0.278	0.000	-0.526	-0.009	-0.141	-0.033	-1.725	-0.027
SANTA BRANCA	-0.223	-0.077	-10.135		-0.262	-0.051	-7.497		-0.366	-0.014	-5.107		-0.133	-0.109	-7.339	
SANTA CLARA - PR	-0.646	-0.106	-17.837	-0.003	-0.711	-0.033	-6.496	-0.003	-0.796	-0.010	-3.668	-0.001	-0.554	-0.157	-18.501	-0.005
SÃO ROQUE	-0.350	-0.092	-30.875	-0.003	-0.398	-0.031	-10.887	-0.003	-0.473	-0.005	-3.190	-0.001	-0.405	-0.026	-9.508	-0.003
SÃO SIMÃO	-0.586	-0.043	-294.613		-0.590	-0.040	-276.546		-0.677	-0.008	-96.499		-0.670	-0.010	-102.712	
SERRA DA MESA	-0.750	-0.013	-147.626	-0.008	-0.912	-0.005	-74.907	-0.010	-1.116	-0.001	-47.688	-0.003	-1.051	-0.002	-50.276	-0.008
SERRA DO FACAO	-0.491	-0.022	-39.178	-0.013	-0.540	-0.015	-26.630	-0.023	-0.695	-0.002	-8.971	-0.007	-0.358	-0.033	-35.902	-0.040
SINOP	-0.163	-0.083	-80.937	-0.009	-0.197	-0.033	-39.467	-0.009	-0.247	-0.014	-34.086	-0.005	-0.123	-0.112	-69.751	-0.012
SOBRADINHO	-0.145	-0.018	-84.685	-0.010	-0.173	-0.011	-59.922	-0.012	-0.245	-0.003	-50.767	-0.006	-0.233	-0.003	-48.814	-0.010
TRÊS MARIAS	-0.281	-0.014	-60.200	-0.004	-0.372	-0.004	-22.195	-0.006	-0.478	-0.001	-15.091	-0.002	-0.377	-0.004	-21.268	-0.004
TUCURUI	-0.391	-0.080	-855.548	-0.018	-0.437	-0.051	-582.278	-0.021	-0.583	-0.009	-293.664	-0.010	-0.553	-0.014	-309.773	-0.018

*own calculation based on [127], [150]

** units = $\gamma_Q^{hT,pln}$: (MW·s/m³); $\gamma_V^{hT,pln}$: (MW/hm³); $\gamma_o^{hT,pln}$: (MW); $\gamma_S^{hT,pln}$: (MW·s/m³).

Table II-6. Production function coefficients for hydropower plants with reservoir – Part 2*.

Planes	**5**	**5**	**5**	**5**	**6**	**6**	**6**	**6**	**7**	**7**	**7**	**7**	**8**	**8**	**8**	**8**
Coefficients	$\gamma_Q^{hT,pln}$	$\gamma_V^{hT,pln}$	$\gamma_o^{hT,pln}$	$\gamma_S^{hT,pln}$	$\gamma_Q^{hT,pln}$	$\gamma_V^{hT,pln}$	$\gamma_o^{hT,pln}$	$\gamma_S^{hT,pln}$	$\gamma_Q^{hT,pln}$	$\gamma_V^{hT,pln}$	$\gamma_o^{hT,pln}$	$\gamma_S^{hT,pln}$	$\gamma_Q^{hT,pln}$	$\gamma_V^{hT,pln}$	$\gamma_o^{hT,pln}$	$\gamma_S^{hT,pln}$
A. A. LAYDNER (Jurumirim)	-0.312	-0.001	-7.922	-0.003	-0.243	-0.002	1.028	-0.006	-0.243	-0.002	1.028	-0.006	-0.243	-0.002	1.028	-0.006
ÁGUA VERMELHA	-0.418	-0.047	-254.559		-0.520	-0.007	-78.310		-0.520	-0.007	-78.310		-0.520	-0.007	-78.310	
AMADOR AGUIAR I (campim branco I)	-0.472	-0.250	-52.010		-0.478	-0.146	-30.052		-0.494	-0.033	-7.190		-0.478	-0.142	-28.992	
BALBINA	-0.171	-0.003	-28.079	-0.014	-0.220	0.000	-0.911	-0.006	-0.171	-0.003	-24.136	-0.014	-0.175	-0.003	-20.218	-0.014
BARRA BONITA	-0.064	-0.041	-10.192	-0.009	-0.200	-0.003	-9.292	-0.003	-0.200	-0.003	-9.292	-0.003	-0.200	-0.003	-9.292	-0.003
BARRA GRANDE	-1.474	-0.002	-10.172	-0.001	-1.206	0.000	71.440	-0.006	-1.206	0.000	71.440	-0.006	-1.206	0.000	71.440	-0.006
BATALHA	-0.389	-0.001	-2.000	-0.003	-0.294	-0.003	2.225	-0.009	-0.294	-0.003	2.225	-0.009	-0.294	-0.003	2.225	-0.009
BOA ESPERANÇA	-0.327	-0.016	-48.431	-0.011	-0.383	-0.004	-20.965	-0.005	-0.383	-0.004	-20.965	-0.005	-0.383	-0.004	-20.965	-0.005
CACONDE	-0.406	-0.084	5.432	-0.011	-0.854	-0.003	-1.188	-0.007	-0.854	-0.003	-1.188	-0.007	-0.854	-0.003	-1.188	-0.007
CACU	-0.218	-0.163	-30.151	-0.007	-0.248	-0.030	-6.622	-0.003	-0.228	-0.093	-17.818	-0.006	-0.215	-0.010	3.431	-0.007
CAMARGOS	-0.080	-0.054	-3.351		-0.224	-0.005	-3.586		-0.224	-0.005	-3.586		-0.224	-0.005	-3.586	
CAMPOS NOVOS	-1.592	-0.081	-104.656		-1.643	-0.005	-6.707		-1.592	-0.080	-102.61		-1.570	-0.005	13.171	
CAPIVARA (Escola Engenharia Mackenzie)	-0.217	-0.051	-172.725	-0.010	-0.403	-0.003	-31.143	-0.004	-0.403	-0.003	-31.143	-0.004	-0.403	-0.003	-31.143	-0.004
CHAVANTES	-0.581	-0.016	-87.806	-0.011	-0.675	-0.002	-14.643	-0.004	-0.675	-0.002	-14.643	-0.004	-0.675	-0.002	-14.643	-0.004
CORUMBÁ	-0.305	-0.205	-42.276	-0.011	-0.695	-0.013	-16.347	-0.007	-0.695	-0.013	-16.347	-0.007	-0.695	-0.013	-16.347	-0.007
CORUMBA III	-0.370	-0.004	-3.089	-0.004	-0.324	-0.009	-0.863	-0.009	-0.324	-0.009	-0.863	-0.009	-0.324	-0.009	-0.863	-0.009
CORUMBÁ IV	-0.640	-0.001	-5.083	-0.005	-0.576	-0.003	-3.272	-0.013	-0.576	-0.003	-3.272	-0.013	-0.576	-0.003	-3.272	-0.013
CURUA-UNA	-0.183	-0.005	-2.243	-0.005	-0.128	-0.013	-0.298	-0.011	-0.128	-0.013	-0.298	-0.011	-0.128	-0.013	-0.298	-0.011
EMBORCAÇÃO	-0.544	-0.054	-113.160		-1.204	-0.002	-28.327		-1.204	-0.002	-28.327		-1.204	-0.002	-28.327	
ESPORA	-0.420	-0.006	-0.814	-0.003	-0.410	-0.009	-1.055	-0.004	-0.410	-0.009	-1.055	-0.004	-0.410	-0.009	-1.055	-0.004
FUNIL	-0.260	-0.188	-25.762	-0.010	-0.574	-0.012	-10.219	-0.005	-0.574	-0.012	-10.219	-0.005	-0.574	-0.012	-10.219	-0.005
FURNAS	-0.543	-0.027	-47.656	-0.007	-0.810	-0.001	-31.237	-0.002	-0.810	-0.001	-31.237	-0.002	-0.810	-0.001	-31.237	-0.002

GOV. BENTO MUNHOZ (Foz do Areia)	-0.540	-0.147	-22.850	-0.032	-0.785	-0.099	-130.786	-0.018	-1.241	-0.006	-35.994	-0.005	-0.869	-0.066	-72.382	-0.018
GOV. NEY BRAGA (Ex UHE Segredo)	-1.042	-0.011	-31.609	-0.002	-0.993	-0.015	-10.975	-0.009	-0.993	-0.015	-10.975	-0.009	-0.993	-0.015	-10.975	-0.009
GOV. PARIGOT SOUZA (Capivari-Cachoeira)	-6.602	-0.006	-1.070		-6.602	-0.006	-1.070		-6.602	-0.006	-1.070		-6.602	-0.006	-1.070	
I. SOLT. EQV	-0.405	-0.007	-237.031	-0.004	-0.349	-0.010	43.524	-0.010	-0.349	-0.010	43.524	-0.010	-0.349	-0.010	43.524	-0.010
IRAPÉ	-1.000	-0.043	-66.624	-0.015	-1.581	-0.001	-3.466	-0.005	-1.581	-0.001	-3.466	-0.005	-1.581	-0.001	-3.466	-0.005
ITAPARICA	-0.458	-0.006	-61.795	0.000	-0.458	-0.006	-61.795		-0.458	-0.006	-61.795		-0.458	-0.006	-61.795	
ITUMBIARA	-0.355	-0.087	-147.280	-0.021	-0.736	-0.004	-54.738	-0.007	-0.736	-0.004	-54.738	-0.007	-0.736	-0.004	-54.738	-0.007
JAGUARI	-0.543	-0.001	-1.429		-0.379	-0.001	4.284		-0.379	-0.001	4.284		-0.379	-0.001	4.284	
MACHADINHO	-0.936	-0.005	-16.982	-0.004	-0.818	-0.038	-48.277	-0.015	-0.818	-0.038	-48.277	-0.015	-0.818	-0.038	-48.277	-0.015
MANSO	-0.390	-0.017	-60.728	-0.011	-0.530	-0.001	-7.056	-0.003	-0.530	-0.001	-7.056	-0.003	-0.530	-0.001	-7.056	-0.003
MARIMBONDO	-0.215	-0.165	78.671	-0.022	-0.522	-0.010	-51.470	-0.008	-0.522	-0.010	-51.470	-0.008	-0.522	-0.010	-51.470	-0.008
MASCARENHAS DE MORAES (Peixoto)	-0.187	-0.088	-73.176	-0.012	-0.375	-0.009	-32.131	-0.005	-0.375	-0.009	-32.131	-0.005	-0.375	-0.009	-32.131	-0.005
MAUA	-1.077	-0.003	-6.133	-0.004	-0.995	-0.007	-0.607	-0.011	-0.995	-0.007	-0.607	-0.011	-0.995	-0.007	-0.607	-0.011
MIRANDA	-0.631	-0.012	-12.776		-0.603	-0.036	-29.391		-0.603	-0.036	-29.391		-0.603	-0.036	-29.391	
NOVA PONTE	-1.080	-0.001	-15.850	-0.006	-0.828	-0.003	36.835	-0.016	-0.828	-0.003	36.835	-0.016	-0.828	-0.003	36.835	-0.016
PARAIBUNA	-0.747	-0.001	-5.188		-0.600	-0.001	4.011		-0.600	-0.001	4.011		-0.600	-0.001	4.011	
PASSO FUNDO	-2.323	0.000	-0.105		-2.241	-0.001	1.754		-2.241	-0.001	1.754		-2.241	-0.001	1.754	
PASSO REAL	-0.434	-0.001	-2.023		-0.245	0.000	44.675		-0.245	0.000	44.675		-0.245	0.000	44.675	
PEDRA DO CAVALO	-0.949	0.000	-0.225	-0.001	-0.880	-0.001	3.615	-0.004	-0.880	-0.001	3.615	-0.004	-0.880	-0.001	3.615	-0.004
PEIXE ANGICAL	-0.215	-0.056	-99.666	-0.014	-0.224	-0.040	-74.009	-0.012	-0.252	-0.006	-13.838	-0.005	-0.225	-0.038	-69.811	-0.012
PICADA	-1.086	-0.373	-2.048	-0.005	-1.101	-0.054	-0.353	-0.002	-1.101	-0.054	-0.353	-0.002	-1.101	-0.054	-0.353	-0.002
PORTO ESTRELA	-0.357	-0.644	-33.741	0.000	-0.456	-0.062	-5.475	0.000	-0.456	-0.062	-5.475	0.000	-0.456	-0.062	-5.475	0.000
PORTO PRIMAVERA	-0.147	-0.021	-166.441		-0.149	-0.019	-159.200		-0.180	-0.005	-58.266		-0.152	-0.015	-107.968	

PROMISSAO	-0.223	-0.003	-19.114	-0.002	-0.192	-0.009	-42.916	-0.006	-0.192	-0.009	-42.916	-0.006	-0.192	-0.009	-42.916	-0.006
QUEBRA QUEIXO	-1.083	-0.005	-0.676	-0.001	-1.045	-0.049	-4.425	-0.002	-1.045	-0.049	-4.425	-0.002	-1.045	-0.049	-4.425	-0.002
QUEIMADO	-1.646	-0.002	-1.073		-1.538	-0.003	2.648		-1.538	-0.003	2.648		-1.538	-0.003	2.648	
RETIRO BAIXO	-0.294	-0.105	-19.449	-0.010	-0.322	-0.009	-2.018	-0.003	-0.322	-0.009	-2.018	-0.003	-0.322	-0.009	-2.018	-0.003
SALTO SANTIAGO	-0.613	-0.139	-245.615	-0.020	-0.992	-0.006	-36.645	-0.006	-0.992	-0.006	-36.645	-0.006	-0.992	-0.006	-36.645	-0.006
SAMUEL	-0.199	-0.015	-8.454	-0.027	-0.201	-0.014	-8.947	-0.024	-0.278	0.000	-0.196	-0.009	-0.223	-0.007	-2.560	-0.024
SANTA BRANCA	-0.374	-0.009	-3.747		-0.374	-0.009	-3.747		-0.374	-0.009	-3.747		-0.374	-0.009	-3.747	
SANTA CLARA - PR	-0.801	-0.007	-2.965	-0.001	-0.694	-0.024	-1.109	-0.005	-0.694	-0.024	-1.109	-0.005	-0.694	-0.024	-1.109	-0.005
SÃO ROQUE	-0.273	-0.141	-35.036	-0.004	-0.475	-0.003	-2.426	-0.001	-0.475	-0.003	-2.426	-0.001	-0.475	-0.003	-2.426	-0.001
SÃO SIMÃO	-0.575	-0.046	-306.452		-0.681	-0.007	-86.166		-0.681	-0.007	-86.166		-0.681	-0.007	-86.166	
SERRA DA MESA	-0.505	-0.019	-60.935	-0.012	-1.140	-0.001	-31.109	-0.003	-1.140	-0.001	-31.109	-0.003	-1.140	-0.001	-31.109	-0.003
SERRA DO FACAO	-0.704	-0.001	-6.434	-0.004	-0.695	-0.002	-8.896	-0.013	-0.695	-0.002	-8.896	-0.013	-0.695	-0.002	-8.896	-0.013
SINOP	-0.254	-0.009	-25.200	-0.005	-0.179	-0.019	20.508	-0.012	-0.179	-0.019	20.508	-0.012	-0.179	-0.019	20.508	-0.012
SOBRADINHO	-0.098	-0.024	-7.379	-0.014	-0.255	-0.001	-31.555	-0.006	-0.255	-0.001	-31.555	-0.006	-0.255	-0.001	-31.555	-0.006
TRÊS MARIAS	-0.017	-46.886	-0.006	-0.484	-0.001	-11.271	-0.002	-0.484	-0.001	-11.271	-0.002	-0.484	-0.001	-11.271	-0.002	
TUCURUI	-0.132	-219.47	-0.024	-0.597	-0.005	-180.65	-0.010	-0.597	-0.005	-180.65	-0.010	-0.597	-0.005	-180.65	-0.010	

*own calculation based on [127], [150]

** units = $\gamma_Q^{hT,pln}$: (MW·s/m³); $\gamma_V^{hT,pln}$: (MW/hm³); $\gamma_o^{hT,pln}$: (MW); $\gamma_S^{hT,pln}$: (MW·s/m³).

Table II-7. Production function coefficients for ROR hydropower plants*.

Planes	1	1	1	2	2	2	3	3	3	4	4	4
Coefficients	$\gamma_Q^{hT,plnR}$	$\gamma_o^{hT,plnR}$	$\gamma_S^{hT,plnR}$	$\gamma_Q^{hT,plnR}$	$\gamma_o^{hT,plnR}$	$\gamma_S^{hT,plnR}$	$\gamma_Q^{hT,plnR}$	$\gamma_o^{hT,plnR}$	$\gamma_S^{hT,plnR}$	$\gamma_Q^{hT,plnR}$	$\gamma_o^{hT,plnR}$	$\gamma_S^{hT,plnR}$
14 DE JULHO	0.3162	0.0092		0.1148	61.0118		0.1148	61.0118		0.1148	61.0118	
AIMORÉS	0.2607	1.4427		0.2340	17.3301		0.2025	56.1565		0.2025	56.1565	
ÁLVARO DE SOUZA LIMA (Bariri)	0.1882	0.0985	-0.0073	0.1555	19.5417	-0.0105	0.1555	19.5417	-0.0105	0.1555	19.5417	-0.0105
ALZIR DOS SANTOS ANTUNES (ex UHE Monjolinho)	0.5459	0.0004	-0.0026	0.4717	9.1122	-0.0043	0.4717	9.1122	-0.0043	0.4717	9.1122	-0.0043
AMADOR AGUIAR II (campim branco II)	0.3976	0.2308	-0.0053	0.3976	0.2308	-0.0053	0.3976	0.2308	-0.0053	0.3976	0.2308	-0.0053
APERTADOS	0.2441	0.2201	-0.0054	0.2441	0.2201	-0.0054	0.2441	0.2201	-0.0054	0.2441	0.2201	-0.0054
ARMANDO S. OLIVEIRA (Limoeiro)	0.2142	0.0227	-0.0080	0.0845	18.2642	-0.0050	-0.0001	31.8448	0.0000	-0.0001	31.8448	0.0000
BAGUARI	0.1729	0.5979	-0.0066	0.1549	8.7154	-0.0111	0.0617	86.2728	-0.0100	0.0617	86.2728	-0.0100
BAIXO IGUAÇU	0.1582	0.6596		0.1417	10.0088		0.1271	32.1931		0.0914	117.8123	
BARRA DO BRAÚNA	0.2142	0.0584		0.1665	6.9795		0.1665	6.9795		0.1665	6.9795	
BARRA DOS COQUEIROS	0.3318	0.1780	-0.0056	0.2961	8.3039	-0.0059	0.2961	8.3039	-0.0059	0.2961	8.3039	-0.0059
BELO MONTE	0.8371	3.9125	-0.0185	0.5957	2892.8807	-0.0204	0.5957	2892.8807	-0.0204	0.5957	2892.8807	-0.0204
BELO MONTE - Complemento	0.0935	0.8402	-0.0037	0.0841	10.6457	-0.0074	0.0169	159.4266	-0.0085	0.0169	159.4266	-0.0085
BEM QUERER	0.1782	1.2428		0.1382	45.4965		0.1087	138.9538		0.1087	138.9538	
CACHOEIRA CALDEIRÃO	0.1409	0.0028	-0.0048	0.1109	41.0046	-0.0057	0.1109	41.0046	-0.0057	0.1109	41.0046	-0.0057
CACHOEIRA DOURADA	0.2704	1.8326	-0.0090	0.2418	25.4472	-0.0207	0.1661	196.5295	-0.0263	0.1661	196.5295	-0.0263
CANA BRAVA	0.3999	0.6052		0.3591	18.5628		0.1962	195.0842		0.1962	195.0842	
CANOAS I	0.1483	0.1477	-0.0055	0.1248	10.6393	-0.0083	0.1248	10.6393	-0.0083	0.1248	10.6393	-0.0083
CANOAS II	0.1268	0.1409	-0.0058	0.0918	16.6703	-0.0081	0.0918	16.6703	-0.0081	0.0918	16.6703	-0.0081
CASTRO ALVES	0.8509	0.0063		0.7464	12.6461		0.7464	12.6461		0.7464	12.6461	
COARACY NUNES	0.1825	0.0025		0.0903	33.2257		0.0903	33.2257		0.0903	33.2257	
COLIDER	0.2133	2.9063	-0.0104	0.1913	15.0990	-0.0177	0.1715	36.0629	-0.0241	0.1715	36.0629	-0.0241
COMISSARIO	0.3185	0.0545	-0.0048	0.3185	0.0545	-0.0048	0.3185	0.0545	-0.0048	0.3185	0.0545	-0.0048

COUTO MAGALHÃES	1.3606	0.5148		1.3606	0.5148		1.3606	0.5148		1.3606	0.5148	
DARDANELOS	0.8815	0.0350	-0.0106	0.4257	130.5842	-0.0003	0.4257	130.5842	-0.0003	0.4257	130.5842	-0.0003
DONA FRANCISCA	0.3386	0.0336	-0.0075	0.2739	19.5277	-0.0130	0.2739	19.5277	-0.0130	0.2739	19.5277	-0.0130
ERCILANDIA	0.1538	0.4034	-0.0055	0.1372	4.0712	-0.0102	0.1225	11.3794	-0.0122	0.1225	11.3794	-0.0122
ESTREITO	0.2312	9.3786	-0.0147	0.1794	90.9799	-0.0255	0.1397	229.4882	-0.0384	0.1397	229.4882	-0.0384
EUCLIDES DA CUNHA	0.7376	0.0941	-0.0150	0.4040	42.7751	-0.0228	0.4040	42.7751	-0.0228	0.4040	42.7751	-0.0228
FERREIRA GOMES	0.1687	0.0317		0.1504	9.7797		0.1344	32.6353		0.0001	251.9163	
FONTES NOVA	2.6809			2.6809			2.6809			2.6809		
FOZ DO CHAPECÓ	0.4660	0.1885		0.3675	145.0002		0.3675	145.0002		0.3675	145.0002	
FOZ PIQUIRI	0.1487	0.3845	-0.0050	0.1333	4.4245	-0.0108	0.1333	4.4245	-0.0108	0.1333	4.4245	-0.0108
FUNDAO	0.8353	0.0252	-0.0085	0.0000	120.0447	0.0000	0.0000	120.0447	0.0000	0.0000	120.0447	0.0000
FUNIL GRANDE	0.3511	0.0000	0.0000	0.1295	111.5274	0.0000		180.2573	0.0000		180.2573	0.0000
GARIBALDI	0.3922	0.0097	-0.0057	0.2334	71.5505	-0.0016	0.2334	71.5505	-0.0016	0.2334	71.5505	-0.0016
GOV. JOSÉ RICHA (Ex Salto Caxias)	0.5867	0.2057	-0.0087	0.4426	271.1875	-0.0141	0.4426	271.1875	-0.0141	0.4426	271.1875	-0.0141
GUAPORE	1.4094	0.2065	-0.0065	1.4094	0.2065	-0.0065	1.4094	0.2065	-0.0065	1.4094	0.2065	-0.0065
GUILMAN AMORIM	1.0262			1.0262			1.0262			1.0262		
HENRY BORDEN	5.6951			5.6951			5.6951			5.6951		
IBITINGA	0.2043	0.4106	-0.0089	0.1438	34.4123	-0.0089	0.0001	131.3587	-0.0051	0.0001	131.3587	-0.0051
IGARAPAVA	0.1494	0.4427	-0.0032	0.0851	84.2288	-0.0014	0.0851	84.2288	-0.0014	0.0851	84.2288	-0.0014
ILHA DOS POMBOS	0.2805	2.1067		0.1957	51.0009		0.0001	187.0848		0.0001	187.0848	
ITÁ	0.9298	0.1311	-0.0164	0.8201	129.2093	-0.0305	0.8201	129.2093	-0.0305	0.8201	129.2093	-0.0305
ITAIPU 60 HZ	0.8094	86.9803	-0.0367	0.7260	565.7137	-0.0787	0.2940	5946.7619	-0.0992	0.2940	5946.7619	-0.0992
ITAOCARA	0.3191	0.8278	-0.0030	0.3191	0.8278	-0.0030	0.3191	0.8278	-0.0030	0.3191	0.8278	-0.0030
ITAPEBI	0.7279	0.0642	-0.0093	0.5147	122.1234	-0.0052	0.5147	122.1234	-0.0052	0.5147	122.1234	-0.0052
ITAPIRANGA	0.2535	0.0000	0.0000	0.2535	0.0000	0.0000	0.2535	0.0000	0.0000	0.2535	0.0000	0.0000
ITAUBA	0.8104	0.0347	-0.0152	0.5777	123.8325	-0.0246	0.5777	123.8325	-0.0246	0.5777	123.8325	-0.0246
ITIQUIRA I	0.7926	0.0000		0.0079	60.5067		0.0079	60.5067		0.0079	60.5067	

ITIQUIRA II	1.2463	0.1966	-0.0037	1.2463	0.1966	-0.0037	1.2463	0.1966	-0.0037	1.2463	0.1966	-0.0037
ITUTINGA	0.2518	0.0967		0.2114	6.8285		0.0000	52.0402		0.0000	52.0402	
JACUI	0.8407	0.0137	-0.0080	0.5504	59.4640	-0.0005	0.0000	181.8311	0.0000	0.0000	181.8311	0.0000
JAGUARA	0.4054	0.9551		0.3155	84.4947		0.3155	84.4947		0.3155	84.4947	
JAURU	0.9303	0.1308	-0.0080	0.7987	16.0082	-0.0094	0.7987	16.0082	-0.0094	0.7987	16.0082	-0.0094
JIRAU	0.1700	0.8716	-0.0144	0.1357	428.5026	-0.0289	0.0527	2440.3989	-0.0294	-0.0005	3819.0119	-0.0300
JLM GODOY PEREIRA (Ex Foz do Rio Claro)	0.2479	0.4158	-0.0100	0.0072	66.3711	-0.0045	0.0072	66.3711	-0.0045	0.0072	66.3711	-0.0045
JUPIA	0.1990	19.7707	-0.0133	0.1760	85.6445	-0.0215	0.1554	187.7529	-0.0300	0.1094	536.4174	-0.0371
L. E. MAGALHÃES (Ex UHE Lajeado)	0.3481	2.3367	-0.0316	0.0435	768.3864	-0.0286	0.0005	900.6137	-0.0210	-0.0003	903.0749	-0.0168
LUCAS N. GARCEZ (Salto Grande)	0.1498	0.1971	-0.0075	0.0370	54.4056	-0.0051	0.0001	73.9404	-0.0019	0.0001	73.9671	-0.0002
LUIZ CARLOS BARRETO (Estreito)	0.5590	0.7559	-0.0071	0.5590	0.7559	-0.0071	0.5590	0.7559	-0.0071	0.5590	0.7559	-0.0071
MASCARENHAS	0.1918	1.4807	-0.0140	0.1505	30.1671	-0.0209	0.0001	197.8628	-0.0170	0.0003	197.7115	-0.0160
MONTE CLARO	0.3762	0.0072		0.0588	108.3969		0.0588	108.3969		0.0588	108.3969	
NILO PEÇANHA	2.4575			2.4575			2.4575			2.4575		
NOVA AVANHANDAVA	0.2818	1.0641	-0.0105	0.0253	313.0044	-0.0042	0.0001	347.2680	0.0000	0.0001	347.2680	0.0000
OURINHOS	0.0939	0.2154		0.0836	2.0622		0.0577	13.2836		0.0577	13.2836	
PARANHOS	0.2685	0.0000	0.0000	0.2685	0.0000	0.0000	0.2685	0.0000	0.0000	0.2685	0.0000	0.0000
PASSO SÃO JOÃO	0.2732	0.0244	-0.0071	0.1855	23.2995	-0.0055	0.0000	79.7488	0.0000	0.0000	79.7488	0.0000
PEREIRA PASSOS	0.3414		-0.0008	0.3070	2.0816	0.1711	0.3070	2.0816	0.1711	0.3070	2.0816	0.1711
PIRAJU	0.2283	0.2055	-0.0058	0.2038	5.6381	-0.0094	0.2038	5.6381	-0.0094	0.2038	5.6381	-0.0094
PONTE DE PEDRA	2.0386	0.2978		1.1769	63.9152		-0.0162	154.5913		-0.0162	154.5913	
PORTO COLÔMBIA	0.1723	0.1368	-0.0031	0.0558	216.9435	-0.0004	0.0558	216.9435	-0.0004	0.0558	216.9435	-0.0004
RISOLETA NEVES (Ex-Candonga)	0.4446	0.2047	-0.0116	0.3757	17.2247	-0.0170	0.3757	17.2247	-0.0170	0.3757	17.2247	-0.0170
RONDON II	0.5495	0.2656		0.2907	33.1375		0.2907	33.1375		0.2907	33.1375	
ROSAL	1.7352	0.0110		0.7511	29.7421		0.7511	29.7421		0.7511	29.7421	
ROSANA	0.1930	1.4554	-0.0103	0.1540	36.1593	-0.0178	0.1146	112.6619	-0.0176	-0.0005	355.3011	-0.0061
SÁ CARVALHO	1.0075	0.0000	0.0000	0.1763	63.7432	0.0000		77.8162	0.0000		77.8162	0.0000

SALTO	0.4431	0.5013	-0.0070	0.3696	17.7995	-0.0107	0.3696	17.7995	-0.0107	0.3696	17.7995	-0.0107
SALTO APIACÁS	0.2218			0.2218			0.2218			0.2218		
SALTO GRANDE - MG	1.0243	0.0873		0.2627	74.1876		0.0000	101.4031		0.0000	101.4031	
SALTO OSORIO	0.6354	0.4819	-0.0125	0.6354	0.4819	-0.0125	0.6354	0.4819	-0.0125	0.6354	0.4819	-0.0125
SALTO PILAO	1.7859	0.0093	-0.0046	1.1004	71.3369	0.0000	1.1004	71.3369	0.0000	1.1004	71.3369	0.0000
SALTO RIO VERDINHO	0.3639	0.5951	-0.0072	0.2976	15.8543	-0.0114	0.2976	15.8543	-0.0114	0.2976	15.8543	-0.0114
SANTA CLARA - MG	0.4431	0.0048		0.1961	29.9786		0.1961	29.9786		0.1961	29.9786	
SANTO ANTONIO	0.2113	26.9588	-0.0144	0.1412	409.3336	-0.0236	0.0935	1050.1091	-0.0145	0.0610	1777.7597	-0.0080
SANTO ANTONIO JARI	0.2516	0.0597	-0.0072	0.2242	14.8633	-0.0191	0.0549	278.6291	-0.0172	0.0549	278.6291	-0.0172
SÃO DOMINGOS	0.2914	1.6359	-0.0054	0.2914	1.6359	-0.0054	0.2914	1.6359	-0.0054	0.2914	1.6359	-0.0054
SÃO JOSE	0.1992	0.0136	-0.0046	0.0169	46.3226	-0.0002	0.0000	50.9450	0.0000	0.0000	50.9450	0.0000
SAO LUIZ TAPAJOS	0.3407	122.9134		0.3060	335.6572		0.2721	854.4328		0.2721	854.4328	
SÃO MANOEL	0.2443	2.5994	-0.0113	0.2164	26.4495	-0.0223	0.1914	70.7385	-0.0326	0.1685	132.2065	-0.0443
SÃO SALVADOR	0.2065	0.0230	-0.0041	0.2065	0.0230	-0.0041	0.2065	0.0230	-0.0041	0.2065	0.0230	-0.0041
SERRA QUEBRADA	0.2637	1.4181	-0.0091	0.2354	55.7857	-0.0232	0.2354	55.7857	-0.0232	0.2354	55.7857	-0.0232
SIMPLICIO	0.9451		-0.0045	0.9451		-0.0045	0.9451		-0.0045	0.9451		-0.0045
SOBRAGÍ	0.6616	0.0000		0.5769	7.3032		0.5769	7.3032		0.5769	7.3032	
TABAJARA	0.2572	2.0304	-0.0086	0.2280	12.7332	-0.0146	0.2049	31.0561	-0.0216	0.2049	31.0561	-0.0216
TAQUARUCU (Escola Politécnica)	0.2232	0.4403	-0.0069	0.1997	27.7763	-0.0132	0.1026	262.9145	-0.0126	0.1026	262.9145	-0.0126
TELEMACO BORBA	0.4522	0.0374		0.4522	0.0374		0.4522	0.0374		0.4522	0.0374	
TELES PIRES	0.5199	1.5907	-0.0162	0.4647	101.0626	-0.0306	0.1327	1331.0063	-0.0283	0.1327	1331.0063	-0.0283
VOLTA GRANDE	0.2445	0.5407		0.2445	0.5407		0.2445	0.5407		0.2445	0.5407	
XINGÓ	1.0966	6.7980	-0.0123	0.7583	899.2673	-0.0055	0.7583	899.2673	-0.0055	0.7583	899.2673	-0.0055

*own calculation based on [127], [150]

** units = $\gamma_Q^{hT,plnR}$: (MW·s/m³); $\gamma_o^{hT,plnR}$: (MW); $\gamma_S^{hT,plnR}$: (MW·s/m³).

E. Transmission system data

Table II-8. Power Transfer Distribution Factor (PTDF)*.

Bus/Line		BUS-1	BUS-2	BUS-3	BUS-4	BUS-5	BUS-6	BUS-7-8	BUS-9	BUS-10	BUS-IMP	BUS-XIN	BUS-IV
BUS-1	BUS-IMP	0.380952	-0.19048	-0.14286	-0.14286	0	0	0	0	0	-0.2381	-0.14286	0
BUS-1	BUS-7-8	0.619048	0.190476	0.142857	0.142857	0	0	0	0	0	0.238095	0.142857	0
BUS-2	BUS-IMP	-0.04762	0.52381	0.142857	0.142857	0	0	0	0	0	-0.09524	0.142857	0
BUS-2	BUS-XIN	0.047619	0.47619	-0.14286	-0.14286	0	0	0	0	0	0.095238	-0.14286	0
BUS-3	BUS-XIN	0	0	1	0	0	0	0	0	0	0	0	0
BUS-4	BUS-XIN	0	0	0	1	0	0	0	0	0	0	0	0
BUS-5	BUS-7-8	0	0	0	0	1	0	0	0	0	0	0	0
BUS-6	BUS-7-8	0	0	0	0	0	1	0	0	0	0	0	0
BUS-7-8	BUS-IMP	-0.2381	-0.38095	-0.28571	-0.28571	0	0	0	0	0	-0.47619	-0.28571	0
BUS-7-8	BUS-XIN	-0.14286	-0.42857	-0.57143	-0.57143	0	0	0	0	0	-0.28571	-0.57143	0
BUS-7-8	BUS-9	0	0	0	0	0	0	0	-0.5	-0.25	0	0	-0.25
BUS-7-8	BUS-10	0	0	0	0	0	0	0	-0.25	-0.5	0	0	-0.25
BUS-7-8	BUS-IV	0	0	0	0	0	0	0	-0.25	-0.25	0	0	-0.5
BUS-9	BUS-10	0	0	0	0	0	0	0	0.25	-0.25	0	0	0
BUS-9	BUS-IV	0	0	0	0	0	0	0	0.25	0	0	0	-0.25
BUS-10	BUS-IV	0	0	0	0	0	0	0	0	0.25	0	0	-0.25
BUS-XIN	BUS-IMP	-0.09524	0.047619	0.285714	0.285714	0	0	0	0	0	-0.19048	0.285714	0

*own calculation

Table II-9. Transmission Lines Capacity*.

Transmission Line		$CapTx_{line,lim+}$ (MW)	$CapTx_{line,lim-}$ (MW)
BUS-1	BUS-IMP	4849	8200
BUS-1	BUS-7-8	6936	6500
BUS-2	BUS-IMP	8518	8518
BUS-2	BUS-XIN	2700	2700
BUS-3	BUS-XIN	2700	2700
BUS-4	BUS-XIN	11000	11000
BUS-5	BUS-7-8	7092	485
BUS-6	BUS-7-8	10500	0
BUS-7-8	BUS-IMP	5598	5380
BUS-7-8	BUS-XIN	6540	8000
BUS-7-8	BUS-9	0	5500
BUS-7-8	BUS-10	9420	9108
BUS-7-8	BUS-IV	0	6800
BUS-9	BUS-10	2112	192
BUS-9	BUS-IV	6300	0
BUS-10	BUS-IV	2317	2426
BUS-XIN	BUS-IMP	4115	4115

* based on [104]

F. Additional data

Table II-10. Wind hotspot localization*.

Name	X (long.)	Y (lat.)	Name	X (long.)	Y (lat.)
HS-1-Parnaíba	41.601	2.919	HS-14-Paranaíba	51.180	19.670
HS-2-Macau	36.633	5.117	HS-15-Arraial do Cabo	42.032	22.984
HS-3-Ceará Mirim	35.417	5.649	HS-16-São Paulo-Congonhas	46.656	23.627
HS-4-Florânia	36.818	6.122	HS-17-Chapecó	52.618	27.096
HS-5-Campo Sales	40.390	6.994	HS-18-Florianópolis	48.550	27.671
HS-6-Paulistana	41.136	8.135	HS-19-São Joaquim	49.932	28.294
HS-7-Garanhuns	36.512	8.884	HS-20-São Luiz Gonzaga	54.961	28.408
HS-8-Petrolina	40.503	9.381	HS-21-Torres	49.734	29.335
HS-9-Barra	43.150	11.091	HS-22-Rivera	55.533	30.891
HS-10-Morro do Chapéu	41.156	11.550	HS-23-Bage	54.107	31.331
HS-11-Caetité	42.578	14.049	HS-24-Pelotas	52.342	31.783
HS-12-Espinoza	42.845	14.920	HS-25-Santa Vitoria do Palmar	53.368	33.519
HS-13-Diamantina	43.600	18.249			

* based on [133] and [134].

Table II-11. Installed capacity for small thermal and hydro power plants.

	Capacity (MW)	
Power bus	**Small thermal power plant**	**Small hydropower plant**
B1	1388.1	209.67
B2	110.1	359.23
B3	551.2	
B5	82.2	134.59
B6	1081.4	
B7-8	9216.59	4962.88
B10	964.9	2659.73

* based on [133] and [134].